

Aus der Medizinischen Klinik I  
der Universität zu Lübeck  
Direktor: Prof. Dr. med. Jürgen Steinhoff

**An Evaluation of  
Poly(ADP-Ribose)Polymerase Inhibitor  
Efficacy in Head and Neck Cancer  
Cell Lines**

Inauguraldissertation  
zur Erlangung der Doktorwürde  
der Universität zu Lübeck

aus der

- Sektion Medizin -

vorgelegt von

Jana Heitmann  
aus Hamburg

Lübeck 2015

1. BERICHTERSTATTER: PD DR. MED. SEBASTIAN FETSCHER

2. BERICHTERSTATTER: PROF. DR. DR. MED. JENS K. HABERMANN

3. BERICHTERSTATTER: PROF. DR. MED. CHRISTOPH THORNS

TAG DER MÜNDLICHEN PRÜFUNG: 19.12.2016

ZUM DRUCK GENEHMIGT. LÜBECK, DEN 19.12.2016

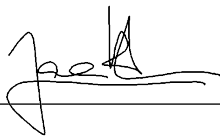
PROMOTIONSKOMMISSION DER SEKTION MEDIZIN

# Declaration of Authorship

I, Jana Heitmann, declare that this thesis titled, ‘An Evaluation of Poly(ADP-Ribose)Polymerase Inhibitor Efficacy in Head and Neck Cancer Cell Lines’ and the work presented in it are my own. I confirm that:

- This work was done wholly while in candidature for a research degree at the University of Lübeck.
- Where I have consulted the published work of others, this is always clearly attributed.
- Where I have quoted from the work of others, the source is always given. With the exception of such quotations, this thesis is entirely my own work.
- Where the thesis is based on work done by myself jointly with others, I have made clear exactly what was done by others and what I have contributed myself.
- This work was done after consultation and consent of the local ethics committee.

Signed: \_\_\_\_\_



Date: 01.02.2015

*Dedicated to my grandfather, who died of cancer*

*The nontoxic curative compound remains undiscovered, but not undreamt of.*

Prof. James F. Holland

# *Abstract*

**Objectives:** Synthetic lethality induced by poly(ADP-ribose)polymerase inhibitors (PARPi) as single agent treatment can occur in tumors with deficiencies in the DNA repair mechanism homologous recombination including, but not limited to those harboring BRCA mutations. This “homologous recombination deficiency” (HRD)-phenomenon has been observed in ovarian and triple negative breast cancers, but its role in other malignancies is not known. This study aims to evaluate the potency of PARPi in the context of HRD in head and neck cancer (HNC), where BRCA mutations are rare.

**Materials and Methods:** The comparative potency of three PARPi (veliparib, olaparib and rucaparib) was evaluated using cell viability assays in a panel of HNC cell lines. More robust IC<sub>50</sub> values were subsequently established for rucaparib in ten cell lines using colony-forming assays and response was compared to BRCA-deficient breast cancer cell lines. Furthermore, the change in foci formation after exposure to rucaparib of  $\gamma$ H2AX and RAD51 was assessed using immunofluorescent staining to determine the capability for homologous recombination. Baseline gene expression was analyzed using microarray data and gene set analysis was used to identify groups of genes correlated with rucaparib IC<sub>50</sub>.

**Results:** We identified rucaparib as the most potent of the PARPi tested. This compound showed single agent activity in a subset of HNC cell lines that was comparable to BRCA-deficient breast cancer cell lines. Rucaparib-sensitive and -resistant groups showed significant differences in  $\gamma$ H2AX and RAD51 foci formation after rucaparib exposure suggesting that differences in DNA repair capability may contribute to sensitivity. In consonance, baseline RAD51 expression was correlated with rucaparib IC<sub>50</sub>. However, foci formation of RAD51 did not serve as a post-treatment biomarker as previously shown for ovarian cancer by others. Expression of genes involved in chromosome structure was strongly associated with rucaparib resistance.

**Conclusion:** For the first time, we demonstrated that PARPi are effective in a subset of HNC cell lines suggesting that these compounds could play a role in the treatment of head and neck tumors that exhibit the HRD phenotype. Further studies elucidating the exact underlying mechanism of this phenotype as well as predictive measures of sensitivity are warranted<sup>1</sup>.

---

<sup>1</sup>The content of this thesis was published as: **J. Heitmann**, P. Geeleher, Z. Zuo, R.R. Weichselbaum, E.E. Vokes, S. Fetscher, T.Y. Seiwert. Poly(ADP-ribose)polymerase inhibitor efficacy in head and neck cancer. *Oral Oncology*, 50(9):825-31, 2014

# Contents

<b>Reviewers</b>	<b>i</b>
<b>Declaration of Authorship</b>	<b>ii</b>
<b>Dedication</b>	<b>iii</b>
<b>Quote</b>	<b>iv</b>
<b>Abstract</b>	<b>v</b>
<b>List of Figures</b>	<b>ix</b>
<b>List of Tables</b>	<b>x</b>
<b>Abbreviations</b>	<b>xi</b>
<b>1 Introduction</b>	<b>1</b>
1.1 Head and Neck Cancer . . . . .	1
1.1.1 Anatomy and Epidemiology . . . . .	1
1.1.2 Risk Factors . . . . .	2
1.1.3 Carcinogenesis . . . . .	2
1.1.4 Prevention . . . . .	3
1.1.5 Clinical Presentation and Diagnosis . . . . .	5
1.1.6 Classification . . . . .	6
1.1.7 Treatment . . . . .	7
1.1.7.1 Conventional Treatment . . . . .	7
1.1.7.2 Targeted Therapy . . . . .	8
1.2 Poly(ADP-Ribose)Polymerase - PARP . . . . .	9
1.2.1 Genomic Instability . . . . .	9
1.2.2 DNA Damage and Response . . . . .	10
1.2.3 The Role of PARP in DNA Repair . . . . .	11
1.2.4 Homologous Recombination Deficiency and Synthetic Lethality . . . . .	11
1.2.5 PARP Inhibitors . . . . .	13
1.3 Aim of this Thesis . . . . .	14
<b>2 Materials and Methods</b>	<b>16</b>
2.1 Materials . . . . .	16

---

2.1.1	Chemicals, Disposable Materials and Equipment . . . . .	16
2.1.2	Compounds . . . . .	18
2.1.3	Cell Lines . . . . .	18
2.1.4	Antibodies . . . . .	20
2.2	Methods . . . . .	20
2.2.1	Cell Culture . . . . .	20
2.2.2	Resazurin Viability Assay . . . . .	21
2.2.3	Colony-Forming (Clonogenic) Assay . . . . .	21
2.2.4	Syto60 <sup>®</sup> Viability Assay . . . . .	22
2.2.5	Western Blotting . . . . .	22
2.2.5.1	Drug Treatment and Lysate Aquisition . . . . .	22
2.2.5.2	Protein Determination . . . . .	22
2.2.5.3	Sample Preparation . . . . .	23
2.2.5.4	SDS-PAGE . . . . .	23
2.2.5.5	Western Blot and Analysis . . . . .	24
2.2.6	Immunofluorescent Staining . . . . .	24
2.2.7	Gene Expression Analysis . . . . .	25
2.2.8	Targeted Sequencing . . . . .	26
2.2.9	ImageJ Analysis . . . . .	26
2.2.9.1	Colony Counting . . . . .	26
2.2.9.2	Foci Counting . . . . .	26
2.2.10	Statistical Analysis . . . . .	26
<b>3</b>	<b>Results</b>	<b>28</b>
3.1	BRCA Alterations in Head and Neck Cancer . . . . .	28
3.2	Comparison of Three PARPi in HNC Cell Lines . . . . .	30
3.3	Establishment of Robust IC <sub>50</sub> Values for Rucaparib . . . . .	32
3.4	Comparison to BRCA-deficient Breast Cancer . . . . .	33
3.5	Predicting Sensitivity . . . . .	34
3.5.1	Estimating HR Competency by RAD51 Formation Assay . . . . .	34
3.5.1.1	RAD51 Foci Formation . . . . .	35
	2 Gy Treatment Regimen . . . . .	35
	Rucaparib Treatment Regimen . . . . .	35
3.5.1.2	$\gamma$ H2AX Foci Formation . . . . .	38
	2 Gy Treatment Regimen . . . . .	38
	Rucaparib Treatment Regimen . . . . .	39
3.5.2	Expression Analysis . . . . .	39
<b>4</b>	<b>Discussion</b>	<b>43</b>
4.1	BRCA Variations in Head and Neck Cancer Cell Lines . . . . .	43
4.2	PARP Inhibitors in Head and Neck Cancer . . . . .	44
4.3	Prediction of PARP Inhibitor Susceptibility . . . . .	45
4.3.1	Gene Signature . . . . .	46
4.3.2	Functional RAD51 Assay . . . . .	46
4.3.2.1	RAD51 . . . . .	46
4.3.2.2	$\gamma$ H2AX . . . . .	47
4.3.3	Gene Set Analysis . . . . .	48



---

4.4	Future Prediction Prospects . . . . .	48
4.5	Limitations of this Study and Future Improvements . . . . .	48
4.6	Conclusion . . . . .	49
	<b>Bibliography</b>	<b>49</b>
	<b>Appendix</b>	<b>63</b>
	<b>A German Summary</b>	<b>64</b>
A.1	Einführung . . . . .	64
A.2	Material und Methoden . . . . .	65
A.3	Ergebnisse . . . . .	66
A.4	Diskussion . . . . .	68
	<b>B ImageJ Analysis</b>	<b>70</b>
B.1	Analysis Path for Colony Counting . . . . .	70
B.2	Macro for Foci Counting . . . . .	70
	<b>C R Code</b>	<b>73</b>
C.1	Code for Generalized Linear Regression Model . . . . .	73
C.2	Code for Spearman's Rank Correlation . . . . .	73
C.3	Code for Pearson's Correlation . . . . .	74
	<b>D Gene Ontology</b>	<b>75</b>
	<b>E Colony-forming Assays</b>	<b>76</b>
	<b>F Acknowledgements</b>	<b>77</b>

# List of Figures

1.1	Sagittal Section of the Upper Aerodigestive Tract. Adapted from [1] . . .	1
1.2	Clinical, Pathological and Molecular Progression of HNC. Adapted from [2, 3] . . . . .	4
1.3	Treatment Algorithm for Locoregionally-Advanced HNC. Sourced from [4]	8
1.4	Simplified Model of DNA Repair and How PARPi Interfer . . . . .	12
1.5	Chemical Structure of Veliparib, Olaparib and Rucaparib . . . . .	13
3.1	BRCA Mutations in TCGA HNC Cohort . . . . .	29
3.2	Comparison of Three PARPi . . . . .	30
3.3	Comparison of AUC Values for Three PARPi . . . . .	31
3.4	Rucaparib Response in Ten HNC Cell Lines . . . . .	32
3.5	Comparison of PARPi Sensitivity in HNC to Breast Cancer . . . . .	33
3.6	Immunofluorescence Images for RAD51 Formation Assay . . . . .	34
3.7	Foci Changes within Cell Lines . . . . .	36
3.8	Foci Changes Group Comparison . . . . .	37
3.9	Western Blot Assessing RAD51 Levels . . . . .	38
3.10	Baseline RAD51 Expression Correlated with Rucaparib IC <sub>50</sub> . . . . .	40
E.1	Examples of Colony-forming Assay 6-well-plates . . . . .	76

# List of Tables

1.1	TNM Classification of HNC . . . . .	6
2.1	Disposable Materials . . . . .	16
2.2	Chemicals and Solutions . . . . .	17
2.3	Equipment . . . . .	18
2.4	Description of Cell Lines . . . . .	19
2.5	Origin of Cell lines . . . . .	19
2.6	Primary Antibodies . . . . .	20
2.7	Secondary Antibodies . . . . .	20
3.1	BRCA1/2 Variations in HNC Cell Lines . . . . .	29
3.2	Whole Genome Expression Correlated to Rucaparib IC <sub>50</sub> . . . . .	41
3.3	GO and Uniprot Terms enriched in Genes Inversly Correlated to Rucaparib IC <sub>50</sub> . . . . .	41
D.1	15 Genes of GO Term Category “Chromosome” . . . . .	75

# Abbreviations

<b>%</b>	<b>P</b> ercent
<b>°C</b>	Degree <b>C</b> elcius
<b>5-FU</b>	<b>5-F</b> luorouracil
<b>APS</b>	<b>A</b> mmonium <b>P</b> ersulfide
<b>ATCC</b>	<b>A</b> merican <b>T</b> ype <b>C</b> ulture <b>C</b> ollection
<b>avg</b>	<b>A</b> verage
<b>BER</b>	<b>B</b> ase <b>E</b> xcision <b>R</b> epair
<b>BSA</b>	<b>B</b> ovine <b>S</b> erum <b>A</b> lbumine
<b>DMEM</b>	<b>D</b> ulbecco's <b>M</b> odified <b>E</b> agles <b>M</b> edium
<b>DNA</b>	<b>D</b> esoxy <b>N</b> ucleic <b>A</b> cid
<b>DSB</b>	<b>D</b> ouble <b>S</b> trand <b>B</b> reak(s)
<b>EDTA</b>	<b>E</b> thylenediaminetetraacetic <b>A</b> cid
<b>EGFR</b>	<b>E</b> pidermal <b>G</b> rowth <b>F</b> actor <b>R</b> eceptor
<b>EtOH</b>	<b>E</b> thanol
<b>FBS</b>	<b>F</b> etal <b>B</b> ovine <b>S</b> erum
<b>g</b>	<b>G</b> ram
<b>g</b>	<b>G</b> ravitational <b>F</b> orce
<b>Gy</b>	<b>G</b> ray
<b>h</b>	<b>H</b> our(s)
<b>HNC</b>	<b>H</b> ead and <b>N</b> eck <b>C</b> ancer
<b>ddH<sub>2</sub>O</b>	double distilled <b>W</b> ater
<b>HPV</b>	<b>H</b> uman <b>P</b> apilloma <b>V</b> irus
<b>HR</b>	<b>H</b> omologous <b>R</b> ecombination
<b>IC<sub>50</sub></b>	<b>H</b> alfmaximal <b>I</b> nhibitory <b>C</b> oncentration
<b>ICC</b>	<b>I</b> mmunocytochemistry

---

<b>IF</b>	<b>I</b> mmunofluorescence
<b>Ig</b>	<b>I</b> mmunoglobulin
<b>IMDM</b>	<b>I</b> scove's <b>M</b> odified <b>D</b> ulbeccos <b>M</b> edium
<b>IR</b>	<b>I</b> onizing <b>R</b> adiation
<b>kDa</b>	<b>K</b> ilo <b>D</b> alton
<i>l</i>	<b>L</b> iter
<b>LOH</b>	<b>L</b> oss <b>O</b> f <b>H</b> eterozygosity
<b>m</b>	<b>M</b> illi
<b>M</b>	<b>M</b> olar
$\mu$	<b>M</b> icro
<b>mAb</b>	<b>M</b> onoclonal <b>A</b> ntibody
<b>min(s)</b>	<b>M</b> inute(s)
<b>ms</b>	<b>M</b> ouse
<b>n</b>	<b>N</b> ano
<b>NaCl</b>	<b>S</b> odium <b>C</b> hloride
<b>NHEJ</b>	<b>N</b> on- <b>H</b> omologous <b>E</b> nd <b>J</b> oining
<b>PAGE</b>	<b>P</b> olyacrylamide <b>G</b> el <b>E</b> lectrophoresis
<b>PARP</b>	<b>P</b> oly( <b>A</b> DP- <b>R</b> ibose) <b>P</b> olymerase
<b>PARPi</b>	<b>P</b> oly( <b>A</b> DP- <b>R</b> ibose) <b>P</b> olymerase inhibitor
<b>PBS</b>	<b>P</b> hosphor <b>B</b> uffered <b>S</b> aline
<b>PFA</b>	<b>P</b> ara- <b>F</b> ormaldehyde
<b>rb</b>	<b>R</b> abbit
<i>r<sub>P</sub></i>	Pearson's correlation coefficient
<i>r<sub>S</sub></i>	Spearman's correlation coefficient
<b>RT</b>	<b>R</b> oom <b>T</b> emperature
<b>SDS</b>	<b>S</b> odium <b>D</b> odecyl <b>S</b> ulfate
<b>SSB</b>	<b>S</b> ingle <b>S</b> trand <b>B</b> reak(s)
<b>TCGA</b>	<b>T</b> he <b>C</b> ancer <b>G</b> enome <b>A</b> tlas
<b>TEMED</b>	<b>N</b> , <b>N</b> , <b>N,N</b> - <b>T</b> etramethyl- <b>E</b> thylen- <b>D</b> iamine
<b>TNM</b>	<b>T</b> umor <b>N</b> ode <b>M</b> etastasis
<b>UICC</b>	<b>U</b> nion <b>I</b> nternational <b>C</b> ontre le <b>C</b> ancer
<b>V</b>	<b>V</b> olt
<b>WB</b>	<b>W</b> estern <b>B</b> lot

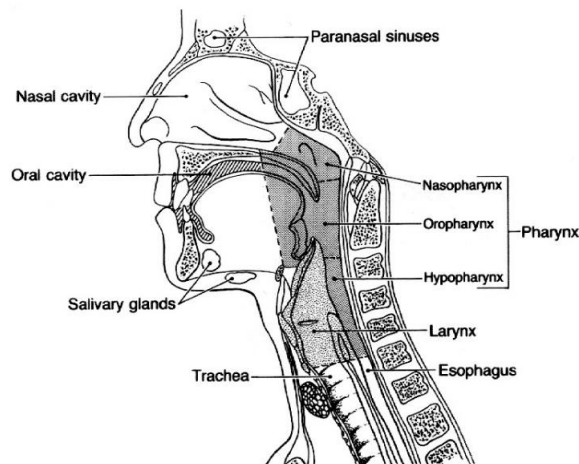
# Chapter 1

## Introduction

### 1.1 Head and Neck Cancer

#### 1.1.1 Anatomy and Epidemiology

Head and neck cancer (HNC) comprises a group of diverse malignancies arising in the upper aerodigestive tract. The primary sites are subdivided anatomically: pharynx (nasopharynx, oropharynx and hypopharynx), larynx, oral and nasal cavity, including paranasal sinuses (Fig. 1.1). Over 90% of these tumors originate from squamous epithelium cells.



---

FIGURE 1.1: Sagittal Section of the upper aerodigestive tract showing anatomic sites of HNC. Adapted from [1]

HNC is the 6<sup>th</sup> most common malignancy worldwide accounting for over 600,000 new cases and approximately 350,000 deaths every year [5]. It was estimated that in 2014, over 12,000 HNC patients died in the United States alone [6]. Men and women are affected in a ratio of 2.5:1 respectively, however this ratio varies by anatomic site of the tumor (up to 4:1 for cancers of the larynx) [6].

### 1.1.2 Risk Factors

It has recently become clear that two distinct types of HNC exist: Approximately one third of HNC tumors are linked to a human papilloma virus (HPV) infection as a risk factor [7]. It is on the rise: Incidence of HPV-related tumors has increased more than four-fold in the past two decades in the United States [8]. There are several types of HPV including type 16, that has been proven to contribute to carcinogenesis through its oncogenes E6 and E7 that inactivate tumor-suppressor genes [9]. Patients with HPV-positive tumors are typically younger and show an improved treatment response resulting in a better overall survival rate (5-year relative survival rate HPV-positive 70%-80% vs. 25%-40% HPV-negative) [10]. Novel research has revealed that despite its unifying squamous cell origin, HNC is a very heterogeneous disease [11]. Our group has recently investigated the genetic make-up of both, HPV-positive and HPV-negative tumors and found remarkable differences in mutational status and copy number aberrations, underlining again that these tumor groups should be treated differently [12]. Hence, HPV status will need to be considered in future therapeutic approaches. Because the group of HPV-negative tumors is much larger and associated with a worse prognosis, we primarily focused on HPV-negative cell lines in this study.

The remaining two thirds of HNC cases (“HPV-negative”) are attributed to alcohol and tobacco consumption (with strong dose-response-relationships for each substance [13]), yielding a worse overall survival rate [14, 15]. Interestingly, the combined carcinogenic effect of both, tobacco smoking and alcohol consumption, is greater than the additive joint effect [13, 15]. Besides the above-mentioned external risk factors, genetic predisposition and some inherited disorders, like Fanconi anaemia, also predispose for developing malignancies in the head and neck [16, 17].

### 1.1.3 Carcinogenesis

In 1953, the term “field cancerization” was proposed by Slaughter and colleagues to describe the high likelihood of multiple HNC lesions and the tendency for local recurrence after treatment [18]. The annual rate of second primary tumors ranges between 3%-7%, which is higher than for any other type of cancer adding up to a 35% chance for a HNC

survivor to develop a second primary tumor within five years after initial occurrence of the malignancy [19]. Since the proposal of this theory, it has been possible to delineate the process of field cancerization molecularly. The surrounding tissue of cancerous lesions has been shown to often contain genetic alterations in terms of dysplasia or pre-cancerous lesions. These surrounding cells have genetic profiles that are clonal to the invasive carcinoma giving rise to the hypothesis that a field of preneoplastic cells proceed the carcinoma to form a multi-step genetic pathogenesis [20]. The first multi-step model for HNC was introduced in 1996 by Califano et al., who studied the genetic characterization of histopathological changes in the epithelium. In a histopathological context, this multi-step model ranges from normal squamous cells over hyperplasia, mild, moderate and severe dysplasia, carcinoma in situ, invasive carcinoma to finally metastasis (Fig. 1.2) [2]. Underlying genetic alterations include loss of heterozygosity, upregulation or amplification of oncogenes (such as Epidermal Growth Factor Receptor (EGFR)) and downregulation or deletion of tumor-suppressor genes (such as p53). The latter has consecutively been shown to often occur early in carcinogenesis of HNC and to contribute to the immortalization of a clone [2]. Recently, multiple classes of genetic data from The Cancer Genome Atlas (TCGA) revealed that the p53 mutation not only contributes to carcinogenesis, but that it is also associated with a worse survival in HNC patients [21].

#### 1.1.4 Prevention

In order to primarily prevent HNC, an important aspect is to stop exposure to causative carcinogens, such as tobacco and alcohol. Encouragingly, the relative risk of HNC decreases sharply after cessation of smoking and reaches an equal risk compared to never-smokers after ten years of abstinence [13]. Cessation of alcohol intake on the other hand only reaches a reversal of HNC risk after over 20 years of abstinence [22]. Furthermore, there seems to be an association between poor oral hygiene and dental care and HNC, lending support to the hypothesis that improved oral hygiene may aid prevention [23]. It has additionally been hypothesized that conservative sexual behavior might stop the sharp rise of HPV-positive HNC, which has been attributed to a lower age at first sexual activity as well as higher numbers in sexual partners [24]. It still remains to be studied whether the HPV-vaccination currently administered to prevent cervical cancer also contributes to prevention of HPV-positive HNC [25].



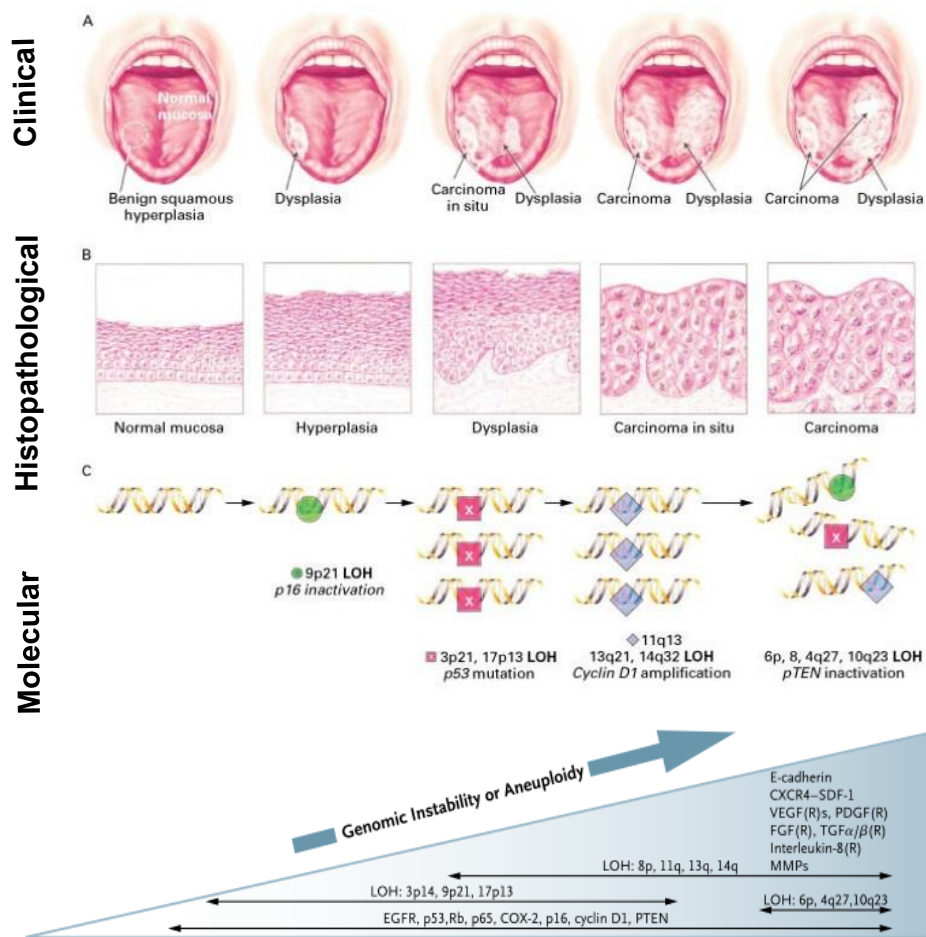


FIGURE 1.2: Progression of HNC

**A** shows the clinical presentation of oral cancer. Benign lesions can look very similar to healthy mucosa. Different stages of the disease can often be observed next to each other as proposed in the field cancerization theory [18]. In **B** the histopathological pattern of HNC lesions is shown at various stages. While different patterns may be observed as shown, they are often based on a clonal relationship. In **C** the underlying genetic instabilities including the loss of heterozygosity (LOH), upregulation of oncogenes and downregulation of tumor-suppressor genes are shown. Strikingly, benign lesions already harbor some of these genetic alterations. Genes of the right side of the triangle, such as E-Cadherine (CDH1), vascular endothelial growth factor (VEGF) or fibroblast growth factor (FGF) are finally involved in the progression of the tumor towards metastasis.

Adapted from [2, 3].

Secondary prevention of HNC aims for an early detection of the malignancy, as diagnostic delay has been linked to decreased overall survival [26]. Alarmingly, the mean time from onset of first symptoms to treatment was 206 days in a recent study. Increased public awareness and knowledge of early symptoms could contribute to sooner detection of HNC, as the longest delay occurred before consultation with a physician [26]. An effective screening of HNC still remains elusive and the only conducted randomized

clinical trial on HNC-screening through clinical examination in India resulted in no difference in mortality rate between the screened and not-screened population [27].

The goal of tertiary prevention is to avoid recurrence or emergence of a second primary tumor. Discontinuance of smoking and alcohol consumption are again key interventions at this stage. Because HNC is especially prone to recurrence as discussed above, adherence to these lifestyle changes is of utmost importance after the diagnosis. There are a number of substances discussed in the literature for tertiary chemoprevention of HNC. Agents range from natural compounds (green tea polyphenols in patients with leukoplakia [28]), to more targeted substances such as the EGFR inhibitor erlotinib, selective cyclooxygenase inhibitors and very recently the combination of both [29], peroxisome activator receptor gamma (PPAR $\gamma$ ) agonists, p53-targeted compounds [30] and retinoid receptor ligands. For the latter a double-blind placebo-controlled trial was conducted as early as 1986, but despite its favorable response rates in histological improvement, the treatment did not reach the clinic due to adverse effects and rapid relapse [31].

### 1.1.5 Clinical Presentation and Diagnosis

The most commonly seen premalignant lesion is oral leukoplakia defined as a white plaque in the mucosal lining that cannot be removed by scraping. The annual transformation rate to an invasive carcinoma amounts to 1%-2% with risk factors for transformation including female gender, grade of dysplasia as well as the size of lesion [32, 33]. However, there is no marker that can reliably predict transformation, which can occur at the site of the lesion or elsewhere in the aerodigestive tract [33]. As of today, no effective treatment has been found to avoid this transformation in patients with leukoplakia and even removal of the lesion does not result in prevention of recurrence [34].

Early symptoms of HNC may be minor, they vary across the different anatomical sites and are easily overseen, which is the reason for treatment delay as discussed above. Symptoms can range from nasal obstruction or otitis (nasopharynx), hoarseness (larynx), sinusitis or epistaxis (nasal cavities), ulcers, changes in the fit of dentures or the above-mentioned leukoplakia (oral cavity) [1].

First diagnostic steps should include a thorough patient history (stressing the risk factors) and clinical examination. The next step could be endoscopy and biopsy of suspicious lesions (such as leukoplakia). Ultrasound of the neck can aid in defining the extent of the disease in the lymphnodes where biopsies may again be taken [1]. In order to estimate a prognosis and choose the right treatment regimen for the patient, staging of the tumor needs to be performed as discussed in the next section.

### 1.1.6 Classification

Aside from lifestyle factors such as smoking (discussed above), the prognosis for patients with HNC is largely determined by the stage at diagnosis, conveyed by the Tumor-Node-Metastasis (TNM) classification of the UICC (Union International Contre Cancer)[35]. Originally established by Pierre Denoix in the 1940s, the classification is still used in clinic today [36]. It is based on the anatomic extent of the primary tumor (T1-T4), as well as the lymph node infiltration (N0-N3) and metastasis to other organs (M0/M1). The stage is determined by clinical examination, imaging, cytology of lymphnodes and definite histopathology after surgery (Tab. 1.1). The head and neck tumors comprise neoplasms at various anatomic sites, which is why there is no general TNM classification. An example of the current UICC TNM classification for HNC in the oral cavity and larynx is summarized below (effective since 2010). Tumor grading is dependent on the histological pattern tumor cells exhibit ranging from G1 (well differentiated) to G4 (undifferentiated).

Stage	Tumor	Node	Metastasis
0	Tis	N0	M0
I	T1	N0	M0
II	T2	N0	M0
III	T3	N0/N1	M0
	T1	N1	M0
	T2	N1	M0
IVa	T4a	N0/N1/N2	M0
	T1	N2	M0
	T2	N2	M0
	T3	N2	M0
IVb	T any	N3	M0
	T4b	N any	M0
IVc	T any	N any	M1

TABLE 1.1: TNM Classification of HNC

Example classification for tumors arising in the oral cavity and larynx. Classifications for other sites are very similar. Stages 0-II are considered early disease, stages III and IV advanced disease

## 1.1.7 Treatment

### 1.1.7.1 Conventional Treatment

In the beginning of the past century, malignancies were addressed with anatomically-guided treatment such as surgical resection and radiation therapy, which still remain commonly used treatment options today [37]. In the 1970s and 1980s, improvements were accomplished in the patients' quality of life, for example regarding speech and swallowing [38].

DNA damaging therapies continue to be a mainstay of therapy including radiation and chemotherapy. Combinations of platinum-based agents (either cisplatin or carboplatin) with 5-fluorouracil (5-FU) are the most frequently used chemotherapeutic agents in HNC with response rates between 20% and 40% [39]. However, these non-selective treatment approaches yield a high risk for acute toxicities during or shortly after treatment including mucositis, xerostomia, dysphagia, regional alopecia, hoarseness and radiation dermatitis. Specifically mucositis remains one of the most fierce adverse effects of non-selective HNC treatment. It occurs with a mean incidence of 80% and is associated with a high level of discomfort and pain leading to weight loss through eating problems and eventually oftentimes cessation of therapy [39, 40].

Tumors are treated according to the stage of disease: Early stage tumors are treated with either surgery or radiotherapy as they have a comparatively good prognosis [11]. For young patients with moderately advanced tumors, organ-preservation is striven for both, surgically and radiotherapeutically to preserve the quality of life for patients [41, 42]. Multimodality treatment is the standard of care for locoregionally-advanced disease. To date, three approaches are applied: The first is surgery followed by adjuvant concurrent chemoradiotherapy, where precise anatomic staging can be performed. However, total resection cannot be accomplished in a majority of cases, particularly when organ preservation is aimed for. For this goal, definite concurrent chemoradiotherapy with surgery as a consecutive option - the second approach - is the favorable alternative, although it provides no pathological information. Thirdly, induction chemotherapy followed by definite local therapy can be used to treat patients with locoregionally-advanced HNC offering tumor debulking in responders but yielding the risk of metastasis (Fig. 1.3). The different approaches are discussed controversially in the literature to date [4].

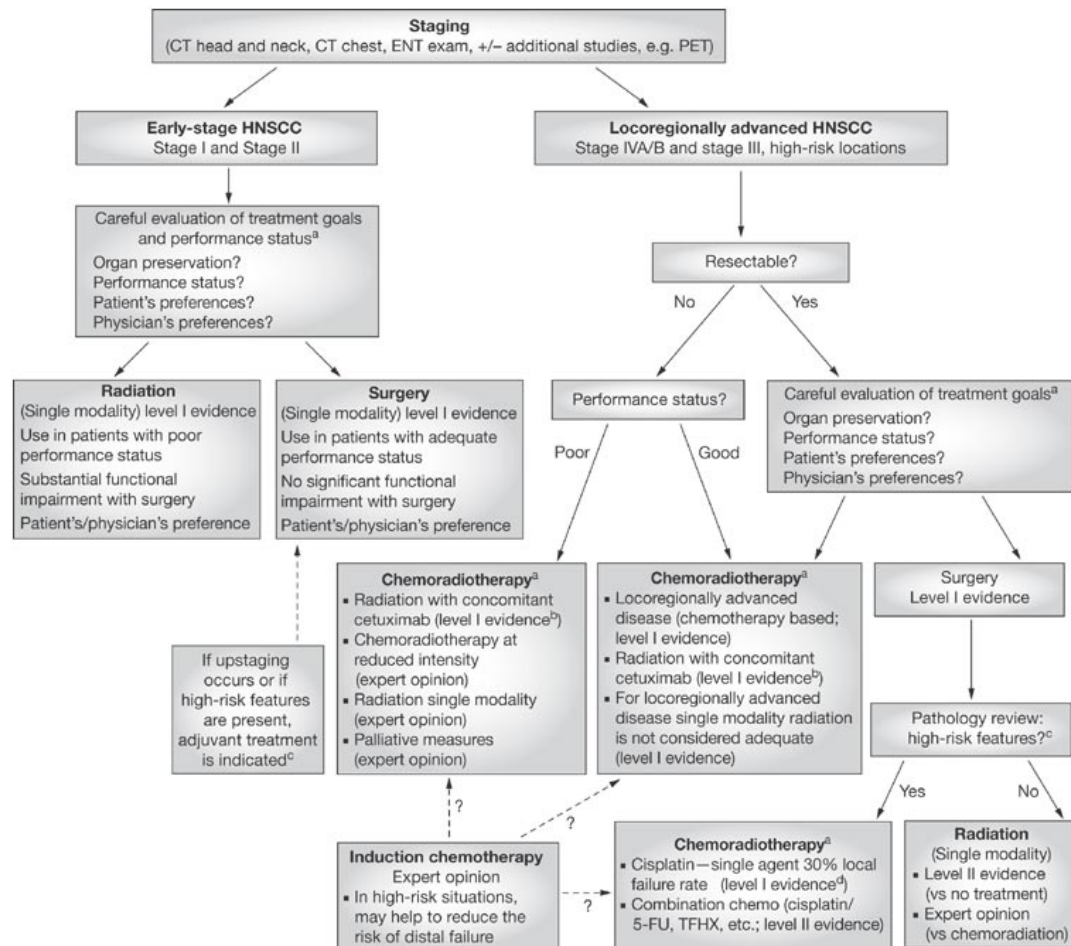


FIGURE 1.3: Treatment algorithm for locoregionally-advanced HNC in the USA based on clinical trials and expert opinion.

“**a** Referral to an experienced center with an adequate support system is recommended. **b** Level 1 evidence compared with radiotherapy as a single modality. No data are available for CRT comparisons; therefore, no clear recommendation can be made in comparison with CRT. This treatment option is an excellent choice for patients with a low performance status who are poor candidates for chemoradiotherapy. **c** High-risk features for recurrence are as follows: involved margins of resection, extranodal or extracapsular spread, perineural invasion, and the presence of two or more involved regional lymph nodes. **d** Cetuximab-based CRT can also be considered as an option, but this therapy has not been studied postoperatively. On the basis of experience with other regimens, the therapy should be considered as a reasonable option, especially in patients who cannot tolerate more-toxic regimens. Abbreviations: CRT, concurrent chemoradiotherapy; ENT: ears, nose, and throat; HNSCC: head and neck squamous cell carcinoma; TFHX: paclitaxel, 5-fluorouracil, hydroxyurea and concurrent radiotherapy.” [4]

### 1.1.7.2 Targeted Therapy

Despite the progress made in identifying and addressing molecular targets in HNC, the overall survival rate of patients with advanced stages of this malignancy has not risen

above 50% since the 1960s highlighting the need for more effective novel therapeutic approaches [38].

The discovery of the DNA structure by Watson and Crick in 1953 allowed for the start of a new era in the understanding of cancer and carcinogenesis. Since then, researchers have endeavored to unravel cancer biology elucidating molecular pathways that facilitated the development of targeted therapies. In 2006, the Food and Drug Administration (FDA) and the European Medicines Evaluations Agency (EMA) approved the first targeted therapy in HNC treatment: Cetuximab, an EGFR inhibitor that showed a promising overall survival benefit in a neoadjuvant treatment regime for patients in a phase III study [43]. The drug - a monoclonal antibody binding to the external portion of EGFR - showed favorable results without adding toxicity to the conventional ionizing radiation (IR) treatment [43, 44]. The targeted drug is approved for two further clinical settings: As second-line treatment for metastatic or recurrent disease as a single agent and secondly in combination with platinum-based agents or 5-FU in this cohort as first-line treatment [45]. However, to date no biomarkers have been found that predict clinical response to cetuximab [45]. Since the introduction of cetuximab to the clinic, more potential drug targets have been identified in the laboratories and continuing research aims to develop novel compounds that exclusively harm cancer cells and spare healthy cells to avoid severe side effects like mucositis. In this study, we too focused on targeting a single protein called poly(ADP-ribose)polymerase.

## 1.2 Poly(ADP-Ribose)Polymerase - PARP

### 1.2.1 Genomic Instability

One of the hallmarks of cancer is genome instability and mutation [46]; therefore, the survival of cancer cells depends on their ability to constantly repair their own DNA. In malignant cells, genomic instability can occur through chromosomal instability and changes of DNA structure. The former meaning that there is an alteration in the number or structure of chromosomes and the latter comprising insertions, deletions, and nucleotide substitutions. In cancer, a large number of mutations are passenger mutations. These mutations are merely a side effect of general genome instability with no capacity to drive disease. On the other hand, mutations occurring in so-called driver genes are capable of changing the behavior of the cell promoting a selective advantage and triggering disease [47].

### 1.2.2 DNA Damage and Response

DNA damage occurs constantly in all cells of the body. It has been estimated that every single cell might suffer up to  $10^5$  DNA lesions per day [48]. The damage can be caused endogenously, for example by oxidation or depurination, or exogenously by UV-light, IR, tobacco smoke, or chemotherapeutic agents [49]. Cytotoxic chemotherapeutics continue to be the mainstay in cancer therapy as they induce breaks in the DNA through various mechanisms, either by alkylating the DNA (e.g. cyclophosphamide), inducing crosslinks (e.g. cisplatin), intercalating between DNA helices (e.g. doxorubicine) or many others. However, these chemotherapeutic agents do not distinguish between normal cells and malignant cells, resulting in severe side effects, especially in tissues that likewise regenerate often, like mucous membranes for example.

Because DNA damage is common, yet constitutes a threat to the cells' survival, many DNA repair mechanisms have evolved. Most of them include the detection of the break and recruitment of repair factors to the damage site, followed by the actual repair [47]. Single strand breaks (SSB) in the DNA are mostly repaired by base excision repair (BER), where bases are removed and replaced. Mismatch repair is the mechanism through which incorrect bases are replaced, nucleotide excision repair replaces an entire nucleotide, e.g. after dimerization of pyrimidines [49]. The major mechanisms that cope with DNA double strand breaks (DSB) are non-homologous endjoining (NHEJ) and homologous recombination (HR). NHEJ simply reconnects the broken DNA ends and therefore contains the high possibility of inaccurate mending. HR however is an exact mechanism to repair DNA DSB, because it utilizes the sister chromatide as a template [50].

While an obvious link is lacking between defects in DNA repair and carcinogenesis, some examples point towards its importance nevertheless. For instance, there is a mutational pattern found in some sporadic and hereditary colorectal tumors called microsatellite instability. This phenomenon is associated with an inability of the cells to perform the DNA repair mechanism mismatch repair [51]. An even better known example of the importance of DNA repair pathways in cancer are the BRCA1 and BRCA2 genes. These genes are involved in the DNA DSB repair mechanism HR. Loss-of-function mutations or epigenetic silencing of these genes have been reported in various types of malignancies, including breast, ovarian, pancreatic, and non-small cell lung cancer [52–54]. Altogether, the DNA repair machinery plays an important role in cancer. While genome instability and inability of cancer cells to stop the cell cycle before DNA is repaired furthers carcinogenesis, it also constitutes a treatment opportunity to target the proteins involved. DNA repair is carried out by a multitude of enzymes, such as ligases, nucleases, topoisomerases and polymerases (the latter are discussed in the next subsection).

### 1.2.3 The Role of PARP in DNA Repair

Poly(ADP-ribose)polymerases (PARP) comprise a family of 17 nuclear enzymes that catalyze ADP-ribosylation of proteins. PARP-1 is thought to be crucial for SSB repair, namely BER, PARP-2 seems to be important for the stability of PARP-1 [55, 56]. PARP recognize SSB in the DNA and bind to the DNA with an N-terminal zinc finger, thus activating their C-terminal catalytic domain to hydrolyze  $NAD^+$  and form poly(ADP-ribose)chains. These chains are attached to acceptor proteins, such as histones, to relax the chromatin structure for easier access to the break, or to repair factors recruiting them to the damage site [55]. Poly(ADP-ribose)polymers have a large negative charge and lead to extensive autoPARylation of PARP itself, resulting in dissociation from the DNA - a crucial step to allow the completion of DNA repair [57] .

### 1.2.4 Homologous Recombination Deficiency and Synthetic Lethality

If PARP is inhibited by PARP inhibitors (PARPi), the accumulating SSB may be converted to DSB during replication. For cancer therapy, PARPi have shown to be effective chemo- and radiation sensitizers as they enforce the effects of DNA damage [58]. Recently, it has been shown that PARPi are highly selectively effective against cells with BRCA1/2 mutations [59, 60]. PARP inhibition can be compensated for by HR in normal cells, however with deleterious mutations in HR genes (e.g. BRCA genes), DSB accumulate during replication and lead to cell death (Fig. 1.4). This is a prime example of “synthetic lethality”, defined as the lethal effect of defects in two genes, where the defect of either one alone is tolerated [61, 62]. The concept has been validated by in vitro studies, as well as clinical trials in breast cancer patients with BRCA mutations [59, 60, 63, 64]. The advantage of synthetic lethality is that toxic effects can be avoided, as normal tissue does not show the homozygous status of the tumor cells.



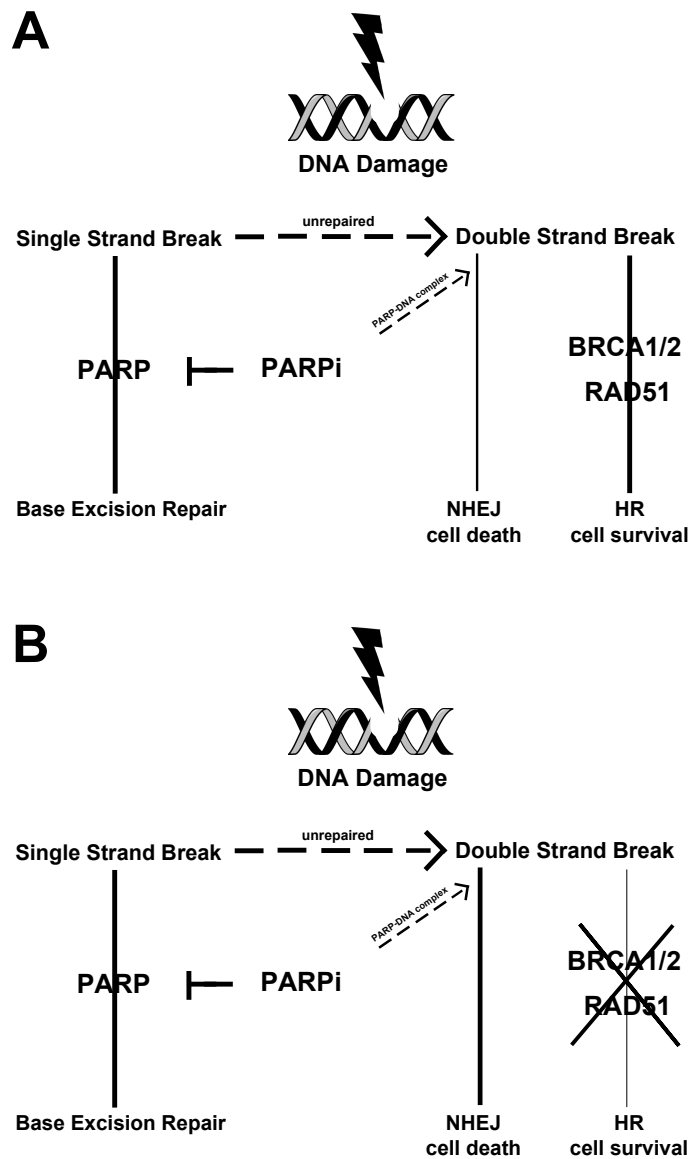


FIGURE 1.4: Simplified model of DNA repair and how PARPi interferes. Frequently occurring DNA SSB are most commonly repaired by base excision repair through PARP. If PARP is inhibited, SSB accumulate and turn into DSB during replication in addition to the DSB occurring when the replication fork reaches a PARP-DNA complex. These DSB then are mainly repaired through HR by a number of proteins here represented by BRCA1/2 and RAD51. The more error-prone mechanism NHEJ leads more frequently to errors and cell death. In **A** the normal situation is shown: HR is mainly used to repair DSB and cell survival is accomplished despite the treatment with PARPi. In **B** the situation in cells with HR deficiency (i.e. through BRCA mutation) is shown: Because HR cannot be performed, NHEJ is used abundantly and genetic instability finally leads to cell death.

Recently, the effects of PARPi have been postulated to also play a role in tumors with defects in the HR pathway in general, and not solely in those tumors containing BRCA mutations [63, 65]. “HR deficiency” (HRD, also known as BRCAness [66, 67]) describes a set of phenotypic characteristics, namely the inability to repair DNA via HR, that some sporadic cancers share with tumors containing germline BRCA mutations [66].

Several mechanisms have been found to contribute to the HRD phenotype, such as silencing of BRCA2 by EMSY [68], downregulation of BRCA1 by the transcription factor ETS-1 [69], or hypermethylation of the BRCA1 promotor [52]. The latter has been associated with PIK3CA copy number gain [70], which frequently occurs in HNC [71]. Beyond BRCA, defects in the Fanconi anaemia pathway, hypermethylation of RAD51C, mutations in the DNA damage recognizing genes ATM and ATR and PTEN, which regulates RAD51 transcription, have been suggested to contribute to a HRD phenotype [67]. Altogether, any defect in the HR machinery may lead to HRD and to PARPi susceptibility in the context of synthetic lethality [47, 58].

### 1.2.5 PARP Inhibitors

In 1971, nicotinamide was found to be a weak inhibitor of PARP [72]. Therefore, the first generation of PARPi, developed in 1980, was a nicotinamide analogue (3-aminobenzamide) [55]. In this study, we used third-generation PARPi, with greater potency and specificity employing their catalytic constraint mainly through the inhibition of PARP-1 [73]. They have a structural resemblance of the substrate  $NAD^+$  and compete for the binding of PARP [74]. Currently, there are nine PARPi in clinical development [75].

We used the inhibitors veliparib (ABT-888), olaparib (AZD2281) and rucaparib (AG014699, PF-01367338, CO-338). They are all orally-available small molecule inhibitors (Fig. 1.5).

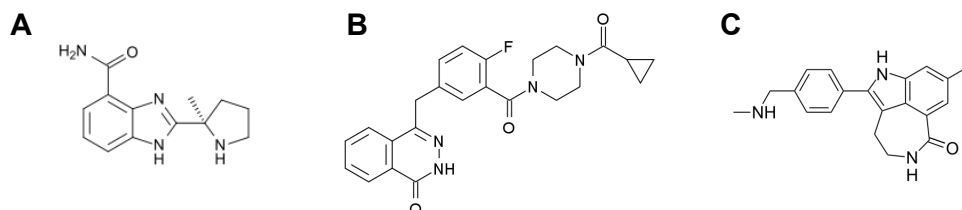


FIGURE 1.5: Chemical structure of **A** veliparib, **B** olaparib and **C** rucaparib

Veliparib and olaparib are potent inhibitors of PARP-1 and PARP-2, rucaparib solely inhibits PARP-1. It has been proposed that there are two main mechanisms by which PARPi employ anti-proliferative activity. Firstly, they inhibit the PARylation, resulting in suppression of factor recruitment to the damage site. Secondly, they bind to the  $NAD^+$  site allosterically, enforcing the N-terminal zinc finger domain of PARP to bind to the DNA. It has been shown, that this PARP-DNA complex forming ability is potentially of larger significance for the anti-proliferative activity than the mere inhibition of the catalytic domain. By decreasing the availability of PARP for further repair and by stalling the transcription fork during mitosis leading to DNA breaks, these PARP-DNA complexes contribute a large proportion of potency [57]. Veliparib does not effectively form PARP-DNA complexes [57], whereas olaparib and rucaparib similarly show strong potentials in trapping PARP-DNA complexes [76].

### 1.3 Aim of this Thesis

Professor James F. Holland, a pioneer in clinical cancer research, stated in a publication about acute lymphocytic leukemia in children in 1970 that “the nontoxic curative compound remains undiscovered, but not undreamt of” [77]. Unfortunately, more than 40 years later, we are still dreaming.

One possible approach to find such “nontoxic compounds” has been the idea of synthetic lethality. This phenomenon occurs when one genetic alteration renders another gene essential in cancer cells only, predestining it as an ideal target for oncological compounds. The BRCA1/2-PARP synthetic lethal interaction is well-established and of clinical importance. Other possible synthetic lethal interaction partners of PARP have been identified as discussed above [52, 67–69]. A current cutting edge study published in *Cell* has now proposed a computational pipeline to discover genome-wide synthetic lethal interactions [78]. Building on this premise that there are more potential synthetic lethal partners of PARP beyond uncommon somatic BRCA mutations in HNC, we hypothesized that PARPi could have a single agent effect on a subset of HNC cell lines leading to synthetic lethality.

To test our hypothesis, we evaluated the comparative potency of veliparib, olaparib and rucaparib in a panel of HNC cell lines using viability assays. We subsequently compared the PARPi sensitivity of HNC cell lines to BRCA-deficient breast cancer cell lines, as the lethal interaction between BRCA and PARP is already well-established. In search for an approach to predict sensitivity to PARPi, we applied a method based on post-treatment RAD51 foci formation and interrogated differences associated to PARPi sensitivity in baseline gene expression of cell lines.

Our study aims to elucidate the potential role of PARPi in the treatment of HNC and extend the knowledge about possible use of such targeted agents, as they are urgently needed in the treatment of this malignancy.

## Chapter 2

# Materials and Methods

### 2.1 Materials

#### 2.1.1 Chemicals, Disposable Materials and Equipment

TABLE 2.1: Disposable Materials

<b>Disposable Materials</b>	<b>Source</b>
Cell Culture Dishes 100mm, polystyrene	BD Falcon™
Cell Scapers	Fisher Scientific, Inc.
Clear 6-well/96-well Microtest Plate	BD Falcon™
Conical Centrifuge Tubes	Fisher Scientific, Inc.
Crystal Violet	Sigma Aldrich®
Dilux™ Dilution Reservoirs	Fisher Scientific, Inc.
EZFlip Centrifuge Tubes	Fisher Scientific, Inc.
Microscopy Slides	Thermo Scientific, Inc.
Millex-GP Filter Unit	EMD Millipore®
Parafilm Laboratory Film	Bemis Flexible Packaging
Poly-D-Lysine-coated coverslips	BD Biosciences #354086
Scalpel	Feather Safety Razor Co
Serological Pipets (2,5,10,25ml)	Denville Scientific, Inc.
Sterile Reagent Reservoirs	Fisher Scientific, Inc.
Threaded Cryogenic Storage Vials	Fisher Scientific, Inc.
TipOne RPT elongated Pipet Tips	USA Scientific®

TABLE 2.2: Chemicals and Solutions

<b>Chemical or Solution</b>	<b>Source</b>
2-Mercaptoethanol	MP Biomedicals
Ammonium Persulfate (APS)	Thermo Scientific, Inc.
Blocking Buffer	Licor <sup>®</sup>
Dimethyl Sulfoxide (DMSO)	American Bioanalytical, Inc.
DME-F12 1:1	Thermo Scientific, Inc.
DME Medium	cellgro <sup>®</sup> Mediatech, Inc.
EMEM	ATCC
Ethyl Alcohol 200 Proof	Decon Laboratories, Inc.
Fetal Bovine Serum	Gemini Bio-Products
Goat Serum	Sigma Aldrich <sup>®</sup>
Halt <sup>™</sup> Phosphatase Inhibitor	Thermo Scientific, Inc.
Hoechst Dye	Life Technologies <sup>™</sup>
IMD Medium	Thermo Scientific, Inc.
Laemmli Loading Buffer 4x	Licor <sup>®</sup>
Methanol, HPLC grade	Fisher Scientific, Inc.
Mounting Medium	Vector Laboratories, # H-1200
NEXT GEL <sup>®</sup> 10% Solution	Amresco <sup>®</sup>
NEXT GEL <sup>®</sup> Running Buffer	Amresco <sup>®</sup>
Nitrocellulose Membrane 0.45	Bio-Rad, Inc.
Odyssey <sup>®</sup> Blocking Buffer	Licor <sup>®</sup>
PageRuler Protein Ladder	Thermo Scientific, Inc.
Para-Formaldehyde (PFA)	Electron Microscopy Sciences
Penicillin-Streptomycin	cellgro <sup>®</sup> Mediatech, Inc.
Phosphate Buffered Saline (PBS)	cellgro <sup>®</sup> Mediatech, Inc.
Phosphatase Inhibitor Cocktail	EMD Millipore <sup>®</sup>
Protease Inhibitor Cocktail Set	EMD Chemicals, Inc.
Protein Assay Dye	Bio-Rad, Inc.
4x Protein Loading Dye	Licor <sup>®</sup>
Quick Start <sup>™</sup> BSA	Bio-Rad, Inc.
Resazurin Sodium Salt, powder	Sigma Aldrich <sup>®</sup>
RIPA buffer	Boston BioProducts, Inc.
RPMI1640	Thermo Scientific, Inc.
Syto60 <sup>®</sup> Nucleic Acid Dye	Life Technologies <sup>™</sup>
TEMED	Bio-Rad, Inc.
10x Tris/Glycine buffer	Bio-Rad, Inc.
Tris-HCl	Sigma Aldrich <sup>®</sup>
Triton X-100	Sigma Aldrich <sup>®</sup>
Trypsin EDTA	cellgro <sup>®</sup> Mediatech, Inc.
Tween <sup>®</sup> 20	Fisher Scientific, Inc.

TABLE 2.3: Equipment

<b>Equipment</b>	<b>Source</b>
Bio Star Microscope	Reichert-Jung, Inc.
Centrifuge 5424R, refrigerated	Eppendorf
CO <sub>2</sub> Incubator Model MCO 18AIC	SANYO Electric Co., Ltd.
Cryo Plus 2 Liquid N <sub>2</sub> tank	Thermo Scientific, Inc.
Genie Blotter	Idea Scientific Company
Hydration Chamber	Simport
Irradiator	Faxitron <sup>®</sup> X-Ray 43855 Series
KC4 <sup>™</sup> Program	BIO-TEK <sup>®</sup> Instruments Inc.
Leica TCS SP2 confocal microscope	Leica Microsystems
Mini-PROTEAN Casting Stand	Bio-Rad, Inc.
Mini-PROTEAN Comb	Bio-Rad, Inc.
Neubauer Hemacytometer	Fisher Scientific, Inc.
Pipet Boy	Drummond Scientific Company
PowerPac HC High-Current Power Supply	Bio-Rad, Inc.
Spacer Plates	Bio-Rad, Inc.
Vortex Genie	Fisher Scientific, Inc.
Western Incubation Boxes	Licor <sup>®</sup>

### 2.1.2 Compounds

Veliparib (ABT-888), olaparib (AZD2281) and rucaparib (AG014699, PF-01367338, CO-338) were purchased from Selleck Chemicals (Houston, TX ; veliparib #S1004; olaparib #S1060; rucaparib #S1098), dissolved in dimethyl sulfoxide (DMSO; American Bioanalytical, Inc., Natick, MA) to a stock solution of 50mM and stored at  $-20^{\circ}\text{C}$ .

### 2.1.3 Cell Lines

Cells lines were fingerprinted in 2011 with the Promega<sup>®</sup> Cell ID System (Promega<sup>®</sup>, Madison, WI). The following cell lines were used (Tab. 2.4):

TABLE 2.4: Description of Cell Lines

Cell line	Medium	Description
93VU-147T	DMEM	58-year-old male; mouth base carcinoma
BB-49	IMDM	70-year-old female
Detroit562	DMEM	pharynx metastatic site (pleural effusion)
FaDu	EMEM	56-year-old male; hypopharynx
HCC1937	RPMI1640	23-year-old female; primary ductal carcinoma
HN4	DMEM	male; T2N0M0
HN5	DMEM	73-year-old male; oral cavity (tongue)
H103	DME-F12	32-year-old male; oral cavity (tongue)
JSQ3	DME-F12	nasal vestibule T3N0M0
SAS	DMEM	oral cavity (tongue)
SCC-61	DME-F12	oral cavity (tongue)
UACC-3199	RPMI1640	mammary gland metastatic site (axillary lymph node)

The BRCA1-mutated (5382insC) [79] breast cancer cell line HCC1937 and the BRCA-methylated [80] cell line UACC-3199 were kindly provided by Prof. Olufumnilayo Olopade (University of Chicago). For remaining origins of cell lines, see Tab. 2.5. The media were obtained from cellgro<sup>®</sup> (DMEM #10-013-CV), Hyclone<sup>™</sup> (DME-F12 #SH30023FS, IMDM #30228FS and RPMI1640 #30027FS) and ATCC (EMEM #302003). All media were supplemented with 10% FBS (Benchmark #0318726), 2mM L-Glutamine (Hyclone<sup>™</sup> #SH3003401), 100 U/ml penicillin and 100 g/ml streptomycin (cellgro<sup>®</sup> #30-002-CI). The RPMI1640 medium was additionally supplemented with 1% HEPES (Sigma Aldrich<sup>®</sup>). All cell lines were confirmed as mycoplasma-free by regular testing (Mycoplasma Alert Detection Kit, Lonza #LT07-118). All experiments were carried out within ten cell passages.

TABLE 2.5: Origin of Cell lines

Cell line	Source
93VU-147T	VU University Medical Center, Amsterdam, Netherlands
BB-49	Ludwig Institute for Cancer Research Brussels, Belgium
Detroit562	American Type Culture Collection (ATCC)
FaDu	ATCC
HCC1937	Prof. Olopade (University of Chicago)
HN4	Dr. Silvio Gutkind, NIDCR, Rockville, MD, USA
HN5	Ludwig Institute for Cancer Research, Oxford, UK
H103	European Collection of Cell Cultures (ECACC), UK
JSQ3	Prof. Weichselbaum (University of Chicago)
SAS	ATCC
SCC-61	Prof. Lingen (University of Chicago)
UACC-3199	Prof. Olopade (University of Chicago)



### 2.1.4 Antibodies

The following primary antibodies were used:

TABLE 2.6: Primary Antibodies

Antibody	Specificity	Application	Dilution	Company
$\gamma$ H2AX (Ser139)	ms mAb	ICC	1:200	EMD Millipore <sup>®</sup>
RAD51 (Ab-1)	rb pAb	WB/ICC	1:2500/1:200	Calbiochem <sup>®</sup>
Actin	ms mAb	WB	1:1000	Cell Signalling <sup>®</sup>

The following secondary antibodies were used:

TABLE 2.7: Secondary Antibodies

Antibody	Specificity	Application	Dilution	Company
anti-ms	donkey pAb	WB	1:20000	Licor <sup>®</sup>
anti-ms	Alexa Fluor546 <sup>®</sup>	ICC	1:200	Molecular Probes <sup>®</sup>
anti-rb	goat pAb	WB	1:20000	Licor <sup>®</sup>
anti-rb	Alexa Fluor488 <sup>®</sup>	ICC	1:100	Molecular Probes <sup>®</sup>

## 2.2 Methods

### 2.2.1 Cell Culture

All cell lines were maintained in 10mm dishes at 37°C in a humidified atmosphere with 5% CO<sub>2</sub>. Medium changes were performed regularly by aspirating the medium, washing twice with pre-warmed phosphor-buffered-saline (PBS) and adding 10ml fresh medium. For subcultures, cells were detached with 1ml trypsin/EDTA for 3-10 mins before inhibiting the detaching reaction by adding fresh medium. The cells were pelleted in a centrifuge for 5 mins at 200 × *g* and 4°C. Cells were re-suspended and split 1:3 to 1:10 depending on the doubling time of the cell line and transferred to new cell culture dishes. Cells were kept in appropriate medium (see above) supplemented with 10% FBS, 100 I.U./ml penicillin-streptomycin and 2mM L-glutamine. Detailed information about the media and origin of the cell lines can be reviewed in Table 2.4 and Table 2.5. To allow working within ten cell passages, cryoconservation was performed as follows: After detachment, cells were re-suspended in freezing medium containing 70% FBS, 20% medium and 10% DMSO. 1 × 10<sup>6</sup> cells were transferred to a cryo tube. Gentle freezing was achieved by keeping the cells for 2-4 h at −20°C, then transferring them to −80°C overnight and finally storing them in liquid N<sub>2</sub>. Cell counting was performed with a Neubauer counting chamber.

### 2.2.2 Resazurin Viability Assay

To assess and compare viability of HNC cell lines in response to three different PARP inhibitors, we performed a resazurin viability assay (also known as Alamar Blue<sup>®</sup>). Resazurin (7-Hydroxy-3H-phenoxazin-3-one 10-oxide) is a redox dye that is reduced to resorufin by mitochondria oxidoreductases, resulting in a color change from blue to fluorescent pink [81].

1000-3000 cells were seeded into 96-well-plates and allowed to attach overnight. The outer wells of the plate were not used for viability testing as too much variation occurred in these wells. Cells were exposed to 0.01 $\mu$ M-50 $\mu$ M veliparib, olaparib or rucaparib or 0.1% DMSO (according to the highest inhibitor concentration) as vehicle control. The plates were rotated by 90° every day to allow even incubation. After three days, resazurin-dye (7.5mg in 50ml *dd*H<sub>2</sub>O, diluted 1:10) was added for 4 h. Finally, fluorescence was measured at 530nm excitation and 590nm emission.

Viability was then calculated as percentage of growth in relation to the control. Triplicate values at each concentration were acquired, averaged and normalized to the control and expressed as percentage of viable cells compared to the DMSO control. Each experiment was performed at least three times independently. Mean values and standard errors were calculated from the independent runs. The area under the curve (AUC) was calculated by the GraphPad Prism<sup>®</sup> Software.

### 2.2.3 Colony-Forming (Clonogenic) Assay

Exponentially growing cells were seeded into 6-well-plates (1000 to 6000 cells per well depending on the doubling time) and allowed to attach overnight. The cells were treated with a range of 0.01 $\mu$ M to 50 $\mu$ M rucaparib or 0.1% DMSO serving as the control in 2ml of medium per well. After 24 h of incubation, the cells were washed twice with PBS and fresh medium was added. The assay was terminated after six to eight days by rinsing with 0.85% NaCl and staining with crystal violet (10g crystal violet, 250ml 95% EtOH, 250ml H<sub>2</sub>O) for 20 mins at room temperature (RT). The 6-well-plates were scanned for analysis with ImageJ. Colonies were counted and normalized to the control. The analysis path, as well as examples for plate scans can be reviewed in Appendix B and E, respectively. At least three independent experiments were performed. The relative IC<sub>50</sub> (halfmaximal inhibitory concentration) was determined using the GraphPad Prism<sup>®</sup> Software. Therefore, raw data was entered, log-transformed, normalized and fitted to a non-linear regression.

### 2.2.4 Syto60<sup>®</sup> Viability Assay

The breast cancer cell lines HCC1937 and UACC-3199 showed poor colony-forming abilities (see Appendix E). In order to compare IC<sub>50</sub> values for rucaparib to our HNC cell lines, we performed the Syto60<sup>®</sup> assay that uses DNA-staining to determine viability.

In a 96-well-plate 300 to 800 cells per well were seeded and allowed to attach overnight. The cells were treated with 0.5 $\mu$ M to 50 $\mu$ M rucaparib or 0.1 % DMSO and incubated for six days. The plates were rotated by 90° every day. Subsequently, the medium was aspirated and the cells were fixed with 150 $\mu$ l per well 4% Para-Formaldehyde (PFA) for 20 mins at RT. To permeabilize the cells they were exposed to 200 $\mu$ l of 0.1% Triton (200ml PBS + 200 $\mu$ l Triton X-100) four times for 5 mins each. After washing twice with PBS-Tween<sup>®</sup> (PBS-T; 200ml PBS + 200 $\mu$ l Tween<sup>®</sup>) for 5 mins, staining was performed using the Syto60<sup>®</sup> Red Fluorescent Nucleic Acid Dye diluted 1:10000 in blocking buffer. 50 $\mu$ l of dye per well was added and 1 h of incubation was allowed at RT protected from light. Afterwards, cells were washed twice for 5 mins with PBS-T, before the 96-well-plate was blotted against paper towels to remove all liquid and finally images were acquired with the Odyssey<sup>®</sup>-scanner and -software. Fluorescence values were normalized to vehicle control.

### 2.2.5 Western Blotting

#### 2.2.5.1 Drug Treatment and Lysate Acquisition

Cells were treated with 10 $\mu$ M rucaparib or 0.05% DMSO for 24 h. For preparation of lysates, cells were washed twice with ice-cold PBS and lysed with 80 $\mu$ l RIPA-buffer, containing 1X Halt Phosphatase Inhibitor Cocktail and 1X Protease Inhibitor Cocktail Set and incubated for 5 mins on ice. Cells were scraped off and transferred into an Eppendorf tube. After thoroughly vortexing the suspension, cells were kept on ice at 4°C for 30 mins before centrifugation at 15000  $\times g$  for 20 mins at 4°C. Supernatants were transferred to new tubes and stored at -80°C for further usage.

#### 2.2.5.2 Protein Determination

To evaluate the protein concentration in lysates, the Bio-Rad Protein Assay was used, which is based on the Bradford method [82]. The binding of protein to Coomassie Brilliant Blue G-250 causes the dye to shift color from red to blue and from an absorption maximum of 465nm to 595nm. It is a fast, stable and reproducible assay [82]. A standard

curve with BSA was prepared and used to align and calculate the protein concentration of the samples.

The Bio-Rad dye was diluted 1:10 in *dd*H<sub>2</sub>O before use. For every sample and every standard 900 $\mu$ l *dd*H<sub>2</sub>O and 100 $\mu$ l dye were mixed in an Eppendorf tube. 2 $\mu$ l of sample-lysate or BSA (equal to concentrations ranging from 2 $\mu$ g/ml to 32 $\mu$ g/ml) was added. Tubes were vortexed and left at RT for 5 mins before triplicates were pipetted into a 96-well-plate for subsequent measuring of absorbance at 595nm with a spectrophotometer.

### **2.2.5.3 Sample Preparation**

For electrophoresis and subsequent Western Blotting, the lysates were prepared in Laemmli-buffer as loading dye. First, the buffer was supplemented with  $\beta$ -Mercaptoethanol that is used to break disulfide bonds of proteins. Samples were diluted in *dd*H<sub>2</sub>O to reach a concentration of 50 $\mu$ g and mixed with 4X Laemmli-buffer in an Eppendorf tube. The tubes were heated to 95°C for 5 mins to denature the proteins, quickly vortexed and spun down before loading.

### **2.2.5.4 SDS-PAGE**

In order to separate the proteins of the lysate, Sodium Dodecyl Sulfate-Polyacrylamide Gel Electrophoresis (SDS-PAGE) was performed. The protein's mobility on the gel is a function of its conformation, charge and molecular weight. To ensure the separation of proteins solely according to their molecular weight, proteins were denatured (with heat) and invariably negatively charged through exposure to SDS. SDS is an anionic detergent that binds to hydrophobic domains of proteins leading to the negative charging of proteins according to their size.

The gel used for electrophoresis was supplemented with TEMED and APS to catalyze the polymerization reaction. For one gel, 15ml Next Gel Solution, 45 $\mu$ l APS and 4.5 $\mu$ l TEMED were mixed and immediately poured between a 1mm spacer plate and a small plate and a comb with ten wells was inserted instantly. The gel was left at RT to polymerize for 1 h and then either immediately used for SDS-PAGE or stored overnight at 4°C wrapped in wet clothes.

After clamping the gel into an electrophoresis chamber and filling it with running buffer, the wells were rinsed several times with a syringe before loading 30 $\mu$ l of sample containing 50 $\mu$ g protein and a protein ladder indicating molecular weight sizes. Electrophoresis was run at 120V for 70-90 mins until the loading dye had run off the gel.

### 2.2.5.5 Western Blot and Analysis

After separating the proteins according to their size, they were transferred from the gel to a nitrocellulose membrane by electro-blotting using the Wet Blot system Genie Blotter. The gel was removed from its glass cage and put onto a filter upon sponges in the blot system. The appropriately cut and pre-soaked membrane was positioned directly on top of the gel, later allowing the proteins to pass to the gel with the electrical current towards the anode. Another filter and sponges were added, carefully avoiding air bubbles, as air does not allow electrical current. The system was filled with sufficient blotting buffer and connected to the current circuit. The blot was run at 12V for 1 h.

Subsequently, the system was dissembled and the membrane was incubated with blocking buffer to block unspecific binding spots for 1 h at RT on a shaker. After blocking, the membrane was cut and incubated with various primary antibodies overnight at 4°C in a cold room or alternatively for 2 h at RT. Following washing with PBS-T three times for 5 mins, the membrane was exposed to the matching secondary antibody for 1 h at RT. These secondary antibodies were IRDye, infrared dyes to be detected near the infrared spectrum. Primary and secondary antibodies were micro-filtered to be used several times. The membranes were washed again before acquiring pictures with the Odyssey<sup>®</sup> Infrared Imaging System followed by analysis with Image Studio<sup>™</sup> software.

### 2.2.6 Immunofluorescent Staining

When DNA DSB occur, the histone H2AX is rapidly phosphorylated at Ser139 to become  $\gamma$ H2AX (the phosphorylated core histone variant)[83]. The latter can be used as a marker of DNA DSB [84]. Poly-D-Lysine-coated coverslips were dipped in 70% ethanol, placed in 6-well-plates and left under UV-light to disinfect for 1 h. Cells were seeded into the wells and allowed to attach overnight. The wells were treated either with 10 $\mu$ M rucaparib or DMSO or with 2 Gy ionizing radiation (IR). Cells were fixed for 20 mins with 4% PFA, 30 mins after irradiation or 24 h after drug treatment, respectively. Cover slips were washed twice with ice-cold PBS, before a 10-min-incubation with 0.25% Triton X-100 to permeabilize the cells. The coverslips were retrieved from the wells with a syringe and tweezers and placed on the plate-lid covered with laboratory parafilm. A lipophilic marker was used to surround the coverslips. 100 $\mu$ l blocking buffer (120 mmol/l KCl, 20 mmol/l NaCl, 10 mmol/l Tris-HCl, 1 mmol/l EDTA plus 0.1% Triton X-100, 2% BSA, 10% milk powder and 10% goat serum) was applied for 1 h. Anti- $\gamma$ H2AX antibody diluted 1:200 was added and incubated for 1 h. After three subsequent 5-min-washes with 0.1% Triton X-100 the anti-RAD51 antibody was added to the slips, left at RT for 2 h and then transferred to a 4°C cold room for overnight incubation. The antibody

solution was aspirated and the slips were washed three times 5 mins with 0.1% Triton X-100 before subsequent application of Alexa Fluor<sup>®</sup> 546 (1:200) and Alexa Fluor<sup>®</sup> 488 (1:100) for 1 h each with three washes in between. Hoechst Dye 1:2000 was applied for 10 mins to counterstain. Finally, after more washes, the coverslips were mounted with mounting medium onto microscopy slides (cell side facing down) and fixed with nail polish. Cells treated with 2 Gy IR were fixed 30 mins after IR, because after this amount of time most H2AX is phosphorylated to form the detected  $\gamma$ H2AX [83]. Images were taken with a Leica TCS SP2 confocal microscope, 100X magnification and 2X optical zoom for all cell lines but SCC-61. Random pictures were acquired from three cover slips allowing analysis for at least 45 cells per treatment regimen. Secondary antibody controls were prepared for every cell line. Lasers were set at the 2 Gy treatment as positive control and not changed for the other treatments. For every cell line, three independent experiments were performed.

### 2.2.7 Gene Expression Analysis

A gene expression microarray dataset (Agilent Technologies 4x44k and 4x44k v2, Santa Clara, CA) of our HNC cell lines had previously been generated by our group (GEO accession number GSE52088 [85]). We tested for gene-drug associations using Pearson's correlation tests of gene expression levels against log-transformed rucaparib IC<sub>50</sub> values. We controlled for the family-wise error rate using Bonferroni correction and for the false discovery rate using the Benjamini and Hochberg (BH) method (see Appendix C). Gene set analysis was performed using the DAVID (Database for Annotation, Visualization and Integrated Discovery) software v.6.7 [86]. This software uses Gene Ontology (GO) terms (as first introduced by Ashburner et al. in 2000 categorizing genes into the groups "biological process", "molecular function" and "cellular component" [87]) and Uniprot terms (a functional protein database [88]) among others. The software then applies an adaption of Fisher's exact test to determine the probability of genes in a given GO term or Uniprot term to appear in the list of genes entered (in our case the 100 genes most positively or inversely correlated with rucaparib sensitivity) compared to chance. Furthermore, we applied several methods in an effort to construct a gene signature, for example PAM, lasso, ridge and ElasticNet regression, but none of these methods were significant in leave-one-out cross validation testing [89–91]. The microarray dataset was generated by cand. rer. nat. Michaela Keck, Dr. Zhixiang Zuo and Dr. Arun Khattri from the Seiwert laboratory and analyses were performed in collaboration with Dr. Paul Geeleher from the Huang laboratory (University of Chicago).

### 2.2.8 Targeted Sequencing

The Seiwert laboratory had previously performed targeted sequencing on 56 HNC cell lines. For a detailed method description, see [12]. This work was done by cand. rer. nat. Michaela Keck, Dr. Zhixiang Zuo and Dr. Arun Khattri.

### 2.2.9 ImageJ Analysis

#### 2.2.9.1 Colony Counting

To avoid counting bias, we developed a computerized algorithm to evaluate colony-forming assays. The 6-well-plates used for the assays were scanned and images were imported into ImageJ (a software provided by the National Institute of Health (NIH)). A binary picture was created and in each well the numbers of colonies depicting ten or more pixels were counted by the software. Afterwards, the colony counts were normalized to the DMSO control. The analysis pipeline can be reviewed in Appendix B.1.

#### 2.2.9.2 Foci Counting

We here provide a solution to the counting-problems the immunofluorescence assay has been criticized for [92]: For  $\gamma$ H2AX and RAD51 foci counting, the single-color pictures (blue = DAPI, green = RAD51, red =  $\gamma$ H2AX) were imported into ImageJ. A binary (255 or 0) image was created and nuclei were counted. The watershed option to separate nuclei was only used when accurate. An intensity threshold was set for the foci (green = 80, red = 60) and foci were counted by the software. By overlaying both, the binary nuclei picture and each of the foci count pictures, the raw intensity per nucleus was calculated by the software. Subsequently, the raw intensity was divided by 255 to calculate the number of foci per nucleus. To accelerate and automate this process, we created a Macro that can be reviewed in Appendix B.2. The average number of foci per nucleus was determined and log-transformed for comparison of sensitive and resistant groups.

### 2.2.10 Statistical Analysis

For PARPi comparison, repeated measures ANOVA was performed using R. The clear outlier (SCC-61) in the rucaparib-treated group was omitted. Analyses of the foci-counts from immunofluorescence experiments were performed in Microsoft Excel 2010 and R. Spearman's rank correlation test for comparison of the different viability assays used in

this study was performed using R (see Appendix C for details). For comparison of foci formation changes within the cell lines, raw count data was analyzed using a generalized linear model (the `glm()` function in R) with a Poisson error-distribution. Details can be reviewed in Appedix C. While count data is often log-transformed to satisfy parametric test assumptions, it has been shown that this generalized linear model approach is more accurate [93]. For the comparison of foci formation of rucaparib-sensitive and rucaparib-resistant groups, we used median log-values of the change in average number of foci per cell and one-tailed t-tests. In both analyses technical replicates were summarized by their median as this is more robust to outliers given the small number of samples.



## Chapter 3

# Results

### 3.1 BRCA Alterations in Head and Neck Cancer

Because mutations in the BRCA genes in HNC have not been described, our first goal was to investigate the BRCA mutational status of the HNC cell lines chosen by us for this study and furthermore in the HNC tumor sample cohort from The Cancer Genome Atlas (TCGA). We investigated variations in the BRCA genes using previously performed targeted sequencing data of the HNC cell lines [12]. We detected possible somatic mutations in four of the ten cell lines and queried the COSMIC database [94] to compare the variations to mutations described in the database. Only the BRCA2 variation **c.53G>A** (Tab. 3.1 highlighted in bold) of the HNC cell line SAS had already been described as a missense mutation in malignancies of the central nervous system [95], although classified as non-pathogenic and of no clinical relevance [96]. We hypothesized that the possible mutations in the other cell lines are likely to be passenger mutations, because they were not listed in the COSMIC database.

Cell line	BRCA1	BRCA2
93VU-147T		c.262C>A
		c.5043G>T
		c.908C>A
		c.2899C>A
		c.3578C>A
HN5		c.5250C>A
		c.908C>A
SAS		c.8686C>A
	c.3467G>T	<b>c.G53G&gt;A</b>
SCC-61		c.2350A>G
	c.4023G>T	c.5744C>T
	c.1326G>T	c.6917C>A

TABLE 3.1: BRCA1/2 Variations in HNC Cell Lines

Listed are the BRCA1/2 variations found in four out of ten tested cell lines. The alteration highlighted in bold has been described elsewhere. Standard mutation nomenclature is used where coding DNA reference sequence is abbreviated as c. followed by the nucleotide number and the base exchange.

Furthermore, we investigated the BRCA mutational status of the HNC tumor samples in the publicly available cohort from TCGA. Somatic BRCA variants were identified for 3%-4% of cases for both, BRCA1 and BRCA2 (Fig. 3.1). We concluded, that HNC cell lines are not commonly mutated in the BRCA genes. Of note, the functional impact on homologous recombination deficiency (HRD) has not been investigated in HNC [97, 98].

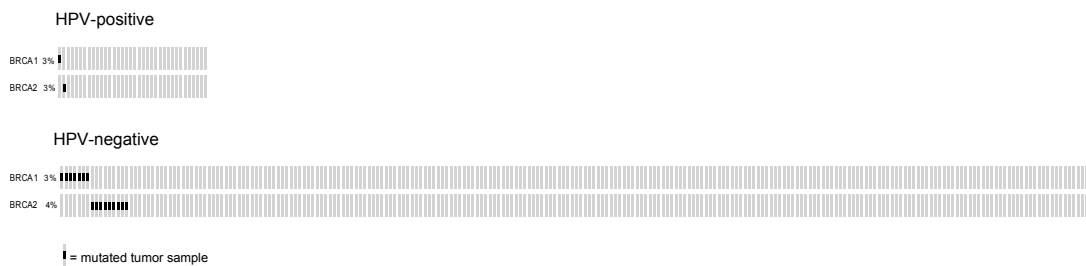


FIGURE 3.1: Oncoprint of BRCA mutations in TCGA HNC cohort  
36 HPV-positive and 243 HPV-negative tumor samples are shown. While BRCA mutations are rare in HNC, they do occur in approximately 6% of tumor samples. Data downloaded and oncoprint adjusted from TCGA.

### 3.2 Comparison of Three PARPi in HNC Cell Lines

To determine the comparative potency of PARPi in HNC, we performed three-day resazurin assays on six HNC cell lines evaluating the compounds veliparib, olaparib and rucaparib (all compounds are currently examined in clinical trials for patients with solid tumors [99])(Fig. 3.2).

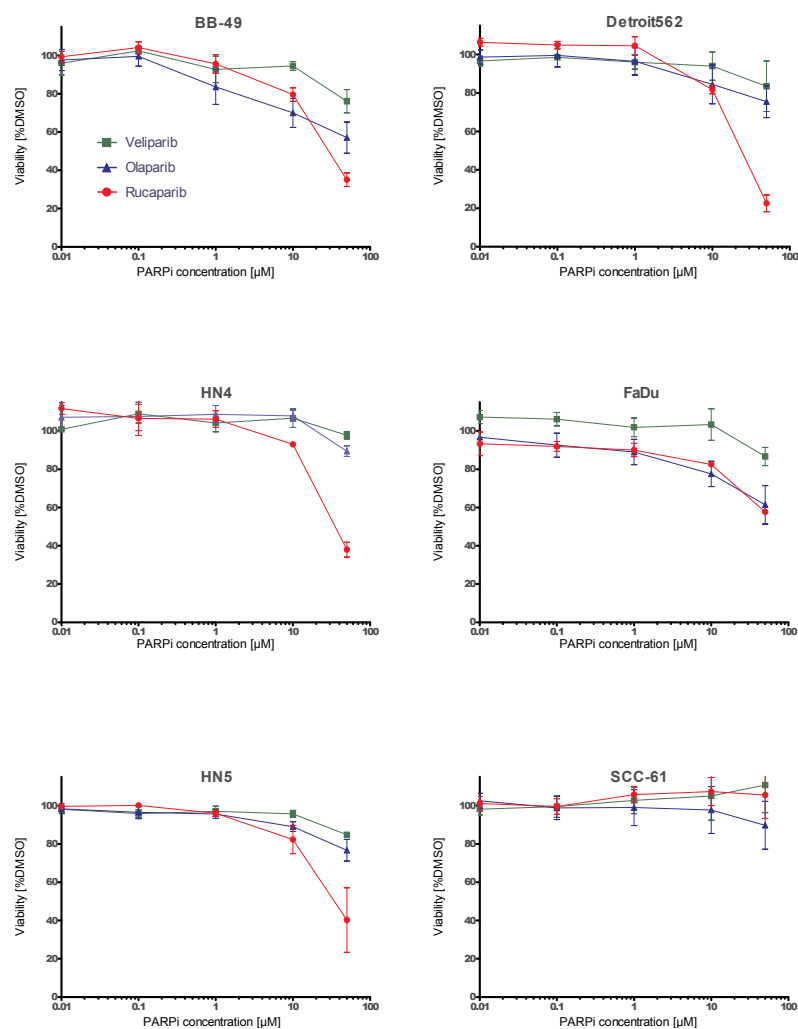


FIGURE 3.2: Survival curves of six HNC cell lines exposed to PARPi. Three-day resazurin assay. Cells were exposed to 0.01  $\mu\text{M}$  to 50  $\mu\text{M}$  veliparib (green), olaparib (blue) or rucaparib (red). Results shown are means  $\pm$ SEM of three independent sets of experiments.

Consistent with prior reports, the standard three-day assay did not allow enough time for the PARPi to unfold their full effect and induce cell death permitting the calculation of robust  $IC_{50}$  values [100] (Fig. 3.2). Therefore, we compared the area under the curve (AUC) for the three compounds (Fig. 3.3). Veliparib, a non-locking PARPi [57], showed only minimal effects on viability even at a drug concentration of  $50\mu M$ . By contrast, olaparib and rucaparib showed a significantly greater effect ( $P = 0.02$  and  $P = 9.8 \times 10^{-5}$ ) compared to veliparib. Rucaparib impaired cell viability significantly more than olaparib ( $P = 0.02$ ). There was also a highly significant difference in PARPi potency when all three drugs were compared ( $P = 6.3 \times 10^{-5}$  from repeated measures ANOVA model comparing the mean of the three groups). When performing Spearman's rank correlation test, we saw that all three drug responses were positively correlated, reinforcing the assumption that some cell lines are more prone to PARPi susceptibility than others (veliparib-olaparib:  $r_S = 0.77$   $P = 0.05$ ; veliparib-rucaparib:  $r_S = 0.89$   $P = 0.02$ ; olaparib-rucaparib:  $r_S = 0.43$   $P = 0.21$ ; from one-sided Spearman's correlation tests. See Appendix C for details). However, the the shortcomings of the assay outlined above prompted us to find an assay to establish more robust  $IC_{50}$  values.

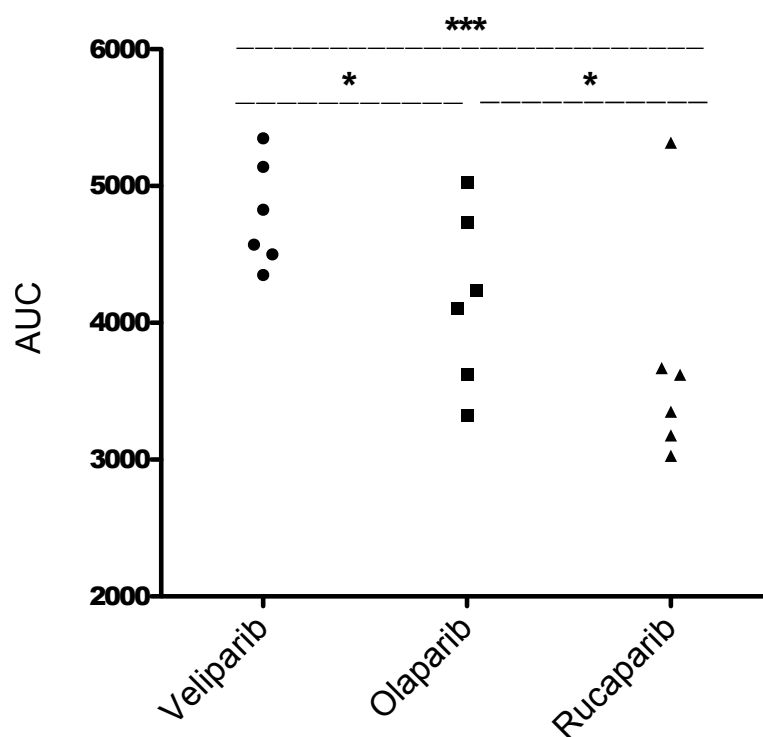


FIGURE 3.3: Comparison of three PARPi  
 Comparison of three PARPi using AUC values for six HNC cell lines. \*  $P \leq 0.05$   
 \*\*\*  $P \leq 0.001$  from repeated measures ANOVA model

### 3.3 Establishment of Robust $IC_{50}$ Values for Rucaparib

Hence, we examined the potency of the most promising agent rucaparib in the cell lines used previously as well as in another four cell lines to increase the sample size. We now performed a more stringent method to establish robust  $IC_{50}$  values. The colony-forming assay was chosen, because a longer time period (six to eight days as opposed to three days in the resazurin assay) is allowed for cells to suffer endogenous or exogenous DNA damage and therefore for the DNA repair targeting PARPi to unfold its effect. An example of plates for a sensitive and a resistant cell line can be reviewed in Appendix E. We found very large variability in drug susceptibility among the ten tested cell lines and categorized them as “sensitive” ( $IC_{50} < 2\mu\text{M}$ , similar to prior reports [101]) or “resistant” (Fig. 3.4).

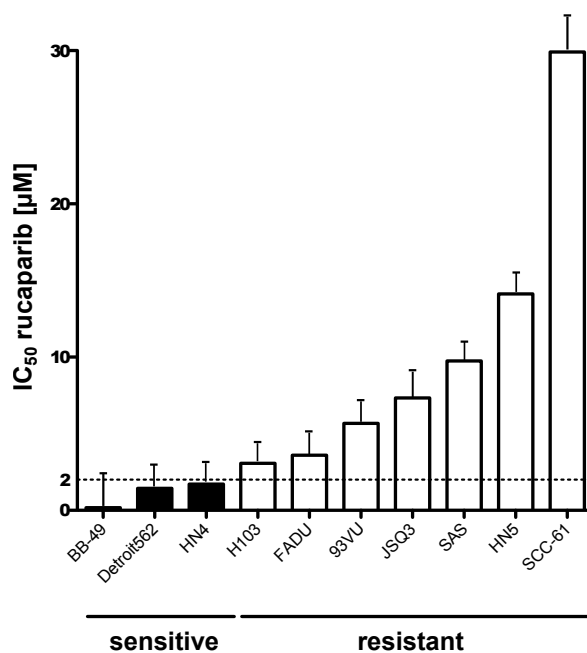


FIGURE 3.4: HNC cell lines respond to rucaparib

Six- to eight-day colony-forming assays were performed on ten HNC cell lines using five rucaparib concentrations ranging from  $0.1\mu\text{M}$  to  $50\mu\text{M}$ .  $IC_{50}$  values were calculated by GraphPad Prism<sup>®</sup> software  $\pm$ SEM. Black: Rucaparib-sensitive cell lines with  $IC_{50} < 2\mu\text{M}$  as previously proposed [101]. Cutoff indicated by a dashed line. White: Resistant cell lines.

Of note, the only HNC cell line harboring a known BRCA2 missense mutation, SAS, was not particularly sensitive to rucaparib and was therefore placed in the “resistant” group (Tab. 3.1 and Fig. 3.4). Encouragingly, the Spearman’s rank correlation between the resazurin assay and the colony-forming assay for the six cell lines used in both assays was  $r_S = 0.77$  ( $P = 0.05$  from one-sided t-test) showing consistency across assays.

### 3.4 Comparison to BRCA-deficient Breast Cancer

After having found three rucaparib-sensitive HNC cell lines, we sought to put these results into perspective by comparing the sensitivity to cell lines that have already shown to be sensitive to rucaparib. Because PARPi have proven to be beneficial for patients with BRCA-deficient breast cancer (BC) [63, 64], we compared our sensitive HNC cell lines to the BC cell line HCC1937, that harbors an inactivating BRCA mutation and UACC-3199, which is BRCA-deficient due to epigenetic silencing. Because of poor colony-forming abilities of the BC cell lines (see Appendix E), we performed the six-day viability assay Syto60<sup>®</sup> to compare rucaparib-susceptibility (Fig. 3.5).

As this is a DNA-based rapid viability assay, the absolute IC<sub>50</sub> values differed from those established with colony-forming assays and resazurin staining, yet the ranking of the three HNC cell lines remained consistent (resazurin assay - Syto60<sup>®</sup>  $r_S = 1$  ; colony-forming assay - Syto60<sup>®</sup>  $r_S = 0.5$ ). Strikingly, the HNC cell lines that were categorized as sensitive (BB-49, Detroit562 and HN4) were notably more susceptible to rucaparib (IC<sub>50</sub> values: 4.4 $\mu$ M, 7.0 $\mu$ M and 9.1 $\mu$ M, respectively) than the BRCA-mutated BC cell line HCC1937 (IC<sub>50</sub> value: 13.1 $\mu$ M). The response of UACC-3199, a cell line that has recently been found to be sensitive to rucaparib [102], was comparable to the response of sensitive HNC cell lines (IC<sub>50</sub> value: 6.4 $\mu$ M)(Fig. 3.5). This strongly suggests, that there is a subset of HNC cell lines susceptible to PARPi, possibly due to HRD.

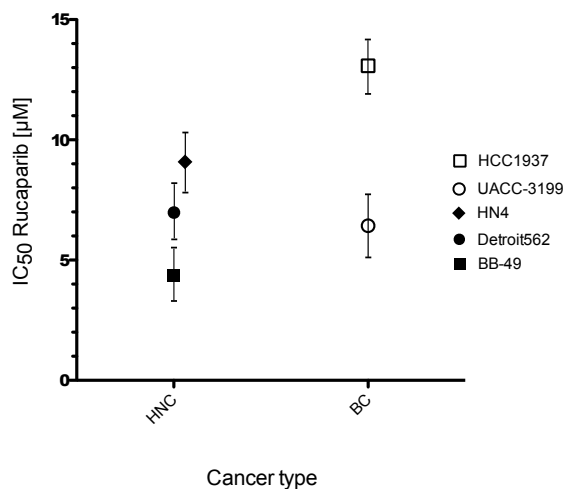


FIGURE 3.5: Comparison of PARPi Sensitivity in HNC to Breast Cancer  
Six-day Syto60<sup>®</sup> viability assays were performed on the three most sensitive HNC cell lines and on the BRCA-mutated breast cancer (BC) cell line HCC1937 and the BRCA-methylated BC cell line UACC-3199. IC<sub>50</sub> values are shown  $\pm$ SEM. The sensitive HNC cell lines show similar responses as UACC-3199. HCC1937 is resistant to rucaparib despite its mutational status.

## 3.5 Predicting Sensitivity

### 3.5.1 Estimating HR Competency by RAD51 Formation Assay

To study the HR competency of HNC cell lines and to investigate possible prediction methods, we employed a HR assay developed by Mukhopadhyay and colleagues for rucaparib response prediction in ovarian cancer cell lines [103]. The group reported a positive predictive value of 93% and a negative predictive value of 100% for rucaparib sensitivity using post-treatment immunofluorescent staining of the HR marker RAD51 [104].

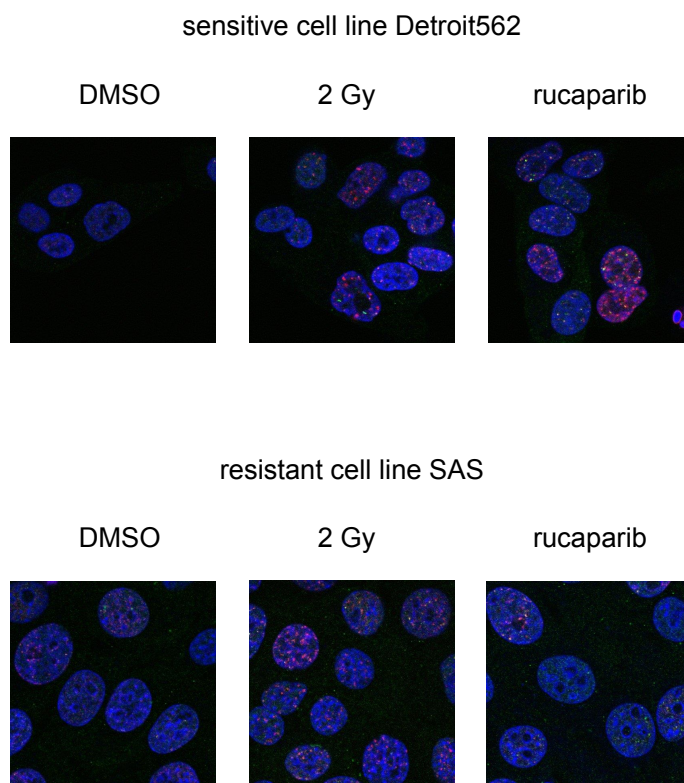


FIGURE 3.6: Immunofluorescence Images for RAD51 Formation Assay

Three sensitive and three resistant cell lines were treated for 24 h with 0.02% DMSO (negative control) or 10 $\mu$ M rucaparib. Serving as positive control were cells fixed 30 mins after exposure to 2 Gy IR. Image acquisition was performed with a confocal microscope (Leica TCS SP2) using the 100X objective and a 2X optical zoom and oil immersion. Red:  $\gamma$ H2AX foci. Green: RAD51 foci. Fluorescence microscopy images of DAPI-stained **A** rucaparib-sensitive (Detroit562) and **B** rucaparib-resistant (SAS)

HNC cell lines treated with DMSO, 2Gy or 10 $\mu$ M rucaparib for 24 h.

We applied this assay to three sensitive (BB-49, Detroit562 and HN4) and three resistant (HN5, SAS and SCC-61) HNC cell lines as categorized by the IC<sub>50</sub> cutoff discussed above (Fig. 3.4). Staining was additionally conducted for the DNA DSB marker  $\gamma$ H2AX.

As a positive control, we added a 2 Gy IR treatment regimen. DMSO-treated cells served as negative control. As illustrated in Figure 3.6, we saw increases in  $\gamma$ H2AX foci formation in the 2 Gy treated cells and a varying response between rucaparib-sensitive and rucaparib-resistant cell lines in the rucaparib treatment regimen. However, the RAD51 foci formation did not serve as a post-treatment biomarker for sensitivity to the PARPi rucaparib. Results of the automated foci counts for both,  $\gamma$ H2AX and RAD51, are discussed in detail for each treatment regimen in the next sections.

### 3.5.1.1 RAD51 Foci Formation

**2 Gy Treatment Regimen** Given the findings of Mukhopadhyay et. al we hypothesized that we would see no increase in RAD51 foci formation in rucaparib-sensitive cell lines and an increase of the same in rucaparib-resistant cell lines. For treatment with positive control (2 Gy IR), we found this to be the case. In sensitive cell lines, the median foci formation decreased (BB-49: -33.2%  $P = 4.5 \times 10^{-4}$ , Detroit562: -12.8% n.s., HN4: -57.2%  $P = 2.7 \times 10^{-3}$ ). Conversely, RAD51 foci formation in resistant cell lines by trend increased after exposure to 2 Gy IR (HN5: +10.4% n.s., SAS: +10.3% n.s., SCC-61: +68.3% n.s.), although results did not yield statistical significance within cell lines (Fig. 3.7). However, the difference between sensitive and resistant cell line groups regarding their RAD51 foci formation after 2 Gy IR compared to DMSO treatment was significant ( $P = 0.02$ ), which suggests that HR is defective in sensitive cell lines (Fig. 3.8).

**Rucaparib Treatment Regimen** Next we examined the change in RAD51 foci formation after treatment with rucaparib. In some cell lines, treatment with rucaparib induced the RAD51 foci formation, suggesting an intact HR process. In others, the number of RAD51 foci remained constant or decreased as compared to the DMSO control. In these cases, one can assume a defective HR pathway and Mukhopadhyay et al. accurately predicted the susceptibility to rucaparib of cell lines showing this pattern. However, the ability of HNC cells to form RAD51 foci after rucaparib treatment was not associated with sensitivity to rucaparib in our experiments. Median percentage change of RAD51 foci formation in sensitive cell lines ranged between -54.1% and +194.3%. Similarly, resistant cell lines responded variably with a range of -31.1% to +18.6% of median percentage foci formation change after rucaparib treatment (Fig. 3.7). The difference between the groups was therefore not significant ( $P = 0.47$ ) (Fig. 3.8).



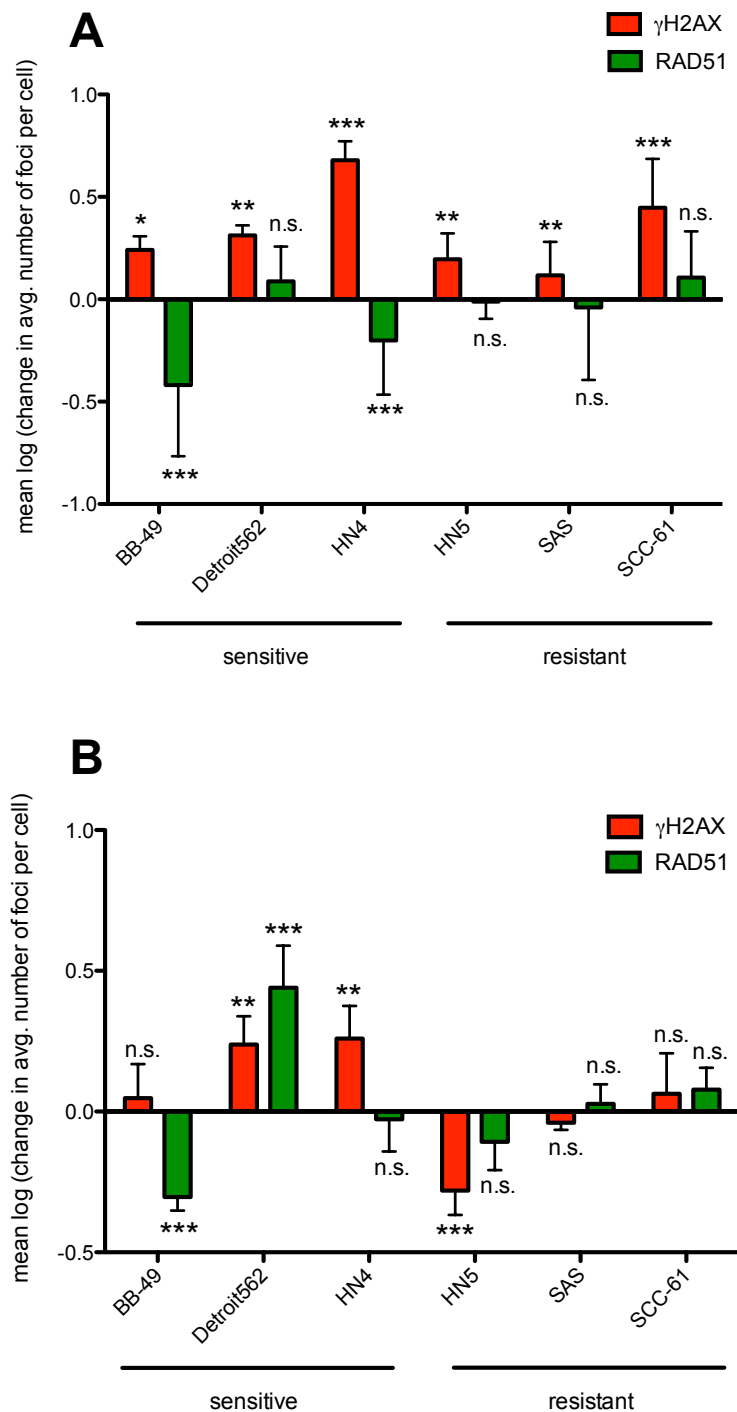


FIGURE 3.7: Changes of foci formation within cell lines  
 Shown are log-transformed means of change in avg. number of foci per cell  $\pm$ SEM. Asterisks are indicating the level of statistical significance using the poisson distribution with \*  $P \leq 0.05$ , \*\*  $P \leq 0.01$  and \*\*\*  $P \leq 0.001$ . **A** Foci formation change after treatment with 2 Gy IR **B** Foci formation change after treatment with rucaparib.

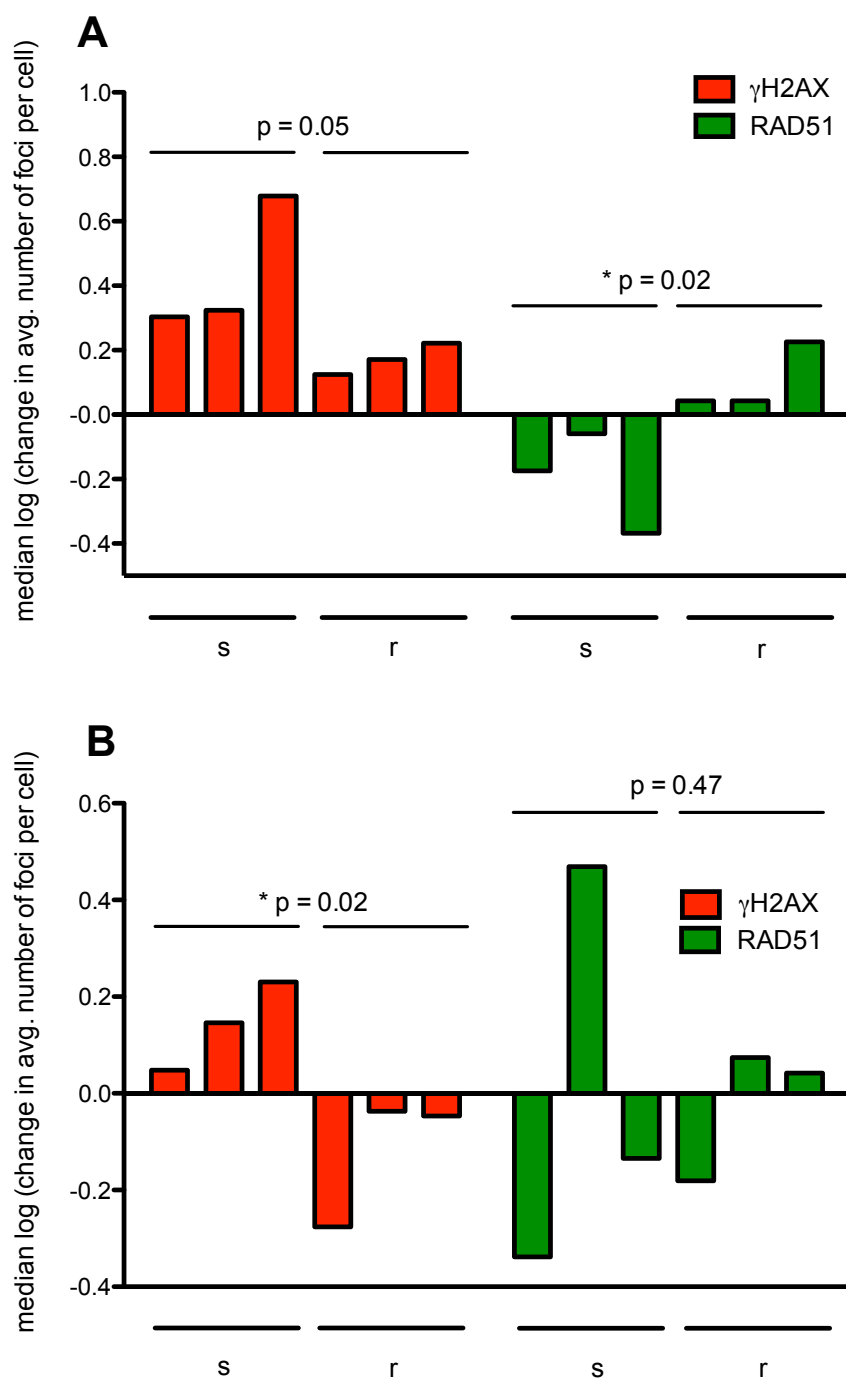


FIGURE 3.8: Comparison of sensitive (s) vs. resistant (r) cell lines for foci formation. Median values are shown of log-transformed changes in average number of foci per cell. **A** Changes in foci formation after treatment with 2 Gy IR. **B** Changes in foci formation after treatment with rucaparib.

Because we were unable to reproduce the impressive predictive values of the assay proposed by Mukhopadhyay et al., we further validated our findings by performing Western Blots, comparing RAD51 protein level before and after rucaparib treatment. Again, RAD51 level change did not coincide with sensitivity, consistent with the results generated by the immunofluorescence assay (Fig. 3.9). While the RAD51 level decreased in the sensitive cell line BB-49 after rucaparib treatment, this trend was not seen in the other two sensitive cell lines.

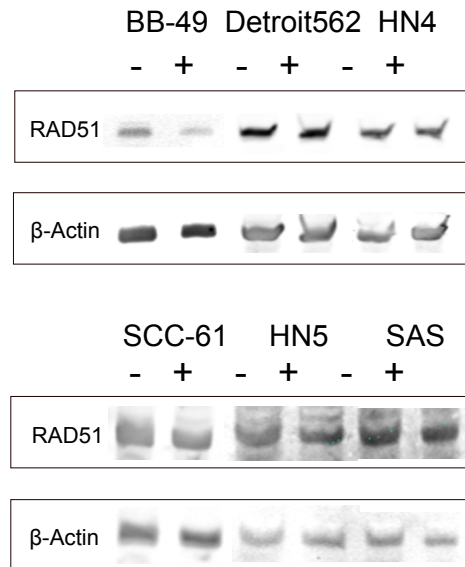


FIGURE 3.9: Protein level assessment of RAD51 after rucaparib treatment  
Immunoblot of RAD51 for three sensitive and three resistant cell lines after treatment with  $10\mu\text{M}$  rucaparib for 24 h (+) compared to DMSO control (-).  $\beta$ -Actin was used as loading control. Results are consistent with foci counts after immunofluorescent staining.

### 3.5.1.2 $\gamma\text{H2AX}$ Foci Formation

**2 Gy Treatment Regimen** As anticipated, the treatment with 2 Gy IR resulted in an increase of  $\gamma\text{H2AX}$ -marked DNA DSB across all cell lines. The median percentage gain of average number of foci per nucleus ranged between +101.2% and +377.4% for rucaparib-sensitive cell lines and between +33.3% and +66.6% for rucaparib-resistant cell lines (Fig. 3.7). The difference between the 2 Gy- and the DMSO-treatment regimen in  $\gamma\text{H2AX}$  foci formation was of statistical significance across all cell lines (Fig. 3.7: BB-49:  $P = 0.03$ , Detroit562:  $P = 1.0 \times 10^{-3}$ , HN4:  $P = 1.8 \times 10^{-7}$ , HN5:  $P = 0.02$ , SAS:  $P = 0.03$ , SCC-61:  $P = 2.7 \times 10^{-6}$ ). Of note, the sensitive cell lines showed a higher increase of DNA DSB after exposure to 2 Gy IR compared to resistant cell lines (Fig. 3.8:  $P = 0.05$ ).

**Rucaparib Treatment Regimen** We hypothesized that the treatment of cells with rucaparib would lead to an increase of  $\gamma$ H2AX foci formation designating DNA DSB in sensitive cell lines and to a constant level of  $\gamma$ H2AX foci formation in resistant cell lines. Indeed, in sensitive cell lines the median percentage gain of average number of foci per nucleus ranged between +11.7% and +70.0% compared to DMSO control. We observed a significant increase of  $\gamma$ H2AX foci formation in two rucaparib-sensitive cell lines (Fig.3.7: Detroit562:  $P = 0.01$ , HN4:  $P = 0.03$ ). However, no statistically significant difference was found in BB-49.

In resistant cell lines,  $\gamma$ H2AX foci formation response was stable in two cell lines and decreased in the third (Fig. 3.7). Interestingly, the difference in DNA DSB formation between sensitive and resistant groups after rucaparib treatment was significant and it was of borderline significance after 2 Gy treatment (Fig. 3.8:  $P = 0.03$  and  $P = 0.05$ ).

Overall, we were able to show that exposure of cells to 2 Gy IR lead to significant increases in  $\gamma$ H2AX foci formation across all cell lines, confirming that the assay is valid. In rucaparib-sensitive cell lines, the formation of  $\gamma$ H2AX foci increased after exposure to rucaparib indicating that DNA DSB were accumulating. Conversely, in rucaparib-resistant cell lines, the  $\gamma$ H2AX foci formation after rucaparib treatment by trend remained constant as exemplified in Figure 3.6. Importantly, the rucaparib-sensitive and -resistant groups showed differences in  $\gamma$ H2AX foci formation both, after treatment with rucaparib and 2 Gy IR. This points towards their differing ability to repair DNA DSB and therefore their susceptibility to PARPi. We investigated this further by analyzing microarray gene expression data of these cell lines.

### 3.5.2 Expression Analysis

A common approach to predict sensitivity is to generate a gene signature based on drug response in a panel of training cell lines, and then to apply this signature to predict the response in out-of-batch sets of samples. Recently, a study identified a 60-gene signature associated with rucaparib sensitivity in familial and sporadic ovarian cancer [105]. The authors used expression data derived from a custom-made microarray designed by the National Cancer Institute that is publicly available [106]. The microarray used for our study measured the expression of only 35 of those 60 genes and we were therefore unable to apply this signature to our dataset. The success and reproducibility of this strategy has been limited for a large variety of reasons [107]. In our case, likewise, it was not possible to generate a reliable gene signature based on the small number of samples (misclassification rate in cross-validation: 36.9% for the gene signature generated with Prediction Analysis for Microarrays (PAM), data not shown). This analysis was conducted in collaboration with Dr. Zhixiang Zuo and Dr. Paul Gleeher.

In cooperation with Dr. Paul Geeleher we subsequently investigated the association of baseline expression of a number of genes thought to be important for HR (e.g. BRCA, EMSY, PTEN) with rucaparib sensitivity. Of these, only RAD51 showed some evidence of an association, with a nominal p-value of 0.04, although this value was not significant after correction for multiple testing. However, we observed a positive correlation ( $r_P = 0.58$ ) between RAD51 baseline expression and rucaparib  $\log(\text{IC}_{50})$  (Fig. 3.10).

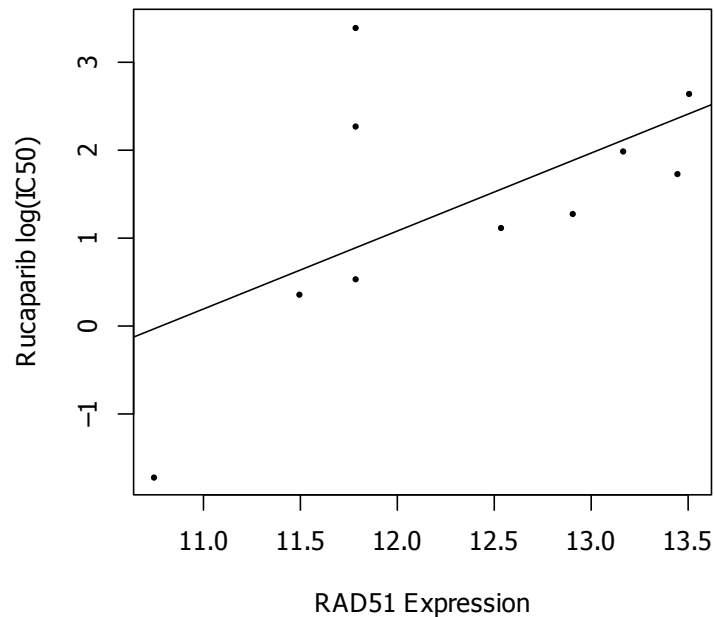


FIGURE 3.10: Baseline RAD51 expression is positively correlated with rucaparib  $\text{IC}_{50}$ . RAD51 baseline expression levels are plotted against rucaparib  $\text{IC}_{50}$  values. The line of best fit (estimated from a linear regression model) is shown. Pearson's  $r_P = 0.58$ ,  $P = 0.04$ .

We also performed correlation tests of rucaparib  $\text{IC}_{50}$  against the 9138 genes measured by microarray (see Methods). This analysis revealed only one gene of borderline significance genome-wide (IL-18) after correction for multiple testing ( $P = 9.9 \times 10^{-6}$ ;  $P_{adj} = 0.09$ ). However, correlations for the top ten genes were high ( $r_P = 0.95$  to  $r_P = 0.81$ ) suggesting that this analysis was underpowered (Tab. 3.2).

Gene name	Pearson's Correlation	p-values	BH
IL-18	0.953	$9.9 \times 10^{-6}$	0.091
NUP62CL	0.890	$2.7 \times 10^{-6}$	0.904
TERF2	0.867	$5.8 \times 10^{-4}$	0.904
PPP1CC	0.849	$9.4 \times 10^{-4}$	0.904
SOCS2	0.838	$1.2 \times 10^{-3}$	0.904
CDK1	0.837	$1.3 \times 10^{-3}$	0.904
ZNF670	0.831	$1.4 \times 10^{-3}$	0.904
C13orf34	0.814	$2.1 \times 10^{-3}$	0.904
TOP2A	0.811	$2.2 \times 10^{-3}$	0.904
KLK8	0.807	$2.4 \times 10^{-3}$	0.904

TABLE 3.2: Whole Genome Expression Correlated to Rucaparib IC<sub>50</sub>  
 Pearsons correlation values and p-values are shown for top ten genes from expression analysis across the whole genome. While correlation with rucaparib sensitivity was high, corrected p-values remained below the level of statistical significance, indicating that this analysis was underpowered. BH = Benjamini and Hochberg.

The low level of enrichment was unsurprising given the small number of samples, thus, we hypothesized that a gene set analysis may improve power to detect genuine biological signal. Hence, we tested for enrichment of Gene Ontology (GO) terms and Uniprot terms among the 100 genes most positively or inversely correlated with rucaparib sensitivity (see Methods and Tab. 3.3).

Category	Term	Count	p-value	BH
GO CC	chromosome	15	$4.6 \times 10^{-8}$	$9.4 \times 10^{-6}$
GO CC	chromosomal part	14	$4.6 \times 10^{-8}$	$4.7 \times 10^{-6}$
GO CC	chromosome, centromeric region	9	$1.8 \times 10^{-7}$	$1.2 \times 10^{-5}$
GO BP	cell cycle	17	$1.0 \times 10^{-5}$	$1.0 \times 10^{-2}$
GO CC	condensed chromosome	6	$1.9 \times 10^{-5}$	$9.6 \times 10^{-4}$
Uniprot	mitosis	8	$3.2 \times 10^{-5}$	$6.1 \times 10^{-3}$
GO CC	kinetochore	6	$4.0 \times 10^{-5}$	$1.6 \times 10^{-3}$
GO CC	condensed chromosome	7	$4.4 \times 10^{-5}$	$1.5 \times 10^{-3}$
GO CC	nuclear pore	6	$4.5 \times 10^{-5}$	$1.3 \times 10^{-3}$
Uniprot	cell division	9	$4.6 \times 10^{-5}$	$4.3 \times 10^{-3}$

TABLE 3.3: Gene terms for chromosomes are correlated with rucaparib resistance  
 Top ten GO and Uniprot terms enriched among genes inversely correlated with rucaparib IC<sub>50</sub>; BH = Benjamini Hochberg; GO = Gene Ontology; CC = cellular component; BP = biological process.

Interestingly, we found that GO terms associated with chromosomal structure were highly significantly enriched among genes that were inversely correlated with rucaparib sensitivity. A list of the 15 genes included in the top hit GO term “chromosome”

---

can be reviewed in Appendix D. Encouragingly, no additional gene sets were identified and this result was strongly consistent with our immunofluorescence data, where we showed that rucaparib-resistant cell lines suffered less DNA DSB after exposure to IR and rucaparib compared to rucaparib-sensitive cell lines (Fig. 3.8). This suggests that there are differences in chromosomal integrity among HNC cell lines that may cause PARPi sensitivity.

# Chapter 4

## Discussion

### 4.1 BRCA Variations in Head and Neck Cancer Cell Lines

In this study, we aimed to evaluate the single agent effect of PARPi in HNC cell lines. Because it has been well established that BRCA-deficient cells are particularly sensitive to these agents due to synthetic lethality, our first goal was to determine whether HNC cell lines harbor any clinically relevant BRCA mutations. We interrogated the publicly available TCGA tumor data as well as existing sequencing data from our cell lines.

Among the 279 head and neck tumor samples in the TCGA cohort, BRCA mutations occurred in 6-7% of samples. In four of our ten cell lines, we found genetic variations in the BRCA genes, only one of which had been described previously. As cancer cells tend to exhibit chromosomal instabilities that lead to a high rate of genetic aberration, it is unsurprising that variations were found in BRCA genes as well. In fact, HNC exhibits a median number of approximately eight somatic mutations per megabase, ranking HNC 9<sup>th</sup> in a panel of 30 malignancies as shown by Alexandrov and colleagues [108].

It therefore seems unlikely that these variations alone contribute to a phenotype that would lead to HRD. We found that the only cell line harboring a known missense mutation (SAS), as well as the the BRCA-mutated breast cancer cell line HCC1937 were rucaparib-resistant. This is consistent with prior reports showing that not all patients with deficiencies in BRCA1 or BRCA2 were PARPi-sensitive [109]. Previous studies have also shown that there are resistance mechanisms to PARPi, including: (a) gain of HR capacity, (b) modified NHEJ capacity, (c) reduced levels of PARP-1 activity or expression, (d) decreased availability of the inhibitor in the cell. For a detailed review see [74]. These mechanisms will need to be investigated in more detail and depth as PARPi enter clinical practice considering that BRCA mutational status alone may not be sufficient to predict responsiveness or resistance to PARPi.



In summary, BRCA mutations are rare but not impossible in HNC. This initial analysis enabled us to attribute any PARPi sensitivity in our cell lines to BRCA mutations and together with the TCGA analysis we were able to draw the broader conclusion that this single existing marker for PARPi sensitivity will most likely not play a role in HNC. It is however probable that not only BRCA mutations, but expression and function of these and other proteins involved in HR may nonetheless lead to the synthetic lethality under PARPi treatment as seen in BRCA-mutated tumors.

## 4.2 PARP Inhibitors in Head and Neck Cancer

The potency of the evaluated PARPi differed significantly in our panel of HNC cell lines. A recent study has shown, that this variability can be attributed at least in part to the inhibitor's ability to form cytotoxic PARP-DNA complexes [57]. Veliparib did not form these complexes in the study, which is in concordance with our finding that veliparib was the least effective PARPi among the agents studied. Rucaparib and olaparib were categorized as locking PARPi by the authors, which was consistent with our results [57, 76]. In the meantime, new PARPi have been developed. Among them is BMN 673, a compound that reportedly exhibits a 100-fold stronger PARP-locking potency compared to the PARPi used in this study. This compound should be investigated for single agent potency in the future [76].

Our results suggest that rucaparib has the largest effect of the studied agents on our HNC cell lines. Interestingly, the determined maximal tolerated dose of the compounds used in current clinical trials are 60mg, 400mg and 360mg for veliparib, olaparib and rucaparib, respectively [110–112]. Together with our results, this suggests that rucaparib is not only the most effective among the tested PARPi, but that it is also comparatively well tolerated by patients, indicating that the role of rucaparib should be further investigated in HNC treatment. Our decision to select rucaparib for the bulk of our analysis stems from the high potency as evidenced by the lowest AUC values in the evaluated HNC cell lines.

A recent publication from the Wellcome Trust Sanger Institute (Cambridge, UK) screened a panel of almost 700 cell lines for sensitivity to 138 compounds, including rucaparib, and correlated results with genetic aberration [100]. 21 HNC cell lines were included in the screening for rucaparib. In this paper, the authors stressed however that a three-day assay was used, which did not allow cells to suffer enough DNA damages for the DNA repair targeting PARPi to unfold its effect. The  $IC_{50}$  values were therefore predominantly estimated from extrapolated data, thus have large associated confidence intervals

and may not be accurate. Hence, given the conclusions of this previous study, we generated more reliable  $IC_{50}$  values for this agent and examined the potency of rucaparib in several HNC cell lines by performing a more suitable method. The colony-forming assay method was chosen due to its longer time period and the unbiased colony counting method that we created for this purpose specifically. The colony-forming assays revealed a profound potency of rucaparib on HNC cell lines showing  $IC_{50}$  values of less than  $2\mu M$  in a subgroup of HNC cell lines, classifying them as “sensitive” as categorized by others [101].

To put our results into perspective with state of the art research, we compared the rucaparib-sensitivity of our HNC cell lines to breast cancer (BC) cell lines deficient in BRCA, because PARPi have proven to be beneficial for patients with BRCA-mutated BC [63]. We found a subset of HNC lines that exhibited similar sensitivity to rucaparib as UACC-3199, a BRCA-methylated BC cell line. Remarkably, it has recently been demonstrated that UACC-3199 is highly sensitive to rucaparib [102]. Furthermore, all of the HNC cell lines tested were much more sensitive to rucaparib than HCC1937, a BRCA-mutated BC cell line. This indicates that non-BRCA-mutant tumors of the head and neck need to be considered in the context of HRD. Consistent with recent findings, this suggests that the therapeutic scope of synthetic lethality of PARPi may be much wider than previously appreciated [63, 113]. On the other hand, these results emphasize again that BRCA mutational status alone may not be sufficient to adequately predict PARPi sensitivity.

In summary, we demonstrated for the first time that despite the sparsity of BRCA mutations, a subset of HNC cell lines was susceptible to the PARPi rucaparib to the same extent as BRCA-deficient BC cell lines. These results need to be replicated in future and sample size needs to be increased as this is arguably a limitation of this study. Nevertheless, this study contains important implications for future investigation of this agent for HNC patients. The next challenge will be to select patients who will benefit from this targeted therapy and we therefore sought to find prediction methods for PARPi susceptibility in cell lines.

### 4.3 Prediction of PARP Inhibitor Susceptibility

It is important to emphasize that not all HNC cell lines were sensitive to PARPi. The variability indicates that patients will also likely exhibit a large variety of responses to these agents, as has already been shown for some other malignancies [63, 74, 114]. It will therefore be crucial to identify biological markers (beyond BRCA as discussed above) that are predictive of drug response.

### 4.3.1 Gene Signature

It is a common approach to generate a gene signature to predict drug response in cell lines, as did Konstantinopoulos et al. for rucaparib response in ovarian cancer cell lines [105]. Of note, this approach has often failed to be of use in the translation to the clinical setting and reproducibility has been limited (as exemplified by our lack of success to reproduce this signature) [107]. However, the value of cell line screening data has recently been shown in a publication that demonstrated that even clinical drug response can in fact be predicted from baseline gene expression. The algorithm uses a model trained on a large panel of cell line drug response leveraging whole-genome information that allows every gene to contribute to the prediction [115]. We therefore hypothesize that a much larger dataset will be needed to generate a signature that can robustly predict rucaparib sensitivity from baseline gene expression levels.

### 4.3.2 Functional RAD51 Assay

In an effort to utilize known synthetic lethal functional interactions (i.e. deficiencies in HR designated by lack of RAD51 foci formation and PARPi treatment), we applied a prediction assay previously proposed by Mukhopadhyay et al. for ovarian cancer cell lines to our HNC cell lines. The authors have proceeded to apply their in vitro results to the clinical setting and reported a significant difference in progression-free survival when comparing HR-competent and HR-deficient primary cell lines as categorized by the above-mentioned assay [103, 116]. While assessing the change in RAD51 foci formation does approximately measure HRD competence, it does not identify the specific gene or protein causing the deficiency upstream of RAD51, which in this case was the rationale for using it as a screening parameter, given the large number of possible disruptions of this DNA repair pathway [92].

#### 4.3.2.1 RAD51

The prediction accuracy of this assay using post-treatment RAD51 foci formation was not recapitulated in HNC. Of note, RAD51 expression is partly cell cycle dependent, possibly leading to false negative results in this assay. Because RAD51 levels are higher in rapidly replicating cells, the accuracy of RAD51 as a HR marker could be imprecise [65]. The other drawback of this approach noted in the literature was the need for a standardized and automated scoring system. We have provided solutions to this issue (see Methods and Appendix B) [92]. Crucially, while our results do not unequivocally prove that the level of RAD51 foci formation is unrelated to variability in rucaparib

response (as exemplified in Fig. 3.10), it strongly suggests that other biomarkers will be necessary to robustly predict drug response in HNC. Novel biomarkers that have been proposed include ATM-mutation, MRE11-mutation, FANCF promotor methylation, PTEN deficiency and PAR levels, although none of them have been validated in clinical trials [57, 117].

We note that although the lack of increased RAD51 foci formation was not predictive of rucaparib sensitivity, we were able to show significant differences in RAD51 foci formation between sensitive and resistant cell lines after exposure to 2 Gy IR (a treatment regimen that was not included in the original assay). This warrants further studies to increase the sample size possibly leading to the development of a new assay for HNC to predict PARPi sensitivity. Together with the DNA DSB assessment discussed below, these findings point towards combination potential with DNA damaging therapeutic options, such as IR or platinating agents (e.g. cisplatin). It has already been shown that PARPi can synergize with IR in vitro and in mouse models in nasopharyngeal carcinoma [118], Ewing's Sarcoma [119], and glioblastoma [114]. One study has confirmed the radiosensitization potential of veliparib in head and neck cancer [117]. Currently, olaparib and veliparib are evaluated in combination with radiation therapy in clinical trials for pancreatic, colorectal and esophageal cancers and we hypothesize that rucaparib could be a candidate agent for a similar trial in HNC [99]. PARP has been proven to play an important role in the initiation NHEJ, the repair mechanism that is used predominantly by cells to repair IR-induced DNA DSB [120]. This makes PARP an ideal target for radiosensitization and although momentarily speculative, our results suggest that rucaparib could potentially be used as an effective radiosensitizer, especially in tumors where RAD51 foci formation is inhibited upon rucaparib treatment and that rucaparib could furthermore synergize with DNA damaging agents in this cohort.

#### 4.3.2.2 $\gamma$ H2AX

Because the histone H2AX is rapidly phosphorylated at DNA DSB sites, we added a staining for  $\gamma$ H2AX to the assay to monitor the extent of DNA DSB in our experiments. Reassuringly, all cell lines showed significantly increased numbers of  $\gamma$ H2AX foci after treatment with 2 Gy IR. Furthermore, the cell lines that were sensitive to rucaparib showed a larger increase in foci compared to rucaparib-resistant cell lines and the difference was of statistical significance. Likewise, after treatment with rucaparib, the sensitive cell lines formed significantly more  $\gamma$ H2AX foci compared to resistant cell lines, where the number of foci remained constant compared to DMSO control. Taken together, these results suggest that there are differences in the tendency of chromosomes to accumulate DSB between the sensitive and resistant cell lines.

### 4.3.3 Gene Set Analysis

As no genes were significantly differentially expressed between sensitive and resistant cell lines (although RAD51 did correlate with rucaparib  $IC_{50}$ ), we tested for enrichment in Gene Ontology (GO) terms to improve power in order to detect differences between sensitive and resistant cell lines. Strikingly, we were able to show a strong enrichment of genes involved in chromosome structure among the sets of genes most highly correlated with rucaparib resistance, lending further support to the hypothesis outlined above that these genes may be potential candidate biomarkers for rucaparib response in HNC.

## 4.4 Future Prediction Prospects

Ruppin and colleagues have recently developed a computational approach integrating large cell line based datasets of copy number variation, gene expression profiles and shRNA screens to detect synthetic lethal interactions in cancer. For PARP specifically, the group reported synthetic lethal interactions with five genes, among them MDC1 (a mediator of DNA damage checkpoint one interacting with BRCA1) and PRKDC (a DNA proteinkinase involved in DSB repair) [78]. Again, these results emphasize that the scope of PARPi can potentially be broadened and that identification of patients that may benefit from such treatment may in future stem from “big data”.

Ultimately, targeted agents like rucaparib will likely be combined with other targeted treatments to enhance the efficacy and exploit pathway interactions with limited side effects. Combination partners for PARPi, that have been proposed in the preclinical setting, include cyclin-dependent kinase 2 inhibitors, histone deacetylase inhibitors or the tyrosine kinase inhibitor imatinib, as all of these agents have shown to disrupt the HR process and reduce RAD51 foci formation [92].

## 4.5 Limitations of this Study and Future Improvements

As already mentioned above, the sample size of our study was limited and needs to be expanded in future. While the concept of synthetic lethality provides a reasonable and satisfying explanation for the PARPi sensitivity we found in a subset of HNC cell lines, it remains to be proven that it is in fact the underlying mechanism. This could be elegantly done with gene knock-out screens of candidate synthetic lethal partners of PARP in resistant cell lines as introduced above. It is furthermore desirable to detect the molecular differences between sensitive and resistant cell lines that lead to the PARPi

sensitivity seen in this study. Again, these differences seem to be too minor to detect in a small panel. HRD seems to be a possible mechanism of sensitivity, but in this study we were unable to prove that it is in fact HRD causing cells to be PARPi-sensitive. It remains unclear, whether the fact that rucaparib is the only PARPi that solely targets PARP-1 may play a role in its superior performance over olaparib and veliparib. As mentioned above, staining for markers that are partly expressed in a cell cycle dependent manner may not be the most accurate way of analyzing exact levels of DNA damage; in future, assays need to be improved and growth rate needs to be controlled for. Finally, it is important to stress that the results of this study solely rely on cell line data and translation to animal models or the clinical setting is yet to be conducted.

## 4.6 Conclusion

In conclusion, we were able to show that there are significant differences in potency between PARPi in HNC cell lines and we have identified rucaparib as the most effective agent. Crucially, we demonstrated that a subset of HNC cell lines, that do not harbor BRCA mutations, were susceptible to rucaparib to the same extent as a BRCA-methylated breast cancer cell line. We furthermore showed that there are significant differences in accumulation of DNA DSB between sensitive and resistant cell lines and we presented emerging evidence that this may be associated with chromosomal integrity. These results strongly support a future investigation of this agent for head and neck cancer patients. The next challenge remains to reliably identify patients, who will benefit from this targeted therapy by pinpointing appropriate biomarkers as well as synthetic lethal partners of rucaparib in an effort to take the next step towards personalized medicine for head and neck cancer patients.

# Bibliography

- [1] E. E. Vokes, R. R. Weichselbaum, S. M. Lippman, and W. K. Hong. Head and Neck Cancer. *N Engl J Med*, 3(328):184–194, 1993.
- [2] R. I. Haddad and D. M. Shin. Recent advances in head and neck cancer. *N Engl J Med*, 359(11):1143–54, 2008.
- [3] A. Forastiere, W. Koch, A. Trotti, and D. Sidransky. Head And Neck Cancer. *N Engl J Med*, 345(26):1890–1900, 2001.
- [4] T. Y. Seiwert, J. K. Salama, and E. E. Vokes. The chemoradiation paradigm in head and neck cancer. *Nat. Clin. Pract. Oncol.*, 4(3):156–71, 2007.
- [5] J. Ferlay, H. Shin, F. Bray, D. Forman, C. Mathers, and D. M. Parkin. Estimates of worldwide burden of cancer in 2008: GLOBOCAN 2008. *Int. J. Cancer*, 127(12):2893–917, 2010.
- [6] R. Siegel, J. Ma, Z. Zou, and A. Jemal. Cancer statistics, 2014. *CA. Cancer J. Clin.*, 64(1):9–29, 2014.
- [7] N. Termine, V. Panzarella, S. Falaschini, A. Russo, D. Matranga, L. Lo Muzio, and G. Campisi. HPV in oral squamous cell carcinoma vs head and neck squamous cell carcinoma biopsies: a meta-analysis (1988-2007). *Ann. Oncol.*, 19(10):1681–90, 2008.
- [8] A. K. Chaturvedi, E. A. Engels, R. M. Pfeiffer, B. Y. Hernandez, W. Xiao, E. Kim, B. Jiang, M. T. Goodman, M. Sibug-Saber, W. Cozen, L. Liu, C. F. Lynch, N. Wentzensen, R. C. Jordan, S. Altekruse, W. F. Anderson, P. S. Rosenberg, and M. L. Gillison. Human papillomavirus and rising oropharyngeal cancer incidence in the United States. *J. Clin. Oncol.*, 29(32):4294–301, 2011.
- [9] H. zur Hausen. Papillomaviruses and cancer: from basic studies to clinical application. *Nat. Rev. Cancer*, 2(5):342–50, 2002.

- [10] M. A. O'Rorke, M. V. Ellison, L. J. Murray, M. Moran, J. James, and L. A. Anderson. Human papillomavirus related head and neck cancer survival: a systematic review and meta-analysis. *Oral Oncol.*, 48(12):1191–201, 2012.
- [11] C. R. Leemans, B. J. M. Braakhuis, and R. H. Brakenhoff. The molecular biology of head and neck cancer. *Nat. Rev. Cancer*, 11(1):9–22, 2011.
- [12] T. Y. Seiwert, Z. Zuo, M. K. Keck, A. Khattri, C. S. Pedomallu, T. P. Stricker, C. D. Brown, T. J. Pugh, P. Stojanov, J. Cho, M. Lawrence, G. Getz, J. Bragelmann, R. DeBoer, R. R. Weichselbaum, A. Langerman, L. D. Portugal, E. A. Blair, K. M. Stenson, M. W. Lingen, E. E. Cohen, E. E. Vokes, K. P. White, and P. S. Hammerman. Integrative and comparative genomic analysis of HPV-positive and HPV-negative head and neck squamous cell carcinomas. *Clin. Cancer Res.*, 2014.
- [13] W. J. Blot, J. K. Mclaughlin, D. M. Winn, D. F. Austin, R. S. Greenberg, L. Bernstein, J. B. Schoenberg, A. Stemhagen, and J. F. Fraumeni. Smoking and Drinking in Relation to Oral and Pharyngeal Cancer Smoking and Drinking in Relation to Oral and Pharyngeal Cancer. *Cancer Res.*, 48(11):3282–3287, 1988.
- [14] J. H. Lubin, M. Purdue, K. Kelsey, Z. Zhang, D. Winn, Q. Wei, R. Talamini, N. Szeszenia-Dabrowska, E. M. Sturgis, E. Smith, O. Shangina, S. M. Schwartz, P. Rudnai, J. E. Neto, J. Muscat, H. Morgenstern, A. Menezes, E. Matos, I. N. Mates, J. Lissowska, F. Levi, P. Lazarus, C. La Vecchia, S. Koifman, R. Herrero, S. Franceschi, V. Wünsch-Filho, L. Fernandez, E. Fabianova, A. W. Daudt, L. D. Maso, M. P. Curado, C. Chen, X. Castellsague, P. Brennan, P. Boffetta, M. Hashibe, and R. B. Hayes. Total exposure and exposure rate effects for alcohol and smoking and risk of head and neck cancer: a pooled analysis of case-control studies. *Am. J. Epidemiol.*, 170(8):937–47, 2009.
- [15] M. Hashibe, P. Brennan, S. Chuang, S. Boccia, X. Castellsague, C. Chen, M. P. Curado, L. Dal Maso, A. W. Daudt, E. Fabianova, L. Fernandez, V. Wünsch-Filho, S. Franceschi, R. B. Hayes, R. Herrero, K. Kelsey, S. Koifman, C. La Vecchia, P. Lazarus, F. Levi, J. J. Lence, D. Mates, E. Matos, A. Menezes, M. D. McClean, J. Muscat, J. Eluf-Neto, A. F. Olshan, M. Purdue, P. Rudnai, S. M. Schwartz, E. Smith, E. M. Sturgis, N. Szeszenia-Dabrowska, R. Talamini, Q. Wei, D. M. Winn, O. Shangina, A. Pilarska, Z. Zhang, G. Ferro, J. Berthiller, and P. Boffetta. Interaction between tobacco and alcohol use and the risk of head and neck cancer: pooled analysis in the International Head and Neck Cancer Epidemiology Consortium. *Cancer Epidemiol. Biomarkers Prev.*, 18(2):541–50, 2009.



- [16] D. I. Kutler, A. D. Auerbach, J. Satagopan, P. F. Giampietro, S. D. Batish, A. G. Huvos, A. Goberdhan, J. P. Shah, and B. Singh. High incidence of head and neck squamous cell carcinoma in patients with Fanconi anemia. *Arch. Otolaryngol. Head. Neck Surg.*, 129(1):106–12, 2003.
- [17] J. Cloos, M. R. Spitz, S. P. Schantz, T. C. Hsu, Z. F. Zhang, H. Tobi, B. J. Braakhuis, and G. B. Snow. Genetic susceptibility to head and neck squamous cell carcinoma. *J. Natl. Cancer Inst.*, 88(8):530–5, 1996.
- [18] D. P. Slaughter, H. W. Southwick, and W. Smejkal. Field cancerization in oral stratified squamous epithelium; clinical implications of multicentric origin. *Cancer*, 6(5):963–8, 1953.
- [19] F. R. Khuri, E. S. Kim, J. J. Lee, R. J. Winn, S. E. Benner, S. M. Lippman, K. K. Fu, J. S. Cooper, E. E. Vokes, R. M. Chamberlain, B. Williams, T. F. Pajak, H. Goepfert, and W. K. Hong. The impact of smoking status, disease stage, and index tumor site on second primary tumor incidence and tumor recurrence in the head and neck retinoid chemoprevention trial. *Cancer Epidemiol. Biomarkers Prev.*, 10(8):823–9, 2001.
- [20] M. P. Tabor, R. H. Brakenhoff, V. M. van Houten, J. A. Kummer, M. H. Snel, P. J. Snijders, G. B. Snow, C. R. Leemans, and B. J. Braakhuis. Persistence of genetically altered fields in head and neck cancer patients: biological and clinical implications. *Clin. Cancer Res.*, 7(6):1523–32, 2001.
- [21] A. M. Gross, R. K. Orosco, J. P. Shen, A. M. Egloff, H. Carter, M. Hofree, M. Choueiri, C. S. Coffey, S. M. Lippman, D. N. Hayes, E. E. Cohen, J. R. Grandis, Q. T. Nguyen, and T. Ideker. Multi-tiered genomic analysis of head and neck cancer ties TP53 mutation to 3p loss. *Nat. Genet.*, 46(9):939–943, 2014.
- [22] M. Marron, P. Boffetta, Z. Zhang, D. Zaridze, V. Wünsch-Filho, D. M. Winn, Q. Wei, R. Talamini, N. Szeszenia-Dabrowska, E. M. Sturgis, E. Smith, S. M. Schwartz, P. Rudnai, M. P. Purdue, A. F. Olshan, J. Eluf-Neto, J. Muscat, H. Morgenstern, A. Menezes, M. McClean, E. Matos, I. N. Mates, J. Lissowska, F. Levi, P. Lazarus, C. La Vecchia, S. Koifman, K. Kelsey, R. Herrero, R. B. Hayes, S. Franceschi, L. Fernandez, E. Fabianova, A. W. Daudt, L. Dal Maso, M. P. Curado, G. Cadoni, C. Chen, X. Castellsague, S. Boccia, S. Benhamou, G. Ferro, J. Berthiller, P. Brennan, H. Møller, and M. Hashibe. Cessation of alcohol drinking, tobacco smoking and the reversal of head and neck cancer risk. *Int. J. Epidemiol.*, 39(1):182–96, 2010.

- [23] W. Ahrens, H. Pohlbeln, R. Foraita, M. Nelis, P. Lagiou, A. Lagiou, C. Bouchardy, A. Slamova, M. Schejbalova, F. Merletti, L. Richiardi, K. Kjaerheim, A. Agudo, X. Castellsague, T. V. Macfarlane, G. J. Macfarlane, Y. Lee, R. Talamini, L. Barzan, C. Canova, L. Simonato, P. Thomson, P. A. McKinney, A. D. McMahon, A. Znaor, C. M. Healy, B. E. McCartan, A. Metspalu, M. Maron, M. Hashibe, D. I. Conway, and P. Brennan. Oral health, dental care and mouthwash associated with upper aerodigestive tract cancer risk in Europe: the ARCAGE study. *Oral Oncol.*, 50(6):616–25, 2014.
- [24] E. Rettig, A. P. Kiess, and C. Fakhry. The role of sexual behavior in head and neck cancer: implications for prevention and therapy. *Expert Rev. Anticancer Ther.*, 15(1):35–49, 2015.
- [25] M. Wierzbicka, A. Józefiak, J. Jackowska, J. Szydowski, and A. Goździcka-Józefiak. HPV vaccination in head and neck HPV-related pathologies. *Otolaryngol. Pol.*, 68(4):157–73, 2014.
- [26] Z. S. Peacock, M. A. Pogrel, and B. L. Schmidt. Exploring the reasons for delay in treatment of oral cancer. *J. Am. Dent. Assoc.*, 139(10):1346–52, 2008.
- [27] R. Sankaranarayanan, K. Ramadas, G. Thomas, R. Muwonge, S. Thara, B. Mathew, and B. Rajan. Effect of screening on oral cancer mortality in Kerala, India: a cluster-randomised controlled trial. *Lancet*, 365(9475):1927–33, 2005.
- [28] N. Li, Z. Sun, C. Han, and J. Chen. The chemopreventive effects of tea on human oral precancerous mucosa lesions. *Proc. Soc. Exp. Biol. Med.*, 220(4):218–24, 1999.
- [29] D. M. Shin, H. Zhang, N. F. Saba, A. Y. Chen, S. Nannapaneni, A. R. M .R. Amin, S. Müller, M. Lewis, G. Sica, S. Kono, J. C. Brandes, W. J. Grist, R. Moreno-Williams, J. J. Beitler, S. M. Thomas, Z. Chen, H. J. C. Shin, J. R. Grandis, F. R. Khuri, and Z. G. Chen. Chemoprevention of head and neck cancer by simultaneous blocking of epidermal growth factor receptor and cyclooxygenase-2 signaling pathways: preclinical and clinical studies. *Clin. Cancer Res.*, 19(5):1244–56, 2013.
- [30] Y. Li, L. Li, S. Zhang, L. Wang, Z. Zhang, N. Gao, Y. Zhang, and Q. Chen. In vitro and clinical studies of gene therapy with recombinant human adenovirus-p53 injection for oral leukoplakia. *Clin. Cancer Res.*, 15(21):6724–31, 2009.
- [31] W. K. Hong, S. M. Lippman, L. M. Itri, D. D. Karp, J. S. Lee, R. M. Bryers, S. P. Schantz, A. M. Kramer, R. Lotan, L. Peters, I. W. Dimery, B. W. Brown, and H. Goeppert. Prevention of second primary tumors with isotretinoin in squamous-cell carcinoma of the head and neck. *N. Engl. J. Med.*, 323(12):795–801, 1990.

- [32] S. S. Napier and P. M. Speight. Natural history of potentially malignant oral lesions and conditions: an overview of the literature. *J. Oral Pathol. Med.*, 37(1):1–10, 2008.
- [33] I. van der Waal. Potentially malignant disorders of the oral and oropharyngeal mucosa; terminology, classification and present concepts of management. *Oral Oncol.*, 45(4-5):317–23, 2009.
- [34] G. Lodi, A. Sardella, C. Bez, F. Demarosi, and A. Carrassi. Interventions for treating oral leukoplakia. *Cochrane database Syst. Rev.*, 1(4):CD001829, 2006.
- [35] S. G. Patel and Shah J. P. TNM Staging of Cancers of the Head and Neck: Striving for Uniformity Among Diversity. *CA Cancer J. Clin.*, 55(4):424–58, 2005.
- [36] P. F. Denoix. Tumor, Node and Metastasis (TNM). *Bull Inst Nat Hyg*, 1(1):1–69, 1944.
- [37] G. Crile. III. On the Technique of Operations upon the Head and Neck. *Ann. Surg.*, 44(6):842–50, 1906.
- [38] P. Bose, N. T. Brockton, and J. C. Dort. Head and neck cancer: from anatomy to biology. *Int. J. Cancer*, 2013.
- [39] S. K. Kundu and M. Nestor. Targeted therapy in head and neck cancer. *Tumour Biol.*, 33(3):707–21, 2012.
- [40] A. Trotti, L. A. Bellm, J. B. Epstein, D. Frame, H. J. Fuchs, C. K. Gwede, E. Komaroff, L. Nalysnyk, and M. D. Zilberberg. Mucositis incidence, severity and associated outcomes in patients with head and neck cancer receiving radiotherapy with or without chemotherapy: a systematic literature review. *Radiother. Oncol.*, 66(3):253–62, 2003.
- [41] R. B. Smith, J. C. Sniezek, D. T. Weed, and M. K. Wax. Utilization of free tissue transfer in head and neck surgery. *Otolaryngol. Head. Neck Surg.*, 137(2):182–91, 2007.
- [42] M. R. Vergeer, P. A. H. Doornaert, D. H. F. Rietveld, C. R. Leemans, B. J. Slotman, and J. A. Langendijk. Intensity-modulated radiotherapy reduces radiation-induced morbidity and improves health-related quality of life: results of a nonrandomized prospective study using a standardized follow-up program. *Int. J. Radiat. Oncol. Biol. Phys.*, 74(1):1–8, 2009.
- [43] J. A. Bonner, P. M. Harari, J. Giralt, N. Azarnia, D. M. Shin, R. B. Cohen, C. U. Jones, R. Sur, D. Raben, J. Jassem, R. Ove, M. S. Kies, J. Baselga, H. Youssoufian,

- N. Amellal, E. K. Rowinsky, and K. K. Ang. Radiotherapy plus cetuximab for squamous-cell carcinoma of the head and neck. *N. Engl. J. Med.*, 354(6):567–78, 2006.
- [44] J. A. Bonner, P. M. Harari, J. Giralt, R. B. Cohen, C. U. Jones, R. K. Sur, D. Raben, J. Baselga, S. A. Spencer, J. Zhu, H. Youssoufian, E. K. Rowinsky, and K. K. Ang. Radiotherapy plus cetuximab for locoregionally advanced head and neck cancer: 5-year survival data from a phase 3 randomised trial, and relation between cetuximab-induced rash and survival. *Lancet. Oncol.*, 11(1):21–8, 2010.
- [45] C. Boeckx, M. Baay, A. Wouters, P. Specenier, J. B. Vermorken, M. Peeters, and F. Lardon. Anti-epidermal growth factor receptor therapy in head and neck squamous cell carcinoma: focus on potential molecular mechanisms of drug resistance. *Oncologist*, 18(7):850–64, 2013.
- [46] D. Hanahan and R. Weinberg. Hallmarks of cancer: the next generation. *Cell*, 144(5):646–74, 2011.
- [47] C. J. Lord and A. Ashworth. The DNA damage response and cancer therapy. *Nature*, 481(7381):287–94, 2012.
- [48] J. H. J. Hoeijmakers. DNA damage, aging, and cancer. *N. Engl. J. Med.*, 361(15):1475–85, 2009.
- [49] A. Ciccia and S. J. Elledge. The DNA damage response: making it safe to play with knives. *Mol. Cell*, 40(2):179–204, 2010.
- [50] S. C. West. Molecular views of recombination proteins and their control. *Nat. Rev. Mol. Cell Biol.*, 4(6):435–45, 2003.
- [51] J. Jiricny. The multifaceted mismatch-repair system. *Nat. Rev. Mol. Cell Biol.*, 7(5):335–46, 2006.
- [52] M. Esteller, J. M. Silva, G. Dominguez, F. Bonilla, X. Matias-Guiu, E. Lerma, E. Bussaglia, J. Prat, I. C. Harkes, E. Repasky, E. Gabrielson, M. Schutte, S. B. Baylin, and J. G. Herman. Promoter hypermethylation and BRCA1 inactivation in sporadic breast and ovarian tumors. *J. Natl. Cancer Inst.*, 92(7):564–9, 2000.
- [53] A. L. Lucas, R. Shakya, M. D. Lipsyc, E. B. Mitchel, S. Kumar, C. Hwang, L. Deng, C. Devoe, J. A. Chabot, M. Szabolcs, T. Ludwig, W. K. Chung, and H. Frucht. High prevalence of BRCA1 and BRCA2 germline mutations with loss of heterozygosity in a series of resected pancreatic adenocarcinoma and other neoplastic lesions. *Clin. cancer Res.*, 19(13):3396–403, 2013.

- [54] M. Lee, R. Tseng, H. Hsu, J. Chen, C. Tzao, W. L. Ho, and Y. Wang. Epigenetic inactivation of the chromosomal stability control genes BRCA1, BRCA2, and XRCC5 in non-small cell lung cancer. *Clin. Cancer Res.*, 13(3):832–8, 2007.
- [55] V. Schreiber, F. Dantzer, J. Ame, and G. de Murcia. Poly(ADP-ribose): novel functions for an old molecule. *Nat. Rev. Mol. Cell Biol.*, 7(7):517–28, 2006.
- [56] J. C. Ame. PARP-2, A Novel Mammalian DNA Damage-dependent Poly(ADP-ribose) Polymerase. *J. Biol. Chem.*, 274(25):17860–17868, 1999.
- [57] J. Murai, S. N. Huang, B. B. Das, A. Renaud, Y. Zhang, J. H. Doroshov, J. Ji, S. Takeda, and Y. Pommier. Trapping of PARP1 and PARP2 by Clinical PARP Inhibitors. *Cancer Res.*, 72(21):5588–99, 2012.
- [58] M. Rouleau, A. Patel, M. J. Hendzel, S. H. Kaufmann, and G. G. Poirier. PARP inhibition: PARP1 and beyond. *Nat. Rev. Cancer*, 10(4):293–301, 2010.
- [59] H. Farmer, N. McCabe, C. J. Lord, A. N. J. Tutt, D. Johnson, T. B. Richardson, M. Santarosa, K. J. Dillon, I. Hickson, C. Knights, N. M. B. Martin, S. P. Jackson, G. C. M. Smith, and A. Ashworth. Targeting the DNA repair defect in BRCA mutant cells as a therapeutic strategy. *Nature*, 434(7035):917–21, 2005.
- [60] H. E. Bryant, N. Schultz, H. D. Thomas, K. M. Parker, D. Flower, E. Lopez, S. Kyle, M. Meuth, N. J. Curtin, and T. Helleday. Specific killing of BRCA2-deficient tumours with inhibitors of poly(ADP-ribose) polymerase. *Nature*, 434(7035):913–7, 2005.
- [61] T. Dobzhansky. Genetics of Natural Populations. Xiii. Recombination and Variability in Populations of *Drosophila Pseudoobscura*. *Genetics*, 31(3):269–90, 1946.
- [62] J. C. Lucchesi. Synthetic lethality and semi-lethality among functionally related mutants of *drosophila melanogaster*. *Genetics*, 59:37–44, 1968.
- [63] M. Audeh, J. Carmichael, R.T. Penson, M. Friedlander, B. Powell, K. M. Bell-McGuinn, C. Scott, J. N. Weitzel, A. Oaknin, N. Loman, K. Lu, R. K. Schmutzler, U. Matulonis, M. Wickens, and A. Tutt. Oral poly(ADP-ribose) polymerase inhibitor olaparib in patients with BRCA1 or BRCA2 mutations and recurrent ovarian cancer: a proof-of-concept trial. *Lancet*, 376(9737):245–51, 2010.
- [64] P. C. Fong, D. S. Boss, T. A. Yap, A. Tutt, P. Wu, M. Mergui-Roelvink, P. Mortimer, H. Swaisland, A. Lau, M. J. O’Connor, A. Ashworth, J. Carmichael, S. B. Kaye, J. H. M. Schellens, and J. S. de Bono. Inhibition of poly(ADP-ribose) polymerase in tumors from BRCA mutation carriers. *N. Engl. J. Med.*, 361(2):123–34, 2009.

- [65] B. Lupo and L. Trusolino. Inhibition of poly(ADP-ribose)ylation in cancer: Old and new paradigms revisited. *Biochim. Biophys. Acta*, 1846(1):201–15, 2014.
- [66] N. Turner, A. Tutt, and A. Ashworth. Hallmarks of 'BRCAness' in sporadic cancers. *Nat. Rev. Cancer*, 4(10):814–9, 2004.
- [67] G. Rigakos and E. Razis. BRCAness: finding the Achilles heel in ovarian cancer. *Oncologist*, 17(7):956–62, 2012.
- [68] L. Hughes-Davies, D. Huntsman, M. Ruas, F. Fuks, J. Bye, S. Chin, J. Milner, L. A. Brown, F. Hsu, B. Gilks, T. Nielsen, M. Schulzer, S. Chia, J. Ragaz, A. Cahn, L. Linger, H. Ozdag, E. Cattaneo, E. S. Jordanova, E. Schuurin, D. S. Yu, A. Venkitaraman, B. Ponder, A. Doherty, S. Aparicio, D. Bentley, C. Theillet, C. P. Ponting, C. Caldas, and T. Kouzarides. EMSY links the BRCA2 pathway to sporadic breast and ovarian cancer. *Cell*, 115(5):523–35, 2003.
- [69] A. Kumar, O. Fernandez-Capetillo, O. Fernandez-Capetillo, and A. C. Carrera. Nuclear phosphoinositide 3-kinase beta controls double-strand break DNA repair. *Proc. Natl. Acad. Sci. U. S. A.*, 107(16):7491–6, 2010.
- [70] J. Z. Press, A. De Luca, N. Boyd, S. Young, A. Troussard, Y. Ridge, P. Kaurah, S. E. Kalloger, K. Blood, M. Smith, P. T. Spellman, Y. Wang, D. M. Miller, D. Horsman, M. Faham, C. B. Gilks, J. Gray, and D. G. Huntsman. Ovarian carcinomas with genetic and epigenetic BRCA1 loss have distinct molecular abnormalities. *BMC Cancer*, 8:17, 2008.
- [71] J. M. G. Pedrero, D. G. Carracedo, C. M. Pinto, A. H. Zapatero, J. P. Rodrigo, C. S. Nieto, and M. V. Gonzalez. Frequent genetic and biochemical alterations of the PI 3-K/AKT/PTEN pathway in head and neck squamous cell carcinoma. *Int. J. Cancer*, 114(2):242–8, 2005.
- [72] J.B. Clark, G.M. Ferris, and S. Pinder. Inhibition of nuclear NAD nucleosidase and poly ADP-ribose polymerase activity from rat liver by nicotinamide and 5-methyl nicotinamide. *Biochim. Biophys. Acta - Nucleic Acids Protein Synth.*, 238(1):82–85, 1971.
- [73] Y. Chen, L. Zhang, and Q. Hao. Olaparib: a promising PARP inhibitor in ovarian cancer therapy. *Arch. Gynecol. Obstet.*, 288(2):367–74, 2013.
- [74] A. Resistance to PARP-Inhibitors in Cancer Therapy. Montoni, M. Robu, E. Pouliot, and G. M. Shah. Resistance to PARP-Inhibitors in Cancer Therapy. *Front. Pharmacol.*, 4:18, 2013.

- [75] M. Javle and N. J. Curtin. The role of PARP in DNA repair and its therapeutic exploitation. *Br. J. Cancer*, 105(8):1114–22, 2011.
- [76] J. Murai, S. N. Huang, A. Renaud, Y. Zhang, J. Ji, S. Takeda, J. Morris, B. Teicher, J. H. Doroshow, and Y. Pommier. Stereospecific PARP Trapping by BMN 673 and Comparison with Olaparib and Rucaparib. *Mol. Cancer Ther.*, 13(2):433–43, 2014.
- [77] J. F. Holland. Hopes for tomorrow versus realities of today: therapy and prognosis in acute lymphocytic leukemia of childhood. *Pediatrics*, 45(2):191–3, 1970.
- [78] L. Jerby-Arnon, N. Pfetzer, Y. Y. Waldman, L. McGarry, D. James, E. Shanks, B. Seashore-Ludlow, A. Weinstock, T. Geiger, P. A. Clemons, E. Gottlieb, and E. Ruppin. Predicting Cancer-Specific Vulnerability via Data-Driven Detection of Synthetic Lethality. *Cell*, 158(5):1199–1209, 2014.
- [79] G. E. Tomlinson, T. T-L. Chen, V. A. Stastny, A. K. Virmani, M. A. Spillman, V. Tonk, J. L. Blum, N. R. Schneider, I. I. Wistuba, J. W. Shay, J. D. Minna, and A. F. Gazdar. Characterization of a Breast Cancer Cell Line Derived from a Germ-Line BRCA1 Mutation Carrier. *Cancer Res.*, 58(15):3237–3242, 1998.
- [80] M. Wei, T. Grushko, J. Dignam, F. Hagos, R. Nanda, L. Sveen, J. Xu, J. Fackenthal, M. Tretiakova, S. Das, and O. I. Olopade. BRCA1 promoter methylation in sporadic breast cancer is associated with reduced BRCA1 copy number and chromosome 17 aneusomy. *Cancer Res.*, 65(23):10692–9, 2005.
- [81] H. Zhang, G. Du, and J. Zhang. Assay of mitochondrial functions by resazurin in vitro. *Acta Pharmacol. Sin.*, 25(3):385–9, 2004.
- [82] M. M. Bradford. A rapid and sensitive method for the quantitation of microgram quantities of protein utilizing the principle of protein-dye binding. *Anal. Biochem.*, 72:248–54, 1976.
- [83] W. M. Bonner, C. E. Redon, J. S. Dickey, A. J. Nakamura, O. A. Sedelnikova, S. Solier, and Y. Pommier.  $\gamma$  H2AX and cancer. *Nat. Rev. Cancer*, 8:957–967, 2008.
- [84] E. P. Rogakou. DNA Double-stranded Breaks Induce Histone H2AX Phosphorylation on Serine 139. *J. Biol. Chem.*, 273(10):5858–5868, 1998.
- [85] M. K. Keck, Z. Zuo, A. Khattri, T. P. Stricker, C. Brown, M. Imanguli, D. Rieke, K. Endhardt, P. Fang, J. Bragelmann, R. DeBoer, M. El Dinalli, S. Aktolga, Z. Lei, P. Tan, S. G. Rozen, R. Salgia, R. R. Weichselbaum, M. W. Lingen, M. D. Story, K. K. Ang, E. E. Cohen, K. P. White, E. E. Vokes, and T. Y. Seiwert. Integrative

- analysis of Head and Neck Cancer identifies two biologically distinct HPV and three non-HPV subtypes. *Clin. cancer Res.*, 2014.
- [86] X. Jiao, B. T. Sherman, D. W. Huang, R. Stephens, M. W. Baseler, H. C. Lane, and R. A. Lempicki. DAVID-WS: a stateful web service to facilitate gene/protein list analysis. *Bioinformatics*, 28(13):1805–6, 2012.
- [87] M. Ashburner, C. A. Ball, J. A. Blake, D. Botstein, H. Butler, J. M. Cherry, A. P. Davis, K. Dolinski, S. S. Dwight, J. T. Eppig, M. A. Harris, D. P. Hill, L. Issel-Tarver, A. Kasarskis, S. Lewis, J. C. Matese, J. E. Richardson, M. Ringwald, G. M. Rubin, and G. Sherlock. Gene ontology: tool for the unification of biology. The Gene Ontology Consortium. *Nat. Genet.*, 25(1):25–9, 2000.
- [88] R. Apweiler, A. Bairoch, C. H. Wu, W. C. Barker, B. Boeckmann, S. Ferro, E. Gasteiger, H. Huang, R. Lopez, M. Magrane, M. J. Martin, D. A. Natale, C. O’Donovan, N. Redaschi, and L. L. Yeh. UniProt: the Universal Protein knowledgebase. *Nucleic Acids Res.*, 32(Database issue):D115–9, 2004.
- [89] R. Tibshirani, T. Hastie, B. Narasimhan, and G. Chu. Diagnosis of multiple cancer types by shrunken centroids of gene expression. *Proc. Natl. Acad. Sci. U. S. A.*, 99(10):6567–72, 2002.
- [90] R. Tibshirani. Regression Shrinkage and Selection via the Lasso. *J. R. Stat. Soc.*, 58(1):267–288, 1996.
- [91] H. Zou and T. Hastie. Regularization and variable selection via the elastic net. *J. R. Stat. Soc. Ser. B Stat. Methodol.*, 67(2):301–320, 2005.
- [92] T. A. Yap, S. K. Sandhu, C. P. Carden, and J. S. de Bono. Poly(ADP-ribose) polymerase (PARP) inhibitors: Exploiting a synthetic lethal strategy in the clinic. *CA. Cancer J. Clin.*, 61(1):31–49, 2011.
- [93] R. B. OHara and D. J. Kotze. Do not log-transform count data. *Methods Ecol. Evol.*, 1(2):118–122, 2010.
- [94] S. A. Forbes, G. Bhamra, S. Bamford, E. Dawson, C. Kok, J. Clements, A. Menzies, J. W. Teague, P. A. Futreal, and M. R. Stratton. The Catalogue of Somatic Mutations in Cancer (COSMIC). *Curr. Protoc. Hum. Genet.*, Chapter 10:Unit 10.11, 2008.
- [95] R. McLendon, A. Friedman, and A. Bigner. Comprehensive genomic characterization defines human glioblastoma genes and core pathways. *Nature*, 455(7216):1061–8, 2008.



- [96] A. B. Spurdle, S. R. Lakhani, S. Healey, S. Parry, L. M. Da Silva, R. Brinkworth, J. L. Hopper, M. A. Brown, D. Babikyan, G. Chenevix-Trench, S. V. Tavtigian, and D. E. Goldgar. Clinical classification of BRCA1 and BRCA2 DNA sequence variants: the value of cytokeratin profiles and evolutionary analysis—a report from the kConFab Investigators. *J. Clin. Oncol.*, 26(10):1657–63, 2008.
- [97] E. Cerami, J. Gao, U. Dogrusoz, B. E. Gross, S. O. Sumer, B. A. Aksoy, A. Jacobsen, C. J. Byrne, M. L. Heuer, E. Larsson, Y. Antipin, B. Reva, A. P. Goldberg, C. Sander, and N. Schultz. The cBio cancer genomics portal: an open platform for exploring multidimensional cancer genomics data. *Cancer Discov.*, 2(5):401–4, 2012.
- [98] J. Gao, B. A. Aksoy, U. Dogrusoz, G. Dresdner, B. Gross, S. O. Sumer, Y. Sun, A. Jacobsen, R. Sinha, E. Larsson, E. Cerami, C. Sander, and N. Schultz. Integrative analysis of complex cancer genomics and clinical profiles using the cBioPortal. *Sci. Signal.*, 6(269):1–19, 2013.
- [99] C. C. O’Sullivan, D. H. Moon, E. C. Kohn, and J. Lee. Beyond Breast and Ovarian Cancers: PARP Inhibitors for BRCA Mutation-Associated and BRCA-Like Solid Tumors. *Front. Oncol.*, 4:42, 2014.
- [100] W. Yang, J. Soares, P. Greninger, E. J. Edelman, H. Lightfoot, S. Forbes, N. Bindal, D. Beare, J. Smith, I. R. Thompson, S. Ramaswamy, P. A. Futreal, D. Haber, M. R. Stratton, C. Benes, U. McDermott, and M. J. Garnett. Genomics of Drug Sensitivity in Cancer (GDSC): a resource for therapeutic biomarker discovery in cancer cells. *Nucleic Acids Res.*, 41(Database issue):D955–61, 2013.
- [101] L. Robillard, T. C. Harding, and A. O. Walter. Preclinical efficacy of the PARP inhibitor rucaparib (AG014699/PF-01367338) as a monotherapy and in combination with PI3K inhibition. In *104th Annu. Meet. Am. Assoc. Cancer Res. Abstr. 3349*, Philadelphia, 2013.
- [102] Y. Drew, E. A. Mulligan, W. Vong, H. D. Thomas, S. Kahn, S. Kyle, A. Mukhopadhyay, G. Los, Z. Hostomsky, E. R. Plummer, R. J. Edmondson, and N. J. Curtin. Therapeutic potential of poly(ADP-ribose) polymerase inhibitor AG014699 in human cancers with mutated or methylated BRCA1 or BRCA2. *J. Natl. Cancer Inst.*, 103(4):334–46, 2011.
- [103] A. Mukhopadhyay, A. Elattar, A. Cerbinskaite, S. J. Wilkinson, Y. Drew, S. Kyle, G. Los, Z. Hostomsky, R. J. Edmondson, and N. J. Curtin. Development of a functional assay for homologous recombination status in primary cultures of epithelial ovarian tumor and correlation with sensitivity to poly(ADP-ribose) polymerase inhibitors. *Clin. Cancer Res.*, 16(8):2344–51, 2010.

- [104] S. Lee, C. Roques, A. C. Magwood, J. Masson, and M. D. Baker. Recovery of deficient homologous recombination in Brca2-depleted mouse cells by wild-type Rad51 expression. *DNA Repair (Amst)*., 8(2):170–81, 2009.
- [105] P. A. Konstantinopoulos, D. Spentzos, B. Y. Karlan, T. Taniguchi, E. Fountzilas, N. Francoeur, D. A. Levine, and S. A. Cannistra. Gene expression profile of BRCAness that correlates with responsiveness to chemotherapy and with outcome in patients with epithelial ovarian cancer. *J. Clin. Oncol.*, 28(22):3555–61, 2010.
- [106] A. A. Jazaeri. Gene Expression Profiles of BRCA1-Linked, BRCA2-Linked, and Sporadic Ovarian Cancers. *CancerSpectrum Knowl. Environ.*, 94(13):990–1000, 2002.
- [107] R. Simon and S. Roychowdhury. Implementing personalized cancer genomics in clinical trials. *Nat. Rev. Drug Discov.*, 12(5):358–69, 2013.
- [108] L. B. Alexandrov, S. Nik-Zainal, D. C. Wedge, S. A. Aparicio, S. Behjati, A. V. Biankin, G. R. Bignell, N. Bolli, A. Borg, A. Børresen Dale, S. Boyault, B. Burkhardt, A. P. Butler, Ca. Caldas, H. R. Davies, C. Desmedt, R. Eils, J. E. Eyfjörd, J. A. Foekens, M. Greaves, F. Hosoda, B. Hutter, T. Ilicic, S. Imbeaud, M. Imielinski, N. Jäger, D. T. W. Jones, S. Knappskog, M. Kool, S. R. Lakhani, C. López-Otín, S. Martin, N. C. Munshi, H. Nakamura, P. A. Northcott, M. Pajic, E. Papaemmanuil, A. Paradiso, J. V. Pearson, X. S. Puente, K. Raine, M. Ramakrishna, A. L. Richardson, J. Richter, P. Rosenstiel, M. Schlesner, T. N. Schumacher, P. N. Span, J. W. Teague, Y. Totoki, A. N. J. Tutt, R. Valdés-Mas, M. M. van Buuren, L. van 't Veer, A. Vincent-Salomon, N. Waddell, L. R. Yates, J. Zucman-Rossi, P. A. Futreal, U. McDermott, P. Lichter, M. Meyerson, S. M. Grimmond, R. Siebert, E. Campo, T. Shibata, S. M. Pfister, P. J. Campbell, and M. R. Stratton. Signatures of mutational processes in human cancer. *Nature*, 500(7463):415–21, 2013.
- [109] K. K. Dhillon, E. M. Swisher, and T. Taniguchi. Secondary mutations of BRCA1/2 and drug resistance. *Cancer Sci.*, 102(4):663–9, 2011.
- [110] S. Kummar, J. Ji, R. Morgan, H. Lenz, S. L. Puhalla, C. P. Belani, D. R. Gandara, D. Allen, B. Kiesel, J. H. Beumer, E. M. Newman, L. Rubinstein, A. Chen, Y. Zhang, L. Wang, J. Kinders, R. E. Parchment, J. E. Tomaszewski, and J. H. Doroshow. A phase I study of veliparib in combination with metronomic cyclophosphamide in adults with refractory solid tumors and lymphomas. *Clin. Cancer Res.*, 18(6):1726–1734, 2012.
- [111] J. F. Liu, S. M. Tolaney, M. Birrer, G. F. Fleming, M. K. Buss, S. E. Dahlberg, H. Lee, C. Whalen, K. Tyburski, E. Winer, P. Ivy, and U. Matulonis. A Phase 1

- trial of the poly(ADP-ribose) polymerase inhibitor olaparib (AZD2281) in combination with the anti-angiogenic cediranib (AZD2171) in recurrent epithelial ovarian or triple-negative breast cancer. *Eur. J. Cancer*, 49(14):2972–8, 2013.
- [112] R. Kristeleit, P. Lorusso, J. Infante, M. Flynn, M. Patel, S. Tolaney, J. Hilton, H. Calvert, H. Giordano, J. Isaacson, J. Borrow, A. Allen, S. Jaw-tsai, and H. Burris. A phase 1 dose-escalation and pharmacokinetic study of continuous oral rucaparib in patients with advanced solid tumors. In *ASCO Annu. Meet. Abstr. 2585*, volume 31, 2013.
- [113] K. J. Dedes, P. M. Wilkerson, D. Wetterskog, B. Weigelt, A. Ashworth, and J. S. Reis-Filho. Synthetic lethality of PARP inhibition in cancers lacking BRCA1 and BRCA2 mutations. *Cell Cycle*, 10(8):1192–1199, 2011.
- [114] L. Barazzuol, R. Jena, N. G. Burnet, L. B. Meira, J. C. G. Jeynes, K. J. Kirkby, and N. F. Kirkby. Evaluation of poly (ADP-ribose) polymerase inhibitor ABT-888 combined with radiotherapy and temozolomide in glioblastoma. *Radiat. Oncol.*, 8(1):65, 2013.
- [115] P. Geeleher, N. J. Cox, and R. S. Huang. Clinical drug response can be predicted using baseline gene expression levels and in vitro drug sensitivity in cell lines. *Genome Biol.*, 15(3):R47, 2014.
- [116] A. Mukhopadhyay, E. R. Plummer, A. Elattar, S. Soohoo, B. Uzir, J. E. Quinn, W. G. McCluggage, P. Maxwell, H. Aneke, N. J. Curtin, and R. J. Edmondson. Clinicopathological features of homologous recombination-deficient epithelial ovarian cancers: sensitivity to PARP inhibitors, platinum, and survival. *Cancer Res.*, 72(22):5675–82, 2012.
- [117] S. Nowsheen, J. A. Bonner, and E. S. Yang. The poly(ADP-Ribose) polymerase inhibitor ABT-888 reduces radiation-induced nuclear EGFR and augments head and neck tumor response to radiotherapy. *Radiother. Oncol.*, 99(3):331–8, 2011.
- [118] J. P. H. Chow, W. Y. Man, M. Mao, H. Chen, F. Cheung, J. Nicholls, S. W. Tsao, M. Li Lung, and R. Y. C. Poon. Poly(ADP-ribose) polymerase 1 is overexpressed in nasopharyngeal carcinoma and its inhibition enhances radiotherapy. *Mol. Cancer Ther.*, 12(11):2517–28, 2013.
- [119] H. Lee, C. Yoon, B. Schmidt, D. J. Park, A. Y. Zhang, H. V. Erkizan, J. Toretzky, D. G. Kirsch, and S. S. Yoon. Combining poly(ADP-ribose) polymerase 1 (PARP-1) inhibition and radiation in Ewings sarcoma results in lethal DNA damage. *Mol. Cancer Ther.*, 12(11):2591–600, 2013.

- 
- [120] J. Mitchell, G. C. M. Smith, and N. J. Curtin. Poly(ADP-Ribose) polymerase-1 and DNA-dependent protein kinase have equivalent roles in double strand break repair following ionizing radiation. *Int. J. Radiat. Oncol. Biol. Phys.*, 75(5):1520–7, 2009.
- [121] O. Guntinas-Lichius, T. Wendt, J. Buentzel, D. Esser, P. Lochner, A. Mueller, S. Schultze-Mosgau, and A. Altendorf-Hofmann. Head and neck cancer in Germany: a site-specific analysis of survival of the Thuringian cancer registration database - Springer. *J. Cancer Res. Clin. Oncol.*, 136(1):55–63, 2010.

# Appendix A

## German Summary

### A.1 Einführung

Plattenepithelkarzinome im Kopf-Hals-Bereich (HNC) stehen mit einer Inzidenz von über 600.000 an sechster Stelle der häufigsten malignen Tumoren weltweit [5]. Bekannte Risikofaktoren sind sowohl Tabak- und Alkoholkonsum, als auch Infektionen mit dem Humanen Papilloma Virus [7, 14]. In Deutschland liegt die Fünf-Jahres-Überlebensrate in Abhängigkeit von der Lokalisation des Primärtumors bei den fortgeschrittenen Stadien III und IV zwischen 21% und 65% [121]. Allerdings bestehen die Behandlungsschemata noch immer aus unspezifischen Regimen, wie Bestrahlung und zytotoxischer Chemotherapie. Es mangelt an gezielteren, nebenwirkungsärmeren und effektiveren Therapieansätzen.

Eine Gruppe gezielter Chemotherapeutika sind Poly(ADP-Ribose)Polymerase Inhibitoren (PARPi), die in anderen malignen Tumoren vielversprechende Aktivität gezeigt haben [99]. Diese Medikamente hemmen den DNA-Reparaturprozess Basen-Exzisions-Reparatur und bedingen so die Akkumulation von Doppelstrangbrüchen in der DNA. Bisher kamen diese Präparate hauptsächlich bei Mamma- und Ovarialkarzinomen zum Einsatz, da ein Teil dieser Tumorentitäten BRCA-Mutationen aufweist [59, 63]. Diese Mutationen prädisponieren Tumoren zu Empfindlichkeit für PARPi, weil BRCA Teil der Protein-Maschinerie für den Doppelstrangbruch-Reparaturmechanismus homologe Rekombination (HR) ist, der unter PARPi-Therapie vermehrt von der Zelle beansprucht wird. Neue Studien haben jedoch gezeigt, dass jegliche Defizite in HR-Kompetenz (nicht allein BRCA-Mutationen) zu einer Effektivität von PARPi führen und haben somit das mögliche Anwendungsgebiet dieser Substanzen auf andere Tumorentitäten erweitert.

Gegenstand vorliegender Studie ist die Beantwortung der drängenden Frage, ob Tumoren des Kopf-Hals-Bereiches zu den malignen Neoplasien gehören, die im Rahmen einer HR-Defizienz auf PARPi ansprechen. Dazu untersuchten wir die Wirksamkeit dreier PARPi am Zellmodell, verglichen die Sensibilitäts-Level mit BRCA-defizienten Brustkrebszelllinien und gingen der herausfordernden Frage nach, ob PARPi-Ansprechen vorhersagbar ist.

## A.2 Material und Methoden

Alle Zelllinien wurden in 10mm-Petrischalen bei 37°C und 5% CO<sub>2</sub> in dem jeweils geeigneten Medium (ergänzt durch FBS, Penicillin-Streptomycin und L-Glutamin) gehalten. Für die Zwecke dieser Studie wurde strikt innerhalb von zehn Zellpassagen gearbeitet. Zellzählungen wurden mithilfe einer Neubauer-Zählkammer durchgeführt.

Zunächst wurde ein Vergleich der Wirksamkeit dreier PARPi, namentlich Veliparib, Olaparib und Rucaparib mithilfe eines dreitägigen Resazurin-Redox-Färbungstests (auch bekannt als Alamar Blue<sup>®</sup>) angestellt. Zur genauen Bestimmung der halbmaximalen inhibitorischen Konzentration (IC<sub>50</sub>) des effektivsten Agens Rucaparib nutzten wir einen sechs- bis achttägigen Kolonie-formenden-Test (siehe auch Appendix E), zu dessen Auswertung wir die vom National Institute of Health zur Verfügung gestellte Software ImageJ für objektive Zählungen nutzten (Appendix B).

Um die PARPi-Sensibilitätslevel der HNC-Zelllinien und der Brustkrebs(BK)-Zelllinien zu vergleichen, nutzten wir einen sechstägigen Test mit Syto60<sup>®</sup> rot fluoreszierender Nucleinsäurefärbung, da die BK-Zelllinien nur sehr spärlich Kolonien formten. Desweiteren untersuchten wir die Unterschiede zwischen Rucaparib-sensiblen und Rucaparib-resistenten Zelllinien mittels Immunfluoreszenzfärbung von  $\gamma$ H2AX (einem DNA-Doppelstrangbruch-Marker) und RAD51 (einem Marker für HR). Für die Auswertung dieser Daten wurde ebenfalls ImageJ genutzt und ein Algorithmus (Macro) entworfen, um für die Zählung der Foci Befangenheit zu eliminieren und den Prozess zu beschleunigen (Appendix B). Die Ergebnisse für RAD51 validierten wir mittels Western Blot.

Außerdem untersuchten wir die in unserem Labor bereits vorhandenen Datensätze zu gezielter Sequenzierung (für die Bestimmung von Varianten in den BRCA-Genen) und Gen-Expression (Microarray: Agilent). Wir analysierten die Expressionsdaten hinsichtlich Gen-Medikament-Assoziationen zu Rucaparib IC<sub>50</sub> mithilfe des Pearson's Korrelationstests. Da die Probengröße gering war (n = 10), zogen wir desweiteren die DAVID-Software heran, um signifikant angereicherte Gen-Ontologie-Begriffe zu identifizieren, die mit Rucaparib-Sensibilität korrelieren.

### A.3 Ergebnisse

Da bereits bekannt ist, dass BRCA-defiziente Tumoren besonders sensibel auf diese Medikamentengruppe reagieren, war unser erstes Ziel, etwaige Mutationen in diesen Genen zu identifizieren. Zusammenfassend ist zu sagen, dass Mutationen in diesen Genen sowohl in unseren Zelllinien, als auch in Tumordaten (TCGA) selten (3-6%), aber nicht abwesend sind (Abb. 3.1 und Tab. 3.1).

Zurzeit werden mehrere PARPi in klinischen Studien untersucht, um ihre Effektivität in soliden Tumoren sowie ihre Verträglichkeit im Menschen zu bestimmen [99]. Neue Studien haben gezeigt, dass die PARPi sich in ihrer Fähigkeit unterscheiden, PARP-DNA-Komplexe zu formen (die zu höherer zytotoxischer Potenz führen), auch wenn die Inhibition der katalytischen Aktivität von PARP gleich ist [57, 76]. Um die Wirksamkeit von einem nicht-blockierenden PARPi (Veliparib) mit zwei blockierenden PARPi (Olaparib, Rucaparib) zu vergleichen, führten wir den Viabilitätstest Alamar Blue<sup>®</sup> in sechs HNC-Zelllinien durch. Wir konnten zeigen, dass Rucaparib der effektivste PARPi in HNC-Zelllinien unter den drei untersuchten PARPi ist (Abb. 3.2 und Abb. 3.3).

Da allerdings nur eine geringe Beeinträchtigung des Zellüberlebens nach drei Tagen zu beobachten war (wie gleichfalls in anderen Studien festgestellt wurde [100]), führten wir Kolonie-formende-Tests durch, um die halbmaximale Inhibitionskonzentration für Rucaparib in zehn HNC-Zelllinien zu bestimmen. Es zeigte sich eine große Variabilität hinsichtlich der Rucaparib-Antwort unter den getesteten Zelllinien und wir kategorisierten sie analog zu vorherigen Veröffentlichungen [101] als „sensibel“ oder „resistent“ (Abb. 3.4).

Um die ermittelten  $IC_{50}$  Werte in Relation zu bereits als sensibel geltenden BK-Zelllinien zu bringen, verglichen wir unsere als sensibel eingestuften HNC-Zelllinien mit den BK-Zelllinien HCC1937 (BRCA-mutiert) und UACC-3199 (BRCA-methyliert) (Abb. 3.5). Auffallend war, dass alle sensiblen HNC-Zelllinien deutlich sensibler auf Rucaparib reagierten, als HCC1937. Der  $IC_{50}$ -Wert für UACC-3199 (eine Zelllinie, die jüngst von einer anderen Studie als Rucaparib-sensibel eingestuft wurde [102]) war vergleichbar mit denjenigen für unsere HNC-Zelllinien. Dieses Ergebnis deutet darauf hin, dass der BRCA-Mutationsstatus von Zelllinien und auch Patienten allein nicht hinreichend zur Prognose von Rucaparib-Ansprechen ist. Ferner konnten wir indes zeigen, dass es eine Untergruppe von HNC-Zelllinien gibt, die sensibel auf eine PARPi-Monotherapie reagiert.

Um eben diese Subgruppe nicht nur in Zelllinien, sondern letztendlich auch in Patienten zu identifizieren, unternahmen wir mehrere Versuche, Rucaparib-Sensibilität vorherzusagen. Zunächst wandten wir eine Immunfluoreszenz-Färbung an, die zuvor für

Ovarialkarzinom-Zelllinien (und anschließend auch für Ovarialkarzinom-Patientinnen) zur Prognose von Rucaparib-Ansprechen veröffentlicht worden war [103, 116]. Während die Foci-Formation nach Rucaparib-Behandlung in unseren HNC-Zelllinien nicht mit Rucaparib-Sensibilität korrelierte, konnten wir dennoch signifikante Unterschiede zwischen sensiblen und resistenten Gruppen sowohl bezüglich der Foci-Formation für RAD51 als auch für  $\gamma$ H2AX feststellen (Abb. 3.7 und Abb. 3.8). Unsere Ergebnisse für RAD51 konnten wir mittels Western Blot reproduzieren (Abb. 3.9).

In Zusammenarbeit mit Dr. Paul Geeleher (Huang Labor, University of Chicago) haben wir desweiteren Methoden der Bioinformatik genutzt, um eventuelle Biomarker-Kandidaten zu ermitteln. Unsere Versuche, eine robuste Gen-Signatur für Rucaparib-Sensibilität zu erstellen, scheiterten an der geringen Zahl der HNC-Zelllinien ( $n = 10$ ). Dennoch untersuchten wir die Basis-Expression wichtiger Gene für HR (z.B. BRCA, EMSY, PTEN) bezüglich Assoziationen zu Rucaparib-Sensibilität. Lediglich RAD51-Expression war signifikant assoziiert mit Rucaparib-Sensibilität ( $P = 0.04$ , allerdings nicht signifikant nach Korrektur für multiples Testen). Gleichwohl fanden wir eine positive Korrelation zwischen RAD51-Basisexpression und Rucaparib-Sensibilität (Abb. 3.10). Bei Analyse aller Gene, für die Expressionsdaten verfügbar waren, konnte nur IL-18 als grenzwertig signifikant unterschiedlich exprimiertes Gen zwischen sensiblen und resistenten Zelllinien festgestellt werden, wenngleich Korrelationen hoch waren (Tab. 3.2). Dieses Ergebnis ist nicht überraschend bei einer Probengröße von zehn, weshalb wir die Anreicherung von Gen-Ontologie-Begriffen für die 100 Gene, die am stärksten positiv oder invers mit Rucaparib-Ansprechen korrelierten, untersuchten (Tab. 3.3). Interessanterweise waren jene Gen-Ontologie-Begriffe, die mit Chromosomenstruktur zusammenhängen, sehr signifikant in den 100 Genen angereichert, die invers mit Rucaparib-Sensibilität (also mit Rucaparib-Resistenz) korrelierten. Das deutet darauf hin, dass es Unterschiede in der Chromosomen-Stabilität zwischen den HNC-Zelllinien gibt. Möglicherweise ist dies auf HR-Defizienz zurückzuführen und mag auch die Unterschiede bezüglich des Rucaparib-Ansprechens bedingen.

Zweifelsohne bedarf es verlässlicherer Prognose-Methoden für neue gezielte antineoplastische Medikamente wie Rucaparib. In Anbetracht unserer Daten, besonders hinsichtlich der Korrelation zwischen chromosomaler Stabilität und Rucaparib-Resistenz, halten wir es für möglich, in der Zukunft Rucaparib-Ansprechen mithilfe von Expressionsdaten größeren Umfangs vorherzusagen.



## A.4 Diskussion

Ziel vorliegender Studie war es, das Ansprechen von Zelllinien von Kopf-Hals-Tumoren auf die gezielten Chemotherapeutika PARPi zu evaluieren. Wir haben zunächst sowohl unsere HNC-Zelllinien, als auch die TCGA-HNC-Kohorte auf BRCA-Mutationen untersucht und sehr seltene Variationen identifiziert. Es ist jedoch wahrscheinlich, dass weitere Mechanismen zu PARPi-Sensibilität beitragen und der BRCA-Mutationsstatus allein nicht als prädiktiver Marker ausreicht, was ebenfalls bereits in klinischen Studien festgestellt worden ist [109].

Wir konnten hier in der Tat zeigen, dass eine Gruppe der HNC-Zelllinien in Abwesenheit von BRCA-Mutationen sehr empfindlich gegenüber PARPi reagierte. Wahrscheinlich ist diese Sensibilität durch eine HR-Defizienz (über BRCA-Mutationen hinaus) bedingt, worauf die fehlende RAD51-Foci-Formation nach Bestrahlung in sensiblen Zellen hindeutete. Die Wirksamkeit der untersuchten PARPi zeigte signifikante Unterschiede, die sich in Übereinstimmung mit früheren Studien mit der unterschiedlichen Fähigkeit zur PARP-DNA-Komplex-Bildung erklären lassen. Interessanterweise sind die in klinischen Studien bestimmten maximal tolerablen Dosen 60mg, 400mg und 360mg für Veliparib, Olaparib und Rucaparib [110–112]. Dies deutet in der Gesamtbetrachtung mit unseren Ergebnissen darauf hin, dass Rucaparib nicht nur *in vitro* die höchste Effektivität aufweist, sondern auch vergleichsweise gut von Patienten toleriert werden könnte. Das gibt Anlass, diese Substanz für die Behandlung von HNC in Betracht zu ziehen.

Wir konnten weiterhin zeigen, dass unsere HNC Zelllinien ebenso Rucaparib-sensibel sind wie BRCA-defiziente Brustkrebszelllinien, die bereits von anderen Gruppen als sensibel eingestuft worden waren [102]. Dieses Ergebnis setzt unsere Resultate in den Kontext des aktuellen Standes der Forschung und unterstreicht die Aussagekraft dieser Studie.

Es ist jedoch äußerst wichtig zu betonen, dass längst nicht alle Zelllinien auf PARPi ansprechen. Die Variabilität unter den Zelllinien legt die Vermutung nahe, dass HNC-Patienten ebenfalls sehr variabel auf eine solche Therapie reagieren würden. Deshalb werden zwingend Methoden zur Prognose von PARPi-Ansprechen benötigt.

Da unsere Probengröße zu klein für die Entwicklung einer verlässlichen Gen-Signatur war, verwendeten wir zunächst einen Immunfluoreszenz-Assay für RAD51, um die HR-Kompetenz der Zelllinien zu untersuchen. Insgesamt konnten wir die prädiktive Leistung dieses Assays nicht reproduzieren, da sich die RAD51-Foci-Formation nicht signifikant zwischen Rucaparib-sensiblen und Rucaparib-resistenten Zellen unterschied. Allerdings konnten wir zeigen, dass es sehr wohl Unterschiede zwischen diesen Gruppen bezüglich ihrer DNA-Doppelstrangbruch-Akkumulationen nach Bestrahlung und

Rucaparib-Behandlung gibt, was uns Anlass gab, der Frage nachzugehen, ob eine generelle Chromosomeninstabilität zu PARPi-Sensibilität führen könnte.

Da keine Gene signifikant differentiell zwischen Rucaparib-sensiblen und -resistenten Zelllinien exprimiert wurden, nutzten wir die DAVID-Software, um Gengruppen zu identifizieren, deren Expression sich in den Gruppen unterscheiden. In der Tat waren die am stärksten signifikant mit Rucaparib-Resistenz assoziierten Gen-Ontologie-Begriffe der Gruppe „Chromosomen“ zugehörig. Zukünftig werden sicherlich größere Datensätze nötig sein, um Rucaparib-Sensibilität verlässlich vorherzusagen. Vielversprechende Methoden-Ansätze wurden kürzlich in der Zeitschrift *Cell* veröffentlicht [78].

Zusammenfassend konnten wir hier erstmals zeigen, dass es eine Subgruppe von Kopf-Hals-Tumor-Zelllinien gibt, die in gleichem Maße sensibel auf den PARPi Rucaparib anspricht, wie BRCA-defiziente Brustkrebszelllinien. Die vorliegende Arbeit gibt weiterhin Hinweise, dass der Unterschied zwischen sensiblen und resistenten Zelllinien in der chromosomalen Anfälligkeit für Doppelstrangbrüche liegen könnte. Diese Ergebnisse geben Anlass zu weiteren Untersuchungen dieser Medikamentengruppe für Patienten mit Kopf-Hals-Tumoren mit dem Ziel, das Anwendungsgebiet dieser relativ nebenwirkungsarmen Medikamente zu erweitern. Die nächste Herausforderung wird sein, Patienten zu identifizieren, die von PARPi profitieren, um einen weiteren Schritt in Richtung personalisierter Krebsmedizin zu gehen.

## Appendix B

# ImageJ Analysis

### B.1 Analysis Path for Colony Counting

This is an example of the colony counts performed on clonogenic assays. Comments in Italics.

```
selectWindow("SCC-61 RUCA 6-28.JPG"); // import the scanned 6-well-plate file
setAutoThreshold("Default");
//run("Threshold..."); // set an appropriate threshold making sure to exclude shadows
setThreshold(0, 116);
run("Convert to Mask");
run("Make Binary"); // create a binary picture 0 or 255
makeRectangle(998, 44, 420, 418); // draw a rectangle around the well to be counted
run("Duplicate...", "title=[SCC-61 RUCA 6-28 DMSO.JPG]");
run("Analyze Particles...", "size=10-Infinity circularity=0.00-1.00 show=Nothing exclude summarize"); // Process → Analyze Particles. Particles with pixel sizes from 10-infinity were counted for all wells.
```

### B.2 Macro for Foci Counting

Open the three pictures (blue, green, red) in that order. Run Macro. When the program asks, one can choose the function “watershed” to divide touching nuclei. If the watershed function is not accurate, the picture can be excluded. Results of “RawIntDen” per cell need to be divided by 255 to calculate the number of foci in that cell. Comments in Italics.

*dir2 = getDirectory("Choose a Directory for saving"); // prompts user to select the folder where files will be saved*

```
t = getTitle();
s = lastIndexOf(t, 'c');
t = substring(t, 0, s);
t = replace(t, " ", "-");
t2 = t + ' green foci';
t3 = t + ' red foci';
run("Images to Stack");
rename("Stack");
selectWindow("Stack");
setSlice(001);
run("Duplicate...", "title=nuclei");
//run("Threshold...");
setAutoThreshold("Default");
//setThreshold(0, 64);
run("Convert to Mask");
run("Make Binary"); // produces a binary picture: 255 or 0
run("Fill Holes"); wait-
ForUser; // this is the point to decide for watershed or excluding the picture
run("Analyze
Particles...", "size=400-Infinity circularity=0.00-1.00 show=Nothing exclude clear");
// 400 should be big enough to only include nuclei that are in the right focal plain
selectWindow("Stack");
setSlice(002);
run("Duplicate...", "title='t2'");
run("Find Maxima...", "noise=80 output=[Single Points] exclude");
roiManager("Show Non");
roiManager("Show All");
roiManager("Measure");
roiManager("Deselect");
//roiManager("Delete");
saveAs("Results", dir2 + t2 + ".csv");
selectWindow("ROI Manager");
run("Close");
selectWindow("Results");
run("Close");
selectWindow("Stack");
setSlice(001);
```

```
run("Duplicate...", "title=nuclei");
//run("Threshold...");
setAutoThreshold("Default");
//setThreshold(0, 64);
run("Convert to Mask");
run("Make Binary");
run("Fill Holes");
waitForUser;
run("Analyze Particles...", "size=400-Infinity circularity=0.00-1.00 show=Nothing exclude add");
selectWindow("Stack");
setSlice(003);
run("Duplicate...", "title='t3'");
run("Find Maxima...", "noise=60 output=[Single Points] exclude");
roiManager("Show None");
roiManager("Show All");
roiManager("Measure");
roiManager("Deselect");
//roiManager("Delete");
saveAs("Results", dir2 + t3 + ".csv");
selectWindow("ROI Manager");
run("Close");
selectWindow("Results");
run("Close");

run("Close All");
```

# Appendix C

## R Code

### C.1 Code for Generalized Linear Regression Model

```
# Comments in Italics.  
  
resp <- c(7.1, 3.59, 3.22, 12.07, 4.26, 9.58) #Insertion of raw count data  
group <- factor(c(1,1,1,0,0,0)) #Establishes two groups, in this case group 1 is DMSO  
control and group two is after 2 Gy IR treatment  
pairs <- factor(c(1,2,3,1,2,3)) #Creates paired values, in this example run of experi-  
ment 1, 2 and 3  
summary(glm(resp~ group+pairs, family="poisson")) #Generates a generalized linear  
model assuming a Poisson distribution as discussed in detail in Methods
```

### C.2 Code for Spearman's Rank Correlation

```
assay1 <- c(1,2,3,4,5,6) #Insertion of cell lines rank for one assay  
assay2 <- c(2,1,3,4,6,5) #Insertion of cell lines rank for other assay  
  
resp <- cor.test(assay1, assay2, method='spearman', alternative='greater') #Per-  
forms Spearman's rank correlation and paired t-test for the two assays
```

### C.3 Code for Pearson's Correlation

```
corsPear <- numeric() #Creates an empty vector called 'corsPear' to store numbers
for p-values
corPsPear <- numeric()for(i in 1:nrow(agiSensRes)) #Creates empty vector for Pear-
son's correlation coefficients. Indexes every row of the microarray matrix called 'agiSen-
sRes'
{
b <- cor.test(agiSensRes[i,], log(ic50s), method="pearson", alternative="greater")
#Tests every gene expression value (9138) for an association with rucaparib IC50 using
Pearson's correlation and paired t-tests
corPsPear[i] <- b$p.value #Produces p-values
corsPear[i] <- b$estimate #Produces Pearson's correlation coefficients
}
bhPs <- p.adjust(corPsPear, method="BH") #Estimates the false discovery rate using
the Benjamini-Hochberg method
```

## Appendix D

# Gene Ontology

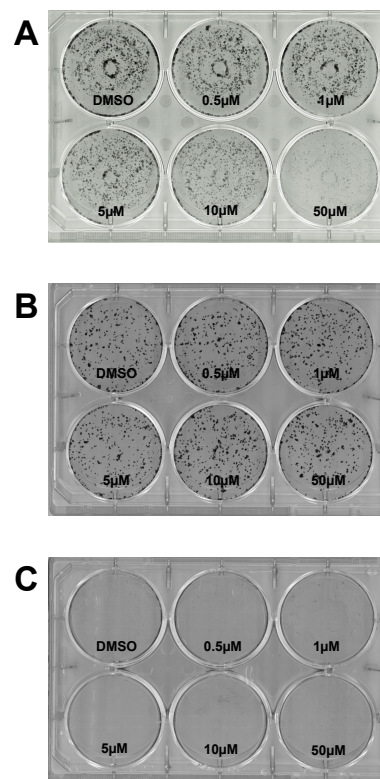
TABLE D.1: 15 Genes of GO Term Category “Chromosome”

Official Gene Symbol	Gene Name
BUB1	budding uninhibited by benzimidazoles 1 homolog (yeast)
CDCA8	cell division cycle associated 8
CENPA	centromere protein A
CENPH	centromere protein H
XPO1	exportin 1 (CRM1 homolog, yeast)
HELLS	helicase, lymphoid-specific
HIST1H4L, HIST1H4C	histone cluster
KIF2C	kinesin family member 2C
NUP37	nucleoporin 37kDa
RFC5	replication factor C (activator 1) 5, 36.5kDa
RPA1	replication protein A1, 70kDa
CBX3	similar to chromobox homolog 3
TERF2	telomeric repeat binding factor 2
TOP2A	topoisomerase (DNA) II alpha 170kDa
ZMIZ2	zinc finger, MIZ-type containing 2



## Appendix E

# Colony-forming Assays



---

FIGURE E.1: Colony-forming assay 6-well-plates  
**A** sensitive cell line BB-49, **B** resistant cell line SCC-61, **C** breast cancer cell line HCC1937 that did not form colonies. Rucaparib was administered for 24 h in concentrations ranging from 0.5  $\mu\text{M}$  to 50  $\mu\text{M}$ .

## Appendix F

# Acknowledgements

Firstly I am indebted to Dr. Tanguy Seiwert at the University of Chicago, who enabled me to work in his laboratory. I am very grateful for the opportunity to join an international team and experience state of the art research at the Knapp Center for Biological Sciences. He let me take initiative and responsibility at all stages of my project and taught me many lessons that will undoubtedly be valuable in the future.

I want to thank the entire Seiwert laboratory, especially Michaela Keck, who taught me resazurin assays, Sabrina Boeser for introducing me to cell culture and Susanne Tepper, who was my constant companion giving me feedback and persevering by my side throughout my research year. At the University of Chicago I also want to thank Lauren Roach and Colles Price for continued support and much appreciated discussion. I am very thankful for the help of Dr. Christine Labno at the Light Microscopy Core Facility, without whom the creation of the counting Macro and interpretation of the immunofluorescence experiments would not have been possible in this way. My appreciation goes out to Professor Olopade for generously providing the breast cancer cell lines used in this study.

Next, I owe my acknowledgments to PD Dr. Sebastian Fetscher, my supervisor at the University of Lübeck. Through my entire endeavor abroad he was always available, full of encouragement and support. Here, I would also like to recognize Prof. Gieseler for his advice and opinion.

I would like to thank the German National Academic Foundation. Through the Foundation I was able to initiate contact to Dr. Seiwert and I am indebted for the financial support they have endowed me with throughout my research year and my studies at both, the University of Chicago and Lübeck.

I acknowledge the TCGA Research Network for generating TCGA datasets used in this manuscript. The data was downloaded from the following webpage: [Http://www.tcgadata.nci.nih.gov](http://www.tcgadata.nci.nih.gov)

I owe my deepest gratitude to Dr. Paul Geeleher, who not only contributed invaluable analyses to this project, taught me countless lessons about research and was of great help in structuring and outlining this study, but also helped me through all the doubts and detours and encouraged me to stand firm. His help was certainly crucial to the success of publishing this study in the peer-reviewed journal *Oral Oncology*.

Lastly, I want to thank my parents for believing in me, for their everlasting support of my decisions in every possible way and for raising me to be resilient. My accomplishments are theirs.

# Jana Heitmann

\* 14. April 1989  
in Hamburg

Kirchenackerweg 7  
8050 Zürich, Schweiz



## Ausbildung

- 11/16 **Zweiter Abschnitt der Ärztlichen Prüfung (mündlicher Teil)**, Ruprecht-Karls-Universität Heidelberg.  
Note: 1,0
- 06/16 **United States Medical Licensing Examination**, Step 2 Clinical Knowledge.
- 10/15 **Zweiter Abschnitt der Ärztlichen Prüfung (schriftlicher Teil)**, Universität zu Lübeck.  
Note: 1,0
- 02/15 **Einreichen der Dissertation**, Universität zu Lübeck.
- 10/12- **Wissenschaftliches Auslandsjahr**, University of Chicago, USA.
- 09/13 Durchführung der Experimente für die medizinische Dissertation im onkologischen Labor von T. Seiwert, MD mit dem Thema "Gezielte Therapien bei Kopf-Hals-Tumoren"
- 09/10 **Erster Abschnitt der Ärztlichen Prüfung**, Universität zu Lübeck.  
Note: 1,0
- 06/08 **Abitur**, Ubbo-Emmius-Gymnasium Leer.  
Note: 1.0
- 05-06 **High School Jahr**, Madison High School, Rexburg, ID, USA.

## Publikationen

S. Diederichs, L. Bartsch\*, J.C. Berkmann\*, K. Fröse\*, **J. Heitmann\***, C. Hoppe\*, D. Iggena\*, D. Jazmati\*, P. Karschnia\*, M. Linsenmeier\*, T. Maulhardt\*, L. Möhrmann\*, J. Morstein\*, S.V. Paffenholz\*, P. Röpenack\*, T. Rückert\*, L. Sandig\*, M. Schell\*, A. Steinmann\*, G. Voss\*, J. Wasmuth\*, M.E. Weinberger\*, R. Wullenkord\* *The dark matter of the cancer genome: aberrations in regulatory elements, untranslated regions, splice sites, non-coding RNA and synonymous mutations* EMBO Mol Med 8(3) 173-303, 2016

**J. Heitmann** P. Geeleher, Z. Zuo, R.R. Weichselbaum, E.E. Vokes, S. Fetscher, T.Y. Seiwert *Poly (ADP-ribose) polymerase inhibitor efficacy in head and neck cancer* Oral Oncology 50(9)825-31, 2014

T. Seiwert, X. Wang, **J. Heitmann** et al. *DNA Repair Biomarkers XPF and Phospho-MAPKAP Kinase 2 Correlate With Clinical Outcome in Advanced Head and Neck Cancer* PLoS ONE 9(7), 2014

## Poster-Präsentationen

- 06/14 **Correlation of homologous recombination deficiency in head and neck cancer with sensitivity to PARP inhibition**, American Society of Clinical Oncology (ASCO) Annual Meeting.  
**J. Heitmann**, Z. Zuo, P. Geeleher, M. Keck, A. Khattri, M. Lingen, J. DeSouza, V. Villafior, M. Beckett, R. Weichselbaum, E. Vokes, T. Seiwert
- 04/14 **An evaluation of Poly(ADP-ribose)Polymerase efficacy in head and neck cancer**, American Association for Cancer Research (AACR) Annual Meeting.  
**J. Heitmann**, P. Geeleher, M. Keck, Z. Zuo, A. Khattri, S. Tepper, M. Beckett, R. Weichselbaum, S. Fetscher, E. Vokes, T. Seiwert

- 04/14 **Influence of growth factors on resistance to EGFR inhibitor treatment in HNSCC – Temsirolimus as a potential concept?**, *AACR Annual Meeting*.  
S. Tepper, Z. Zuo, A. Khattri, **J. Heitmann**, J. Heß, T. Seiwert
- 02/14 **PARP inhibition in Head and Neck Cancer: Do we know who benefits?**, *Multidisciplinary Head and Neck Cancer Symposium Scottsdale, AZ, USA*.  
Vortrag von Jonas DeSouza, MD

## Weiterbildung

- 01/16 **Interdisziplinäres Symposium Thoraxonkologie**, Heidelberg.
- 08/15 **Das Krebsgenom - Entdeckungen aus der dunklen Materie des menschlichen Erbguts**, *Sommerakademie der Studienstiftung des Deutschen Volkes*, Leitung: Prof. Dr. Sven Diederichs, DKFZ.

## Stipendien und Preise

- seit 2009 **Studienstiftung des Deutschen Volkes**, *Auslandsstipendien 2012, 2013 und 2016*.
- 2008 **Preis für das beste Abitur**, *Ubbo-Emmius-Gymnasium Leer*.
- 2006 **All Academic Award**, *Madison High School, Rexburg, ID, USA*.

## Praktika, Freiwilligendienst und Famulaturen

- 06-10/16 **PJ Chirurgie**, *Stadtspital Trimeli, Zürich*.
- 03-06/16 **PJ Interdisziplinäre Onkologie: NCT, Hämatologie, Radioonkologie**, *Universitätsklinikum Heidelberg*.
- 11/15-03/16 **PJ Innere Medizin: Thoraxonkologie und Pneumologie**, *Thoraxklinik Heidelberg*.
- 02-03/15 **Famulatur: Hämatologie und Onkologie**, *Thoraxklinik Heidelberg*.
- 09-10/14 **Famulatur: Hämatologie und Onkologie**, *University of Chicago Hospital, Chicago, USA*.
- 08/14 **Neurologie Summer School**, *Christian Albrechts Universität, Kiel*.
- 07-08/14 **Famulatur: Praxis für Hämatologie, Onkologie und Palliativmedizin**, Leer.
- 08/12 **Famulatur: Radiologie**, *Klinikum Leer*.
- 07/12 **Famulatur: Anästhesiologie**, *Klinikum Leer*.
- 02-03/12 **Famulatur: Viszeralchirurgie**, *UKSH Lübeck*.
- 09/11 **Famulatur: Innere Medizin**, *Borromäus-Hospital, Leer*.
- 03/10 **Praktikum: Praxis für Allgemeinmedizin**, Leer.
- 08-09 **Freiwilliges ökologisches Jahr (FÖJ)**, *Nationalparkhaus Wattenmeer, Norderney*.